

Enclosure 5

MFN 10-044 Supplement 3

**Revised Response (Revision 3) to NRC Request for
Additional Information Letter No. 411
Related to ESBWR Design Certification Application**

Engineered Safety Features

RAI Number 6.2-202 S01

**NEDO-33572, "ESBWR ICS and PCCS Condenser
Combustible Gas Mitigation and Structural Evaluation,"
Revision 3, September 2010**

Public Version

NON-PROPRIETARY INFORMATION NOTICE

This is a non-proprietary version of markups to NEDE-33572P, which has the proprietary information removed. Portions of the document that have been removed are indicated by an open and closed bracket as shown here [[]].



HITACHI

GE Hitachi Nuclear Energy

NEDO-33572

Revision 3

Class I

eDRF Section 0000-0115-2094

September 2010

Licensing Topical Report

ESBWR ICS AND PCCS CONDENSER COMBUSTIBLE GAS MITIGATION AND STRUCTURAL EVALUATION

Copyright 2010, GE-Hitachi Nuclear Energy Americas LLC, All Rights Reserved

NON-PROPRIETARY INFORMATION NOTICE

This is a public version of NEDE-33572P, Revision 3, from which the proprietary information has been removed. Portions of the document that have been removed are indicated by white space within double square brackets, as shown here [[]].

**IMPORTANT NOTICE REGARDING
CONTENTS OF THIS REPORT***

Please Read Carefully

The information contained in this document is furnished as reference to the NRC Staff for the purpose of obtaining NRC approval of the ESBWR Certification and implementation. The only undertakings of GE-Hitachi Nuclear Energy Americas LLC (GEH) respecting information in this document are contained in contracts between GEH and participating utilities, and nothing contained in this document shall be construed as changing those contracts. The use of this information by anyone for any purpose other than that for which it is furnished by GEH, is not authorized; and with respect to any unauthorized use, GEH makes no representation or warranty, express or implied, and assumes no liability as to the completeness, accuracy, or usefulness of the information contained in this document, or that its use may not infringe privately owned rights.

TABLE OF CONTENTS

1.0 SCOPE	10
2.0 PCCS METHODOLOGY	11
2.1 COMBUSTIBLE GAS GENERATION / CONCENTRATION.....	11
2.2 DETONATION LOADS	14
2.2.1 Peak Pressure Ratio	15
2.2.2 Dynamic Load Factor (DLF)	16
2.2.3 Deflagration to Detonation Transition (DDT)	18
2.2.4 Other PCCS Components	18
2.2.5 Vent Line External Pressure	25
2.2.6 Post-Detonation Pressure Relief	27
2.2.7 Thermal Effects.....	28
2.2.8 Single Tube Elongation Due to Post-Detonation Heating	28
2.3 INITIAL SIZING AND STRESS CALCULATION.....	31
2.3.1 Design Criteria	32
2.3.2 Deleted	32
2.4 EFFECT ON HEAT TRANSFER	32
2.4.1 PCCS Unit Heat Removal Capability Type Test.....	32
2.5 POSTULATED DETONATION SCENARIOS	36
2.5.1 Detonation in Tubes.....	36
2.5.2 Detonation in Lower Drum.....	36
2.6 DISCUSSION OF UNCERTAINTY AND CONSERVATIVE ASSUMPTIONS.....	37
2.6.1 Overestimation of Radiolytic Gas Concentration	37
2.6.2 Overestimation of Initial Pressure	37
2.6.3 Underestimation of Initial Temperature	37
2.6.4 Bounding the Effects of Tube Bend Reflections	37
2.6.5 Critical Velocity for Bounding DLF Estimate.....	38
2.6.6 Elastic Range of Material	38
2.6.7 Deleted	38

3.0 CONSIDERATION FOR OTHER PCCS COMPONENTS39

3.1 DELETED39

3.2 APPLICABLE SUBSECTIONS OF ASME CODE SECTION III39

3.3 PCCS COMPONENT DETONATION LOADS40

4.0 ICS METHODOLOGY41

4.1 ICS OPERATION (HIGH PRESSURE).....41

 4.1.1 Analysis of ICS During Station Blackout (SBO) with Venting41

 4.1.2 Radiolytic Gas In Solution Prior to SCRAM.....42

4.2 ICS DURING LOCA (LOW PRESSURE)43

 4.2.1 ICS Vent, Steam, and Drain Lines During LOCA (Low Pressure).....45

4.3 APPLICABLE SUBSECTIONS OF ASME CODE SECTION III45

4.4 DEFLAGRATION TO DETONATION TRANSITION (DDT).....46

5.0 PCCS AND ICS INSPECTIONS AND QUALIFICATION47

5.1 FABRICATION INSPECTIONS47

 5.1.1 PCCS47

 5.1.2 ICS47

5.2 PRE-SERVICE / IN-SERVICE INSPECTIONS47

 5.2.1 PCCS47

 5.2.2 ICS48

5.3 TUBE BENDS48

 5.3.1 PCCS48

 5.3.2 ICS48

5.4 WELD AND WELD FILLER MATERIAL48

6.0 REFERENCES49

APPENDIX A - SUPERSEDED PCCS STRUCTURAL ANALYSIS51

A.1 DESCRIPTION OF MODEL51

A.2 LOAD DEFINITIONS.....52

A.3 LOAD COMBINATIONS52

A.4 FINITE ELEMENT MODEL INPUTS54

A.5 STRESS RESULTS AND MARGIN TO ALLOWABLE57

APPENDIX B - PCCS STRUCTURAL ANALYSIS WITH DETONATION LOADING .58

B.1 DESCRIPTION OF MODEL58

B.1.1 Tube Analysis Model.....58

B.1.2 Lower Header Analysis Model.....58

B.1.3 Global PCCS Condenser Analysis Model59

B.1.4 Lower Header Covers and Lower Header Cover Bolts61

B.2 LOAD DEFINITIONS.....63

B.3 LOAD COMBINATIONS.....63

B.4 FINITE ELEMENT MODEL INPUTS.....65

B.5 STRESS RESULTS AND MARGIN TO ALLOWABLE72

B.6 CONCLUSIONS ON SERVICE LEVEL C ALLOWABLE.....78

B.7 FATIGUE.....78

APPENDIX C - ANCHOR BOLT REACTIONS DUE TO DETONATION AND STRESSES FOR SELECTED PCCS COMPONENTS80

C.1 INTRODUCTION80

C.1.1 Detonation Wave Profile.....80

C.1.2 Load Definition and Modeling Assumptions.....80

C.1.3 Finite Element Model81

C.1.4 Finite Element Model Results.....82

C.1.5 Wave Reflections and Multiplication Factors83

C.1.6 Peak Loads and Calculated Stress Intensities83

C.1.7 References.....87

TABLES

Table 2-1: Tube Elongation Results31

Table 3-1: PCCS Components Applicable ASME Code III Subsection39

Table 3-2: Evaluation of Other Components of the PCCS40

Table 4-1: Thermodynamic Properties of Hydrogen-Oxygen-Steam Mixtures*44

Table 4-1: ICS Components Applicable ASME Code III Subsection.....46

Table A-1: PCCS Load Combinations.....53

Table A-2: Stress Summary of the PCCS Condenser and Supports.....57

Table B-1: Modified PCCS Load Combinations64

Table B-2a: Stress Summary of the PCCS Condenser and Supports72

Table B-2b: Stress Summary of the PCCS Condenser and Supports73

Table B-3a: PCCS Condenser Top Slab Penetration Anchor Bolt Dynamic Reactions75

Table B-3b: PCCS Condenser Top Slab Penetration Anchor Bolt Thermal Reactions75

Table B-4a: PCCS Condenser Support Base Plate Anchor Bolt Dynamic Reactions.....76

Table B-4b: PCCS Condenser Support Base Plate Anchor Bolt Thermal Reactions.....76

Table B-5: Lower Header Condensate Line under DET, Linearized Stress¹77

Table B-5: PCCS Condenser Fatigue Assessment79

Table C-1: Input Data for Detonation Wave Profile and Load.....88

Table C-2: Simulation Parameters89

Table C-3a: Mounting Loads¹90

Table C-3b: Tube End Loads.....90

Table C-4: Loads with 2.5 Multiplier ¹	91
Table C-5: Stresses Due to Detonation Wave in Lower Header ⁴	92
Table C-6: Stress Summary for Selected PCCS Components: Detonation Wave in Lower Header	93
Table C-7: PCCS Condenser Lower Condenser Mount Dynamic Reactions: Detonation Wave in Lower Header	94

ILLUSTRATIONS

FIGURE 1A: PCCS CONDENSER SIMPLIFIED SKETCH	12
FIGURE 1B: PCCS CONDENSER LOWER DRUM SECTION VIEW (NOT TO SCALE).....	12
FIGURE 1C: PCCS CONDENSER ASME JURISDICTIONAL BOUNDARIES	13
FIGURE 2: PORTIONS OF PCCS CONSIDERED FOR DETONATION	14
FIGURE 3: CONCEPTUAL DESIGN FOR IN-LINE CATALYST	21
FIGURE 4: TUBE DEFLECTION.....	30
FIGURE 5: NONCONDENSABLE GAS FRACTIONS IN ICS DURING SBO WITH VENTING (ORIFICE FLOW AREA OF 0.167 CM²).....	42
FIGURE 6: ESBWR POST-SCRAM RADIOLYTIC GAS PRODUCTION OF HYDROGEN AND OXYGEN.....	43
FIGURE A-1A: PCCS CONDENSER AND SUPPORTS.....	54
FIGURE A-1B: PCCS CONDENSER AND SUPPORTS DETAILS.....	55
FIGURE A-2: FEM OF PCCS CONDENSER AND SUPPORTS	56
FIGURE B-1A: TUBE FEM OF AND PRESSURE LOAD.....	65
FIGURE B-1B: LOWER HEADER FEM.....	66
FIGURE B-1C: PCCS CONDENSER FEM.....	67
FIGURE B-1D: LOWER HEADER FEM. NOZZLE, HEAD FITTING, SLEEVE AND FLANGE SECTIONS FOR LINEARIZED STRESS INTENSITIES (MPA).....	68
FIGURE B-2A: PCCS CONDENSER AND SUPPORTS DETAILS.....	69
FIGURE B-2B: PCCS CONDENSER AND SUPPORTS DETAILS.....	70
FIGURE B-2C: PCCS CONDENSER AND SUPPORTS DETAILS.....	71

FIGURE C-1: PCCS CONDENSER..... 95

FIGURE C-2: PRESSURE PROFILE OF DETONATION WAVE AT MIDPOINT OF PCCS LOWER HEADER 96

FIGURE C-3: FINITE ELEMENT MODEL OF PCCS SYSTEM..... 97

FIGURE C-4: FINITE ELEMENT MODEL OF PCCS SYSTEM..... 98

FIGURE C-5: FINITE ELEMENT MODEL OF PCCS SYSTEM..... 99

FIGURE C-6: PCCS CONDENSATE LINE DIMENSION AS MODELED..... 100

FIGURE C-7: LOWER HEADER DISPLACEMENT CONTOUR (PRESSURE WAVE FRONT ¼ THROUGH LOWER HEADER, DISPLACEMENT PLOTS ACTUAL SCALE)..... 101

FIGURE C-8: LOWER HEADER DISPLACEMENT CONTOUR (PRESSURE WAVE FRONT ½ THROUGH LOWER HEADER, DISPLACEMENT PLOTS ACTUAL SCALE)..... 102

FIGURE C-9: LOWER HEADER DISPLACEMENT CONTOUR (PRESSURE WAVE FRONT ¾ THROUGH LOWER HEADER, DISPLACEMENT PLOTS ACTUAL SCALE)..... 103

FIGURE C-10: CONTOURS OF DISPLACEMENT, START OF STEADY STATE PRESSURE IN LOWER HEADER, DISPLACEMENT PLOTSACTUAL SCALE 104

FIGURE C-11: LOWER HEADER DISPLACEMENT CONTOUR AT START OF STEADY STATE PRESSURE (DISPLACEMENT PLOTS ACTUAL SCALE)..... 105

FIGURE C-12: LOWER HEADER DISPLACEMENT CONTOUR AT PEAK LATERAL LOAD ON DRAIN LINE (DISPLACEMENT PLOTS ACTUAL SCALE)..... 106

FIGURE C-13: NET REACTION LOADS AT PCCS LOWER HEADER MOUNT POINTS... 107

FIGURE C-14: INDIVIDUAL HORIZONTAL REACTION LOADS (2 SADDLES AND CONDENSATE LINE)..... 108

FIGURE C-15: INDIVIDUAL MOMENT LOADS (2 SADDLES AND CONDENSATE LINE) 109

FIGURE C-16: FREQUENCY CONTENT IN CONDENSATE LINE, HORIZONTAL FORCE. SIGNALS LESS THAN 2000 HZ WILL BE CAPTURED WITH AT LEAST 5 TIME STEPS.. 110

1.0 SCOPE

The design of the Isolation Condenser System (ICS) and Passive Containment Cooling System (PCCS) as described in Revision 6 of the ESBWR Design Control Document (DCD) are being modified to improve their ability to mitigate the loads resulting from the buildup and possible detonation of radiolytically generated combustible gases. This report describes these changes and the conservative methodology by which the detonation loads are calculated as well as the design philosophy used to ensure the ICS and PCCS have been designed robustly to withstand the most bounding loads while not affecting their heat transfer capability.

2.0 PCCS METHODOLOGY

The PCCS components are first evaluated for accumulation of radiolytically generated hydrogen and oxygen and then the possible range of mixture concentrations is determined. A bounding detonation pressure for a pure stoichiometric mixture of hydrogen and oxygen is calculated using the highest peak pressures during a loss of coolant accident (LOCA). It is then applied statically using dynamic load factors (DLF) in a finite element model for the PCCS condenser using the approved ANSYS computer code. The calculated stresses for the detonation load are combined with those from seismic and LOCA thermal loads. The acceptance criterion for components subject to detonation is based on the ability of those components to retain their pressure integrity without significant plastic deformation following [[]] detonation cycles. Two postulated detonation scenarios are analyzed in the finite element model: a detonation in one tube and a detonation in the lower drum.

Inputs are provided for the finite element analysis that describes increased thicknesses for the PCCS tubes and lower drum that are expected to satisfy the acceptance criteria for elastic-plastic analysis. The impact of increased tube thickness on heat removal capacity is estimated and compensated for by adding additional tubes. This configuration is evaluated in Appendix B.

The specific routing and configuration of components downstream of the lower drum is not yet specified. Therefore, the thickness of downstream piping and components will be sized to accommodate the resulting detonation loads. The magnitude of the detonation load on the downstream components will also be minimized by the addition of a safety-related catalyst module at the entrance of the vent pipe in the condenser lower drum. The catalyst module will function to keep hydrogen concentrations in the PCCS vent below levels at which deflagration-to-detonation (DDT) events can occur.

2.1 COMBUSTIBLE GAS GENERATION / CONCENTRATION

The radiolytic generation of combustible gas is a common occurrence in typical power reactors, including ESBWR. The generation of hydrogen and oxygen gas occurs in a stoichiometric ratio at a rate proportional to the core decay heat. During a LOCA, these gases escape into the containment resulting in very dilute concentrations of combustible gas in the drywell (below concentrations that could result in ignition). The PCCS contains six condensers that are designed to receive this mixture of steam and noncondensable gas, condense the steam, and return the condensate back to the drywell. See simplified sketch, Figures 1a, 1b, and 1c, of the PCCS Condenser.

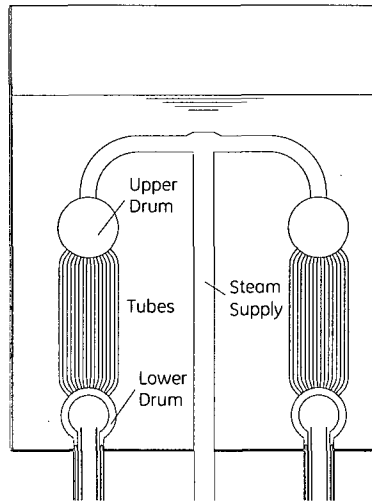


Figure 1a: PCCS Condenser Simplified Sketch

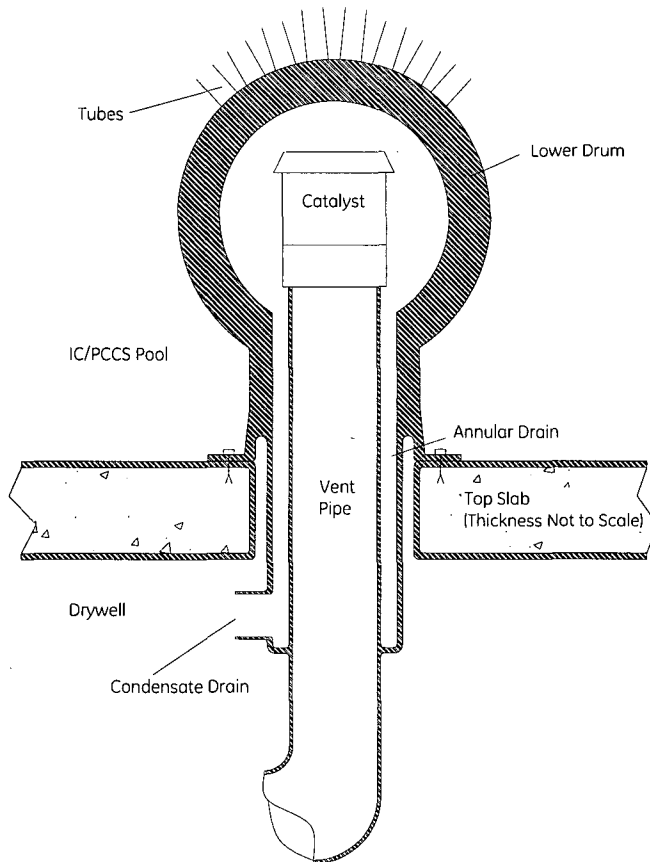
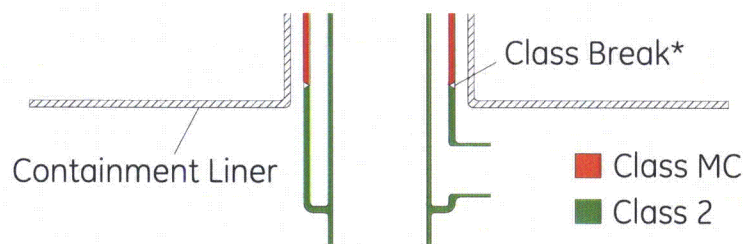


Figure 1b: PCCS Condenser Lower Drum Section View (Not to Scale)



*The specific location of the class break is at the first weld in the annular drain pipe. The transition occurs in this vertical run of pipe downstream of the interface with the pool liner. The pipe that comprises the vent is not part of the containment pressure boundary.

Figure 1c: PCCS Condenser ASME Jurisdictional Boundaries

Each PCCS condenser consists of two modules submerged in a pool of cooling water. Each module contains an upper and lower drum connected by an array of 2-inch diameter tubes. Gas from the drywell passes up a central supply line that feeds both upper drums. The steam component of the gas condenses as it moves downward through the tube array (transferring its heat to the pool water) and condensate collects in the lower drum and drains back to the drywell by gravity. The pool water level drops slowly over the course of the accident as water boils off.

The leftover noncondensable gas can exit the PCCS condenser through a vent line that connects the lower drum to the wetwell. As steam and noncondensables enter, the vent operates passively to bleed gas from the lower drum of the condenser when there is a sufficient pressure differential between the drywell and wetwell. In this way, something close to an equilibrium state is reached in which noncondensables persistently linger in the condenser while small amounts continue to come in with the steam and go out through the vent.

In the initial stage of a LOCA, the majority of the noncondensable gas in the drywell is nitrogen. This gas is eventually forced into the wetwell by the depressurization of the Reactor Pressure Vessel (RPV). Over time, the primary source of noncondensable gas in the drywell is the radiolytically generated hydrogen and oxygen. It has been shown in TRACG that noncondensable gas accumulates in the lower portions of the tubes and lower drum. When this gas transitions from mostly nitrogen to a stoichiometric mixture of hydrogen and oxygen, a combustible concentration may exist.

The relative concentration of steam to hydrogen and oxygen in the PCCS condenser is highly dependent on the conditions in the Isolation Condenser /Passive Containment Cooling System (IC/PCCS) pool subcompartment. Lower pool temperatures will bring down the temperature inside the condenser thereby lowering the steam fraction. The pool level can influence the variation in steam fraction over the height of the condenser tubes. TRACG analyses show that the steam fraction in the upper drum, and upper portion of the PCCS condenser tubes remains above 75%. The steam fraction in the lower portion of the tubes and the lower drum will remain above 30%.

In order to bound the amount of fuel and oxidizer inside the condenser, the atmosphere inside the PCCS is assumed to be 67% hydrogen and 33% oxygen (no steam).

Also, the initial PCCS pressure is assumed equivalent to the peak drywell pressure (407 kPa absolute) for the bounding containment LOCA even though the actual pressure inside the condenser will be significantly lower due to condensation. This approach is conservative because it results in a pure mixture (free from steam diluent) and assumes it is at an initial density greater than it could realistically achieve.

2.2 DETONATION LOADS

The process by which a detonation wave propagates through a medium and imparts stress on its surroundings is a complex subject that has been studied for a variety of applications. References 1 through 9, and 17 are reports that attempt to characterize this phenomenon. Data from these reports have been used to determine a bounding detonation load.

The entire PCCS is considered, but the focus of this report is on the condenser tubes and lower drum because of the complex geometry at the interface between the two and also because of the relatively thin walls of the tubes that make them more vulnerable to internal overpressure. The other portions of the PCCS (vent and drain piping) are considered separately in this report.

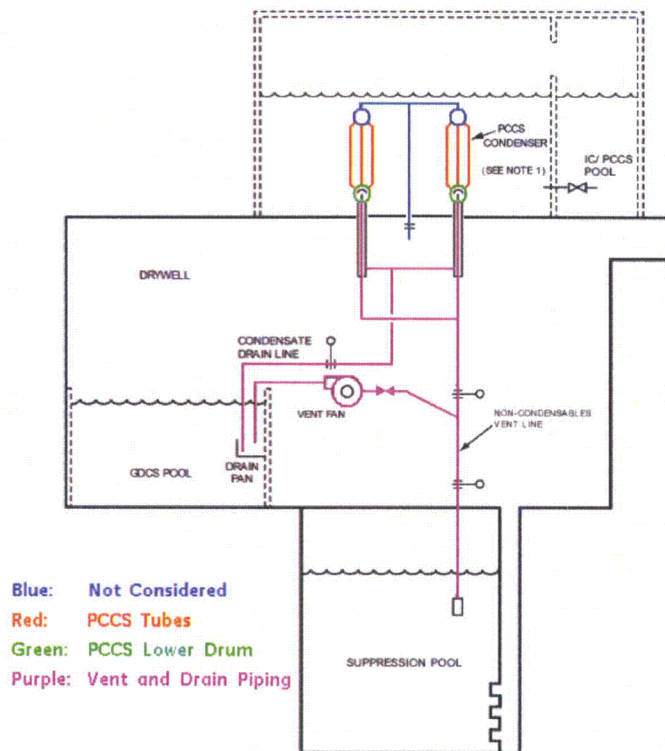


Figure 2: Portions of PCCS Considered for Detonation

The steam supply line and upper drums are not considered in this evaluation because they are constantly being flushed by steam coming from the drywell. The hydrogen and oxygen in this mixture is too dilute to support combustion.

The process used to evaluate the PCCS loads will first estimate the peak pressure resulting from detonation, and then apply this pressure in a finite element model as a static load multiplied by a dynamic load factor.

2.2.1 Peak Pressure Ratio

Many of the studies referenced in Section 6.0 describe the resultant pressure following the passage of a detonation wave, often called the Chapman-Jouguet pressure (or CJ pressure). It has been shown that a correlation can be made between the CJ pressure and the initial pressure prior to detonation. The correlation is dependent on the composition of the fuel-oxidizer mixture, the initial conditions (pressure and temperature), and the geometry of the system.

2.2.1.1 Gas Composition

Reference 3 describes a ratio between CJ pressure and initial pressure for a variety of fuel-oxidizer mixtures. For a stoichiometric mixture of hydrogen and oxygen at an initial temperature of 25°C, this ratio is given as 19:1 (See Table 1 of that report). This ratio is applicable for the PCCS, which also assumes a pure stoichiometric mixture. The assumption of a pure mixture is conservative for the purposes of maximizing the CJ pressure ratio. However, in certain circumstances the presence of steam will be considered as it has the potential to increase pressure loading (explained in Section 2.2.3).

2.2.1.2 Initial Conditions

References 2 and 7 show that lower initial temperatures result in higher peak pressure ratios. Realistic temperatures inside the PCCS at the time of detonation would be approximately 100°C. The assumption of 25°C is considerably lower than the expected temperatures inside the PCCS prior to a detonation and therefore more conservative. Likewise, the initial pressure is assumed to be 407 kPa absolute, which is equivalent to the peak drywell pressure during the most limiting LOCA. Even when the drywell is at this peak pressure, the actual pressure in the PCCS will be considerably lower due to its inherent design (submerged in a pool of cooling water). In this way, the initial conditions for the PCCS are conservatively bounded in the context of the 19:1 peak pressure ratio.

2.2.1.3 PCCS Geometry

Much of the literature cited in Section 6.0 discusses testing using simple straight-tube experiments. These simplified geometries are not necessarily representative of the PCCS condenser, which has a more complex shape with upper and lower drums connected by tubes bending at angles ranging from [[]]. The presence of bends, constrictions, and closed ends creates opportunities for reflections that can create localized peak pressures in excess of the CJ pressure. Reference 9 characterizes this peak pressure for a closed volume as a maximum of 2.5 times the CJ pressure.

The design of the PCCS condenser (in particular the tubes) is more benign in terms of this loading than the tested configuration in Reference 9. Although the condenser tubes do contain bends that are subject to reflection loads, these bends are not as severe as a closed vessel that reflects the full force of the detonation wave. The tube bends range from [[]] to a maximum of [[]], and all have a bend radius of [[]]. Although the presence of bends will introduce some loading due to reflection, the loading will not be to the degree of a closed terminal end. Therefore, the multiplier of 2.5 is a conservative selection for the PCCS to account for effects that could amplify the internal pressure beyond the CJ pressure.

Using the methodology described above, the peak pressure for the PCCS is determined as:
 407 kPa (initial pressure) • 19.0 • 2.5 = 19.3 MPa absolute

2.2.2 Dynamic Load Factor (DLF)

The dynamic load factor (DLF) is a multiplier that is factored into the peak static pressure to determine a maximum bounding load that accounts for dynamic effects resulting from a detonation.

2.2.2.1 DLF Dependence on Detonation Velocity

Reference 3 provides guidance on selecting an appropriate DLF. That study correlates the DLF (also called an amplification factor) to the velocity at which the detonation wave propagates. Low wave speeds are shown to have correspondingly low DLFs (approximately 1). As the wave reaches a “resonance” velocity, the DLF is observed to be as high as 4. At velocities above this resonance threshold, the DLF is shown to decrease and plateau around 2.

The resonance velocity is a characteristic of the tube in which the detonation occurs. A formula for calculating the characteristic resonance velocity or critical velocity (V_{c0}) for the PCCS tubes is given in Reference 3 as:

$$V_{c0} = \left[\frac{E^2 h^2}{3 \rho^2 R^2 (1 - \nu^2)} \right]^{1/4}$$

where

E = Young’s modulus

h = tube thickness

ρ = density

R = mean radius

ν = Poisson’s ratio

When these parameters are applied in accordance with the revised PCCS condenser tube design (see Section 2.3), the equation becomes:

[[

]]

2.2.2.2 Determination of a Conservative Detonation Velocity

Reference 1 describes detonation velocities for a pure stoichiometric mixture of hydrogen and oxygen. The velocities reported there (Figure 1 of that report) are in excess of 2800 m/s, which is considerably higher than the V_{c0} value of [[]]. However, a pure mixture is not necessarily representative of the mixture in the PCCS (although it has conservatively been assumed so in Section 2.2.1.1), and there is also data to suggest that the presence of steam or other diluents could slow the propagation of the detonation wave. To justify using a DLF of 2, it is important to consider the effects of various diluents to ensure that the most limiting case does not reduce the detonation velocity to a value near V_{c0} .

Reference 17 is a thorough report dealing with the topic of combustion of radiolytic gases typical in BWRs. Chapter 5 of that report specifically examines flame accelerations and detonation properties for a range of gas mixtures. Table 5.1.8 of that report contains calculated detonation velocities based on the thermo-chemical properties of the mixture, and shows good agreement with experimental data. The data reported in this table indicates that the CJ velocities are much higher than V_{c0} , justifying the choice of a DLF of 2. It is noted that if extrapolated to 80% steam, CJ velocities could approach the value of V_{c0} , however, the corresponding CJ pressures under these conditions are much lower than the conservative value of 19, which is described in Section 2.2.1.1. At steam concentrations of 65%, the CJ velocity is 1,962 m/s (much higher than V_{c0}). The reported CJ ratio at this steam concentration is 9.3, which is already low enough to accommodate a DLF of 4 while still remaining bounded by a factor of 2 combined with a CJ ratio of 19.

The bounding detonation load (considering dynamic effects) for the condenser tubes is therefore:

$$407 \text{ kPa (initial pressure)} \cdot 19.0 \cdot 2.5 \cdot 2 = 38.7 \text{ MPa absolute}$$

Mitigation strategies for other PCCS condenser components are described in 2.2.4.

2.2.3 Deflagration to Detonation Transition (DDT)

In some cases, an additional factor known as delayed deflagration to detonation transition (or delayed DDT) can increase localized pressures to high values. The delayed DDT phenomenon can occur when the deflagration front undergoes a substantial acceleration period before transitioning to a detonation, or when the un-burnt mixture is compressed due to obstructions or closed ends in the structure. This compression at the onset of detonation has the potential to cause much higher localized pressures loads.

Delayed DDT is a relatively complicated research area and the phenomenon is dependent on many different variables. The detonation cell size is a parameter that is typically used to characterize the sensitivity of the mixture to detonation. Reference 21 is a very comprehensive report on the nature of DDT, and Chapter 3 of that report describes certain conditions that are necessary for DDT to occur, one of which is a minimum cell size. The cell sizes for hydrogen-oxygen mixtures can be small (on the order of 1 mm). Smaller cell sizes are indicative of relatively quick transitions, which are desirable because of the smaller amount of pre-compression.

Reference 4 is an evaluation of the structural response of a tube in conditions favorable to a DDT event. The results of this study characterize the peak loads as those that occur near the closed end of the detonation tube, which maximizes the compression of the un-burnt mixture. The PCCS condenser tubes do not have closed ends, but instead are vented to larger volumes (upper and lower drums). The report concludes that these loads can be accounted for by using a dynamic factor of 4, which is bounded by the assumption used in this report ($2 \cdot 2.5 \cdot P_{CJ}$). As described in the summary of Reference 4, the DDT loads are impulsive and very short in duration and therefore need not be considered as an additional dynamic load on top of the dynamic factors already being applied.

2.2.4 Other PCCS Components

2.2.4.1 Lower Drum

The lower drum of the PCCS condenser is also subject to the accumulation of hydrogen and oxygen (at similar concentrations as the lower portions of the tubes), however, the combustion of these gases is expected to occur by a different mechanism than that described above for the tubes. Whereas the interior of the tube is a relatively restricted volume with a small diameter and long length, the drum interior is a more spacious and open volume. The top of the lower drum is vented through the tubes, which have a cumulative flow area of [[]].

It is conservative to take the same approach for the lower drum as was used for the condenser tubes and to apply the same series of CJ detonation pressure multipliers that was assumed for the tubes in Section 2.2.2.3. The concept of delayed DDT becomes somewhat complicated in the lower drum, because its geometry is less similar to the experimental geometries (which were mostly simple tubes). Reference 21 is a comprehensive report on the subject of flame

acceleration and DDT. Appendix D of that report contains experimental data that characterize the detonation cell size for hydrogen-air mixtures over a range of initial temperatures, pressures, and steam dilutions. Figure D.1-3 of that report indicates that the cell size does not go above 1 cm for a hydrogen-air mixture with 30% steam dilution at initial pressures ranging from 0.1 MPa to 0.4 MPa. The report goes on to describe methods of interpolating for different mixture types, however, this table is sufficient to conclude that the cell sizes in the lower drum also will not exceed 1 cm. Mixtures of hydrogen and oxygen are more sensitive than hydrogen and air, and will therefore have smaller cell sizes than those reported in Ref. 21. Furthermore, the cell size decreases with increasing pressure – a trend that would also result in yet smaller cell sizes for the lower drum. Therefore, because of the small cell size, the dynamic effects of a detonation in the lower drum are considered to be bounded by the combination of factors used in the tubes due to the unlikelihood of a delayed DDT event occurring at a location where it could impart significant loads on the structure of the lower drum.

2.2.4.2 Vent Pipe and Catalyst Recombiner Module

2.2.4.2.1 Description

The PCCS vent line begins with a standpipe in the lower drum, and extends downward to the drywell (routed inside the condensate drain pipe through the top slab) where it separates into an independent line that penetrates the diaphragm floor and terminates at a submerged location in the wetwell. The vent line is designed to conduct noncondensable gases from the PCCS condenser to the wetwell, therefore high concentrations of hydrogen and oxygen would be expected under normal circumstances.

Because of the uncertainties associated with the routing of the PCCS vent line, it is difficult to justify a specific DLF, and even more difficult to make a conclusive statement about the potential for DDT. Therefore, a safety-related catalyst module has been added to the design and will be relied upon to minimize the concentration of noncondensable gas in the vent line.

The catalyst module is bolted to the entrance of the vent pipe in the lower drum so that any gas entering the vent must first pass through the catalyst. The catalyst is composed of an array of platinum or palladium coated plates, arranged in a parallel pattern. The catalyst plates are installed within a housing that is a single piece, thick walled cylinder, which is robust enough to withstand the effects of a detonation inside the lower drum. A cover is provided on the catalyst that prevents condensate from dripping on the plates and also protects the plates against the direct effects of a detonation. A conceptual sketch is shown in Figure 3.

An optimization study was performed on the size of the vent line portion leading to the suppression pool downstream of the branch to the vent fan. This line, which had been sized at 10 inches, has been shown to perform sufficiently with flow areas as low as 2 inches. Therefore, in order to provide optimal structural integrity, the vent pipe is reduced to a 3-inch line.

2.2.4.2.2 Catalytic Performance

This catalyst configuration as depicted in Figure 3, was based on the design attributes (plate dimensions, spacing, etc.) of a similar catalyst that underwent extensive performance testing.

The results of these tests (documented in Reference 18) show that for initial hydrogen concentrations of 4%, the catalyst will recombine virtually all of the hydrogen, provided the flow velocity remains below the tested value of 0.25 m/s. The flow velocity through the vent of the PCCS condenser has been shown to peak at [[]] (nominally much lower). The surface area of the catalyst is based upon the capability for it to recombine twice the mass of hydrogen that is introduced to each PCCS condenser vent, which is conservatively computed to peak at [[]] (nominally much lower). Therefore, it is assumed that the fraction of hydrogen and oxygen downstream of the catalyst is insignificant. Once downstream of the catalyst, it is unlikely that hydrogen concentrations will increase to flammable levels due to the lack of condensation in the downstream portions of the vent line. Additionally, the gas that does enter the line will eventually be pushed into the wetwell due to the slow but steady venting process. Therefore, it is assumed that the safety-related catalyst prevents hydrogen and oxygen in the vent line from reaching flammability limits.

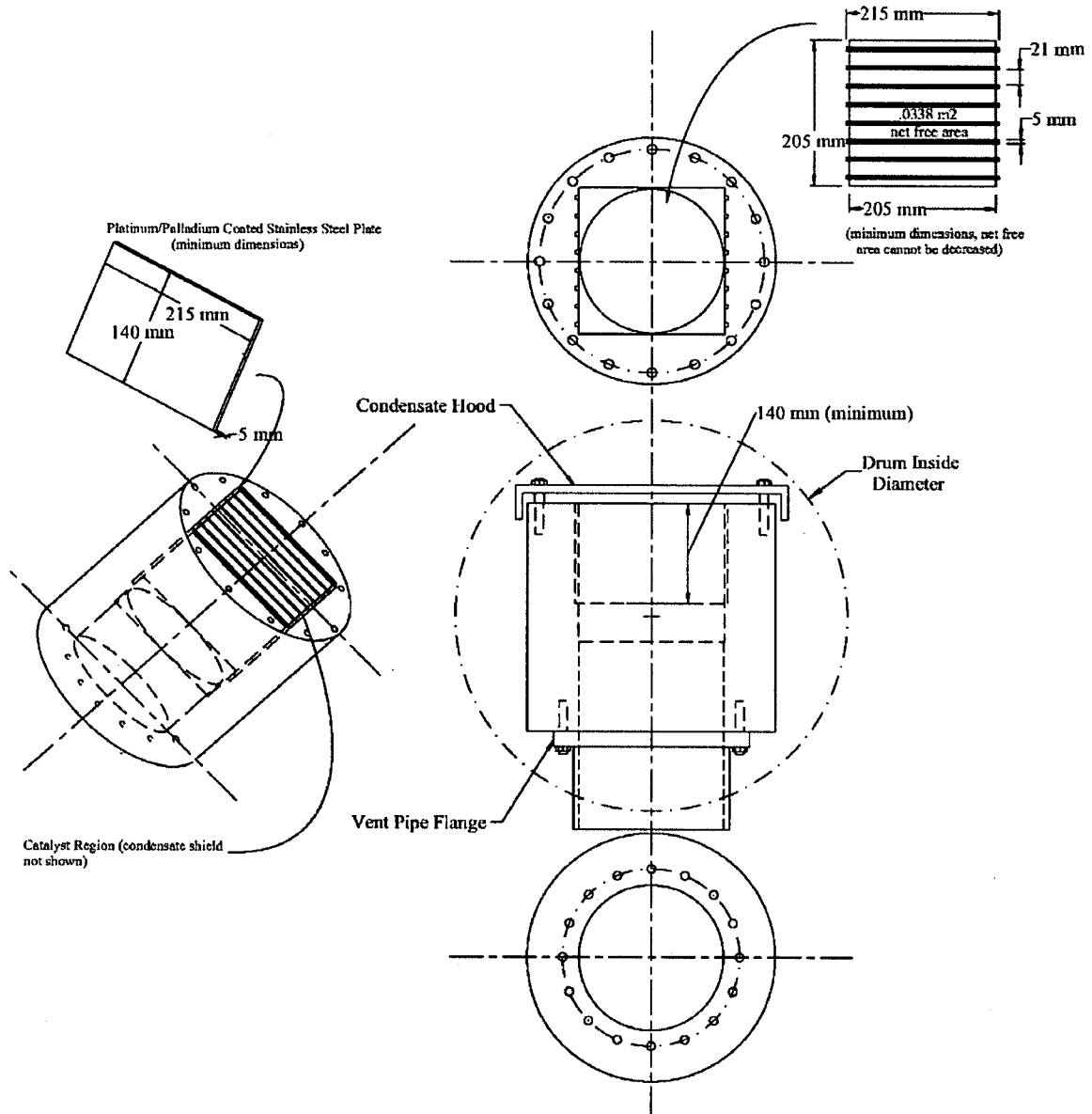


Figure 3: Conceptual Design for In-Line Catalyst

2.2.4.2.3 Effects of Poisons and Inhibitors - Design Basis Accident Conditions

During all design basis accidents postulated for ESBWR, the potential for the generation of significant levels of catalyst poisons or inhibitors is limited by prohibiting materials in containment that could be the source of such poisons or inhibitors during a DBA. Also, poisons or inhibitors that are generated by core melt do not occur during a DBA since the fuel is always covered by water. The discussion of these types of poisons and inhibitors is only applicable during severe accidents.

Liquid water has generally been thought to be an inhibitor; although testing has been performed which would indicate that it is not (See Reference 19, which is introduced in the next section). Even so, a condensate hood is provided which will have design features to mitigate liquid carryover into the vicinity of the catalyst plates.

2.2.4.2.4 Effects of Poisons and Inhibitors - Severe Accident Conditions

The Electric Power Research Institute (EPRI) conducted an extensive study on the subject of passive autocatalytic recombiners (PARs) and documented the results in a report (Reference 19). This EPRI report was submitted to the U.S. Nuclear Regulatory Commission by correspondence dated April 8, 1993. The PARs that EPRI studied utilized platinum/palladium metallic substrates that were configured very similarly to that of the PCCS vent catalyst module and the conclusions of the report are therefore considered relevant to the ESBWR application. The similarity lies in the vertically arranged catalyst racks or plates separated so as to provide flow channels for the bulk of the gasses.

The testing and analysis conducted by EPRI considered poisons and inhibitors such as steam, water, smoke, soot, iodine vapor and carbon monoxide. EPRI noted that there were some noticeable short-term effects of certain poisons and inhibitors, however, these quickly diminished as the catalyst reached operating temperature and the overall performance was not significantly affected. From their testing and analysis, EPRI made the following statements in support of the catalysts:

- “Performance of the catalyst is virtually unaffected by all of the known poisons that were selected for experimental investigation. A presoaked catalyst device functioned normally while being sprayed with water during a test.”
- “Catalyst is self-cleansing (from heat of recombination) with respect to wetness or other types of potential operational contaminants and poisons during accidents.”
- “Catalyst material is not consumed as it functions and is not subject to long-term aging degradation.”

In addition to the extensive testing and analysis that was performed, EPRI conducted a computational analysis that is also documented in the report (Appendix E). This computational analysis demonstrated the negligible impact that aerosols would have on plate-type catalyst during severe accidents involving an in-vessel core melt progressing to lower head penetration and entry to the flooded below-vessel areas of containment (lower drywell and BIMAC). The

computational analysis made very conservative assumptions pertaining to aerosol amounts, particle size, and particle density, to name a few. The analysis based many of its assumptions and input on the ALWR source term work that was documented in Reference 23. The vent catalyst module is designed to accommodate flow channels of equal or larger dimensions as compared to the EPRI prototypical design. These flow channels ensure that the majority of all postulated aerosols are continually swept into the wetwell, with no significant accumulation in the vicinity of the catalyst module.

The EPRI computational analysis results (Reference 19, Appendix E) are adjusted based on the ESBWR specific parameters, namely containment free air volume, accident leak rate, larger core size (as compared to AP600), and maximum PCCS venting velocity. The EPRI result, scaled for ESBWR, indicates that less than 1% of the catalyst plate surface area will be blocked by aerosol deposition during a severe accident. Since the installed catalyst plate surface area is 2 times that which is required, this degree of blockage will have no detrimental affect on recombination and by extension, the venting capacity of the PCCS condenser is also not compromised. It should be noted that no credit is taken for the aerosol stripping that occurs inside the PCCS tubes upstream of the catalyst as steam is condensed (DCD, Tier 2, section 15.4.4.5.2.2)

The significant production of aerosols due to core-concrete-interaction is not possible due to the operation of the GDCS deluge subsystem and the BiMAC (see Reference 25 and 26).

2.2.4.2.5 Environmental Qualification

The catalyst, which has a 60-year design life, will be qualified to operate during the harsh post-accident environment and under the most extreme operating conditions of recombination. The normal operating environment of the catalyst consists of an inerted nitrogen atmosphere with temperatures moderated by the PCCS pools. The catalyst is contained within a cylindrical module located in the lower drum of the PCCS condenser drum above the drywell top slab and is therefore well shielded from the effects of radiation.

2.2.4.2.6 Equipment Qualification

The catalyst module will be qualified to meet both its recombination and structural performance requirements described in Section 2.2.4.2.2 through type-testing by the manufacturer.

2.2.4.2.7 Surveillance Testing and Periodic Inspection

The catalyst module is accessible through either of the bolted covers of the lower drum and the catalyst plates can be readily removed from the module itself. These design features provide for surveillance testing and periodic inspections.

Surveillance testing will be performed on a representative number of catalyst plates of an individual PCCS condenser each refueling outage on a rotating basis and will consist of a laboratory type bench test using an appropriate acceptance criteria which is based upon the performance requirements specified in section 2.2.4.2.2. Visual inspections of the balance of the plates and the entire module assembly may be conducted in parallel with the surveillance test.

2.2.4.2.8 Structural Loading

Detonation loading of the heavy-walled catalyst module consists of both transverse and axial forces imposed by the detonation shock wave, and will be computed during detailed design using a similar analysis performed in Appendix C assuming a pure stoichiometric mixture of hydrogen and oxygen. Detonations do not originate in or propagate into the area of the catalyst plates due to the lack of a combustible mixture. The condensate hood protects the catalyst plates from the direct effects of the shock wave such that the vertically mounted plates experience only the axial on-rush of the venting combustion gases. The plates are designed in such a way that they may not be dislodged during a detonation event.

2.2.4.3 Vent Fan Ball Valve

A ball valve is added to the vent fan branch line upstream of the fan as close as possible to the branch from the main vent line to the suppression pool. The ball valve is designed to protect the vent fan from post-detonation pressure described in 2.2.6, and as such shall be designed robustly to remain operational after withstanding a post-detonation pressure.

The classification of the valve is consistent with the RTNSS function of the vent fans. The valve is nitrogen-operated, normally closed, fail as-is, and provided with an accumulator. It is provided with nonsafety-related power (same power source as the vent fan). While the operation of the ball valve is not safety-related, it is classified as a safety-related component for the purpose of pressure integrity. Because the normally closed ball valve is a safety-related barrier that prevents water redistribution from the GDCS pool to the suppression pool, the safety-related check valve that had been included downstream of the vent fans is no longer required and has been removed from the design. The concern of water transfer from the GDCS pool to the suppression pool only exists in the early stages of an accident when there are large pressure transients in the drywell. After this initial period, the differential pressure between the drywell and wetwell is not large enough to push GDCS pool water back through the vent fan piping, therefore, there are no adverse consequences to the ball valve failing in the open position after the fans have been activated.

2.2.4.4 Drain Pipe

The drain from the PCCS condenser consists of an annular region surrounding the vent pipe. Once the combined vent/drain pipe reaches the drywell, they separate and a series of drain pipes conduct the condensate directly to the submerged discharge location in the GDCS pool. It is not clear to what extent combustible gases can accumulate in the drain lines considering there is a continuous flow of condensate and higher temperatures (resulting in higher steam fractions). Therefore, the drain lines shall be conservatively reinforced as described below to accommodate the same detonation load as the tubes and lower drum. All portions of the drain line that are Class MC have been sized and analyzed in Appendix B. See detail H in Figure B-2b of Appendix B. Drain line pipe that is Class 2 is sized in this section using design by formula as allowed by the ASME Code. To provide flexibility for final routing and supporting of pipes and components, sizing that has been performed by formula can be changed during detailed design to use design by analysis, as permitted by the ASME Code. This analysis will require the use of the

detonation pressure load as defined in this section along with the service level load combinations as defined in Appendix B and acceptance criteria as provided by the ASME Code.

The ASME Code provides guidance for determining an appropriate thickness for cylindrical components. The following correlation used from NC-3641.1

$$t = \frac{P \cdot D_o}{2(S + P \cdot y)}$$

where

t = thickness (mm)

D_o = outer diameter (mm)

P = internal pressure = 38,700 kPa

S = allowable stress = 133,207 kPa for SA-336 F316 at 171°C PCCS design temperature (DCD Tier 2, Table 6.2-10)

In order to maintain a consistent inner diameter ([[]]) while still meeting the allowable stress limit, this correlation was iterated with increasing outer diameters until an appropriate thickness was found. For this Class 2 evaluation, the inner radius and stress limits are satisfied with an outer diameter of ([[]]) and a thickness of ([[]]).

The thickness of ([[]]) shall be used for the annular drain line.

The piping downstream of the annular drain is initially 3" Sch XXS. These 3" lines from each lower drum combine into a single 4" Sch XXS pipe that serves the full condenser. The correlation used above for the annular drain is used as shown below to demonstrate these thicknesses are adequate:

[[

]]

2.2.5 Vent Line External Pressure

Since a detonation is postulated in the annular region of the drain pipe, the vent line is sized to withstand an external pressure of 38.7 MPa minus the initial pressure inside the vent line of 0.407 MPa.

The ASME Code provides guidance for determining an appropriate thickness for cylindrical components. The vent line is an NC component; therefore article NC-3133 of Section III of the ASME Code describes the requirements for designing a structure of cylindrical shells or tubes to withstand an external pressure. To provide flexibility for final routing and supporting of pipes

and components, sizing that has been performed by formula can be changed during detailed design to use design by analysis, as permitted by the ASME Code. This analysis will require the use of the detonation pressure load as defined in this section along with the service level load combinations as defined in Appendix B and acceptance criteria as provided by the ASME Code.

Because the ratio of outer diameter to shell thickness is less than 10 for the proposed vent line, the appropriate formula is given by NC-3133.3(b). That paragraph provides instructions to determine appropriate values for A and B using charts in Part B, Subpart 3 of the ASME Code. The values of A and B are dependent on the geometry of the cylindrical shells and are used to determine an allowable differential pressure (Pa), which is defined as the smaller of the two pressures given by following equations:

$$P_{a1} = \left(\frac{2.167}{\left(\frac{D_o}{T} \right)} - 0.0833 \right) \cdot B$$

and

$$P_{a2} = \frac{2 \cdot S}{D_o/T} \left(1 - \frac{1}{\left(\frac{D_o}{T} \right)} \right)$$

where

Pa = allowable external pressure, kPa gauge

T = thickness (mm)

Do = outside diameter = [[]] mm

B = factor determined from the applicable chart in Section II, Part D, Subpart 3 for the material used in the shell at the design temperature, (kPa); 171 °C is used which is the PCCS design temperature (DCD Tier 2, Table 6.2-10) and by comparison at peak drywell pressure during a LOCA, the temperature is about 149°C.

S = the lesser of twice the allowable stress at design metal temperature from Tables 1A, 1B, and, Section II, Part D, Subpart 1 or 0.9 times the tabulated yield strength at design metal temperature from Tables Y-1, Section II, Part D, Subpart 2, (kPa); vent line material is SA-336 Grade F316 and the lesser of the two is 0.9 times the yield strength giving an allowable of 140,239 kPa.

The previous two equations were iterated until the lesser of the two was just of above the external pressure of 38293 kPa (38700 kPa – 407 kPa). The calculated thickness for the vent line is [[]] mm with the following final inputs used in the above equations.

$$T = [[]] \text{ mm}$$

$$D_o = [[]] \text{ mm}$$

$$L = [[]] \text{ mm}$$

$$A = 0.06$$

$$B = 99974 \text{ kPa (14500 psi)}$$

$$S = 140,239 \text{ kPa}$$

The final allowable pressures with above inputs are Pa1 = 38631 kPa and Pa2 = 43182 kPa.

2.2.6 Post-Detonation Pressure Relief

Following a postulated detonation in the lower drum, the resulting pressurized gas mixture will relieve downward through the vent line, and also upward through the tubes (reverse flow). These relief pathways may briefly be subject to higher pressures as the lower drum equalizes pressure with its surroundings. The pressures seen by the relief pathway will not include the dynamic factors associated with reflected shock waves (factor of 2.5), however a DLF of 2 will still be applied to bound other dynamic effects. The resulting lower drum pressure is 0.407 MPa • 19.0 • 2 = 15.5 MPa. As this gas expands through the relief volume, its pressure is assumed to drop according to the pressure-volume relationship of ideal gases:

$$P_2 = P_1 \left(\frac{V_1}{V_2} \right)$$

The portion of the vent that lies within the annular drain is credited as an expansion volume rather than evaluated for internal pressure because the relief pressure in this part of the vent is balanced by the same relief pressure in the drain (and the drain is reinforced to withstand a full CJ detonation as described in 2.2.4.4). The vent becomes a pressure-retaining boundary when it emerges from the drain line in the upper drywell, and it is downstream of this point that the pressure relief can impose significant stresses on the vent. Likewise, the condenser tubes are considered an expansion volume because they have been designed to withstand a full CJ detonation.

The volumes applicable for calculating pressure reduction have been calculated as follows:

[[

]]

From Section 2.2.5, the PCCS vent is a pipe with a [[]] mm outer diameter and wall thickness of [[]] mm made of SA-336 Grade F316 stainless steel. ASME Section III, Paragraph NC-3324.3 provides a correlation to the minimum wall thickness for a given pressure. The S value for SA-336 Grade F316 at 171°C is 133,207 kPa . The PCCS design temperature is 171°C (DCD Tier 2, Table 6.2-10). At peak drywell pressure during a LOCA, the temperature is about 149°C). Using this information, a conservative allowable pressure for this pipe can be determined as follows:

[[]]

The vent pipe, therefore, is more than capable of relieving the CJ pressure of the lower drum. And, it can withstand the full pressure load of 38.7 MPa as defined for the tubes and the lower drum.

2.2.7 Thermal Effects

In addition to the pressure loads described above, there are thermal stresses that can arise as a result of combustion. Reference 3 contains a discussion of the nature of these thermal stresses, and indicates that while the hoop stress due post-detonation heating do exist in tubes following a detonation, they are much lower than the mechanical loads due to detonation pressure, and also are slow to evolve when compared to the brief pressure pulse. As a result, the thermal effects of a detonation are considered to be bounded by the ability of the condenser to withstand the detonation pressures.

2.2.8 Single Tube Elongation Due to Post-Detonation Heating

A bounding calculation, which assumes all the heat generation due to complete combustion of a pure mixture of hydrogen and oxygen is deposited in the tube, shows tube stresses due to heating from the expanded gases of post detonation are bounded by the stresses reported in the LTR. Table 2-1 presents the results for bending stress and compressive stress due to this heating.

The following describes the methodology and assumptions used.

Methodology

The heat capacity Equation 1 is used to derive the temperature change due to heat addition from a detonation consistent with assumption 1. The temperature change used to find the total elongation or deflection of the tube. The tube is assumed to deflect axially (no bowing) and impart the full deflection to the tube bends at each end (i.e. each tube bend deflects by one half

the calculated axial direction). The deflection at the tube bend is used to determine the maximum bending stress at the tube-to-drum connection.

$$\Delta T = \frac{Q_{\text{combustion}}}{mC_p} \quad (1)$$

Where:

$Q_{\text{combustion}}$ = Total heat (J) generated by the complete combustion of the stoichiometric content of hydrogen with oxygen that can be contained in one condenser tube under worse case temperature and pressure accident conditions.

m = mass of a short condenser tube (kg) per assumption #4.

C_p = Specific heat capacity for condenser tube material, (J/(kg·°K))

Assumptions

1. The total heat of complete combustion for the maximum amount of hydrogen that can be contained in one condenser tube at worse case accident conditions, is assumed to be input to the tube uniformly and instantaneously.
2. The specific heat capacity for the condenser tube material, XM-19, is assumed to be the same as that for type 304 stainless steel.
3. Hydrogen and oxygen are assumed to be present in the condenser tube in their stoichiometric ratio of two hydrogen atoms to every one oxygen atom such that the number of hydrogen moles is 2/3 of the total number of gas moles. The conservative assumption is also made that no steam or water vapor exists inside the tube at the time of detonation. This maximizes the heat generated during a detonation and transferred to the tube. The number of moles of hydrogen is calculated for worse case accident temperature and pressure conditions, saturated state.
4. The tube mass that will yield the greatest ΔT is for shortest possible tube length. This length is taken as the distance between the outer diameters of the upper and lower drums.
5. The tube length that will yield the greatest $Q_{\text{combustion}}$ is the longest possible tube, since it will contain the greatest amount of hydrogen and oxygen. This length is conservatively taken as the upper and lower drum centerline-to-centerline dimension. This tube length is also used in calculating the maximum tube elongation due to tube heatup.
6. Since the total axial elongation of the tube is small as compared to the total tube length, the theoretical highest stresses are induced at the tube-to-drum connection point if it is assumed that “buckling” of the tube does not occur and the full effects of elongation are imparted at the tube bends. It is assumed that one-half of the total axial elongation translates perpendicular to the tube “stub” ends. The tube stub end is modeled as a cantilevered beam. Figure 4 below illustrates these assumptions.
7. The steady-state metal temperatures for material properties is assumed to be 100°C (212°F) since the PCCS/ICS pools are boiling at atmospheric pressure conditions.

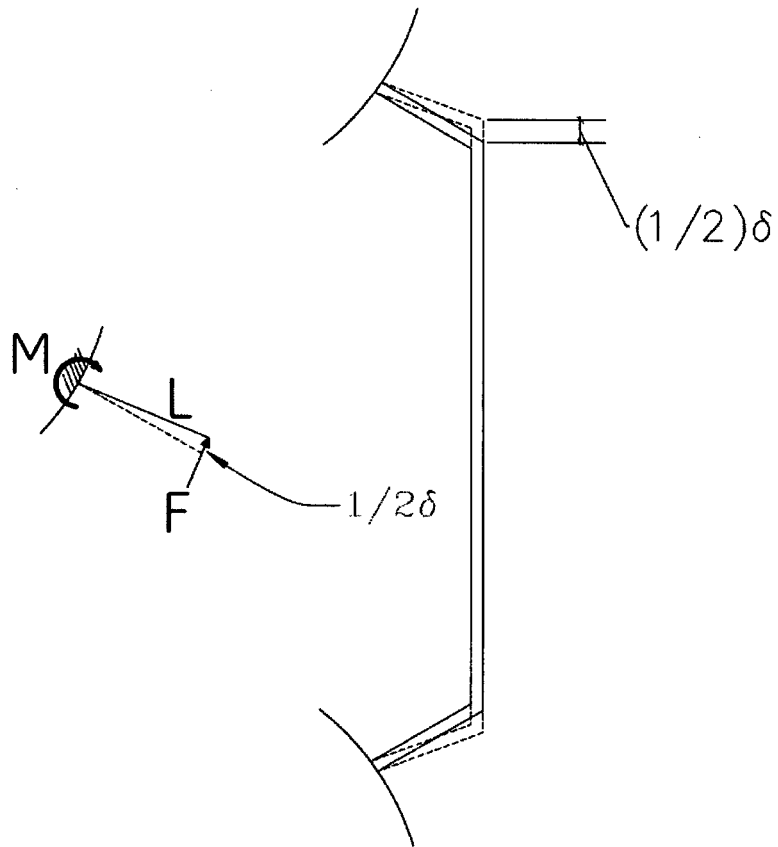


Figure 4: Tube Deflection

Table 2-1: Tube Elongation Results

Parameter	Value	Units	Comments
Min. Tube Length	[[]]	m	Shortest possible tube length
Max. Tube Length	[[]]	m	Longest possible tube length
$Q_{\text{combustion}}$	[[]]	kJ	Heat of combustion from maximum amount of hydrogen and oxygen calculated from longest possible tube.
m	[[]]	kg	Mass of shortest possible tube.
ΔT	[[]]	°C	
δ	[[]]	m	Tube elongation calculated from longest possible tube.
σ_b	94.8	MPa	Bending stress due to deflection (δ) of a simple cantilevered beam (deflection is halved per assumption #6).
σ_c	47.5	MPa	Compressive stress of shortest possible tube length, assumed to be straight, that is restrained at both ends to prevent elongation of δ . All tubes have a bend at the top and bottom before the tube-to-header connection with a smallest angle of [[]] and largest of angle of [[]].

2.3 INITIAL SIZING AND STRESS CALCULATION

The design of the PCCS condenser as described in DCD Revision 6 is not considered robust enough to withstand the very conservative detonation loads postulated in the sections above. This section describes the methodology by which the design has been modified to withstand a detonation.

A seismic and hydrodynamic analysis was performed for the original configuration of the PCCS condenser (See Appendix A) and was described in Revision 6 of the DCD. This analysis has been redone to include detonation loads and the configuration changes described below (analysis is described in Appendix B):

- PCCS condenser tube material changed to SA312 TP XM-19.
- PCCS condenser tube thickness changed to [[]].
- Number of tubes for each module increased from 280 to [[]] (there are two modules in each PCCS condenser).

- PCCS drum material changed to SA182 FXM-19 (both upper and lower drums).
- Thickness of lower drum increased to [[]] (upper drum thickness remains[[]]).
- Catalyst module added to the entrance of the vent in the lower drum of the condenser.
- Ball valve is added to the vent fan branch line upstream of the fan. Check valve has been removed from the design.
- Vent line between the branch for the vent fans and the suppression pool is reduced to a nominal size of 3”.
- Lower drum covers increased to a thickness of [[]].
- Increased sizes for the square tubes of the supporting structure. See Appendix B, Figure B-2a, Note 8 for exact sizes.
- Condensate drain line nozzle and flange. See Appendix B, Figure B-2b for dimensions.

Table of materials for the PCCS as shown in Figure A-1b has been reproduced with updated material changes in Figure B-2a of Appendix B.

2.3.1 Design Criteria

The PCCS condenser is designed to ASME Section III, Subsection NE as a Class MC component. As such it must be designed to accommodate the loads within the acceptance criteria stated in that part of the Code. In the structural evaluation of the PCCS, the detonation will be applied as a Service Level C load. Appendix B contains the details of this evaluation and the results.

2.3.2 Deleted

2.4 EFFECT ON HEAT TRANSFER

The increase in tube thickness and change in material will increase conduction resistance through the tube wall, which will have a negative effect on the overall heat transfer coefficient of the condenser. To compensate for this effect, TRACG evaluations have determined that it is necessary to increase the number of tubes from 280 to [[]] per module in order to keep the containment pressure response bounded by the values described in Revision 7 of the DCD.

2.4.1 PCCS Unit Heat Removal Capability Type Test

To provide confirmation that the revised PCCS design provides adequate heat transfer under DBA conditions with radiolytic hydrogen and oxygen present, a PCCS Unit Heat Removal Capability Type Test will be conducted, using helium and air to simulate hydrogen and oxygen.

The PCC heat removal type test will utilize a production PCCS unit, or a unit of the same design as a production unit, with respect to number of tubes, tube wall thickness, OD, ID, length, header diameter and length, to provide a definitive evaluation of the performance of the condenser

component under conditions that are representative of a LOCA. Satisfactory agreement between the test data and the heat removal calculated in the DBA LOCA analysis provides a high degree of confidence that the performance of the condensers in a post-LOCA environment will be adequate. This description of PCCS heat removal draws on selected parts of the PANTHERS test procedure and facility, relevant to testing the PCCS long term LOCA decay heat removal function.

The test facility will include a PCC unit, steam supply, air supply, helium supply and vent and condensate volumes sufficient to establish boundary conditions and flow-rates corresponding to LOCA conditions. The PCCS will be installed in a water pool having the appropriate volume for one ESBWR PCC assembly.

The instrumentation will be sufficient to ascertain heat exchanger thermal-hydraulic performance by performing mass and energy balances on the facility. The PCCS thermal power (heat rejection rate, W) is calculated by means of the following heat balance:

$$W = F_{\text{steam}} * h_{\text{steam}} + F_{\text{air}} * h_{\text{air}} + F_{\text{liq}} * h_{\text{liq}} - F_{\text{cond}} * h_{\text{cond}} - F_{\text{vent}} * (h_{\text{air_vent}} * X_{\text{vent}} + h_{\text{steam_vent}} * (1 - X_{\text{vent}})) - W_{\text{external}}$$

Where:

W= PCCS heat rejection rate
 F = flowrate
 h = specific enthalpy
 X = mass fraction (air in vent flow)

subscripts:

steam = steam

air=air

liq = liquid (de-superheating water)

cond = condensate

vent = vent discharge

external = heat losses external to the PCCS pool, e.g. through insulation

The test facility will be insulated to minimize heat losses from inlet, vent and drain lines. External heat loss from the PCCS and test system will be determined, and subtracted from the heat rejection rate if they are significant. The energy from the helium flow is not separately added, which is a small conservatism in determining the energy balance.

The overall heat rejection rate from the PCCS heat exchanger will be compared to the DBA LOCA analysis value.

Instrument List

Instrumentation will be provided to measure the following parameters to determine the PCCS heat rejection rate:

Steam flowrate
Air flowrate
Helium flowrate
Condensate flowrate
Vent flowrate

Steam pressure
Air pressure
Helium pressure
Condensate pressure
Vent pressure

Steam temperature
Air temperature
Helium temperature
Condensate temperature
Vent fluid temperature

Note fluid enthalpies will be derived from the pressure and temperature measurements.

Because a production heat exchanger may be used, the test will be non-destructive, and invasive instrumentation will not be used. A limited amount of external instrumentation will be included, for example temperature elements or thermocouples attached to a limited number of tubes on the outside of the array, at several axial locations. These external instruments are not required to determine overall heat removal by the PCCS, but they will provide some information on the flow distribution and non-condensable distribution in the tubes.

The testing will be performed under an approved quality assurance program and using approved procedures or specifications that satisfy the requirements of Title 10CFR, Part 50, Appendix B. The test facility and setup will meet the requirements of NIST Handbook 150, and of ANSI/ISO/IEC 17025-2005, "General Requirements for the Competence of Testing and Calibration Laboratories."

The testing will be steady state. As necessary LOCA conditions corresponding to different times in the DBA will be established, to determine heat removal with the range of parameters that exist during a LOCA. The facility will be placed in a condition where steam, air/steam, and air/steam/He mixtures supplied to the PCC, and the condensed vapor and vented gases are collected. All inlet and outlet flows will be measured. The condensate may be returned to the steam supply, and the vented gas may be released to the atmosphere. Once steady-state conditions are established, data will be collected for a period of approximately 15 minutes.

The tests will simulate the post-LOCA condition with the PCC carrying the decay heat load. In this case, the drywell pressure is slightly greater than the PCC vent submergence pressure, but less than the LOCA vent submergence pressure. Thus, water is forced out of the PCC vent line, clearing a gas-venting path to the suppression pool.

Consistent with the PANTHERS prototype tests, the range of conditions will begin after the DPV opening has depressurized the reactor. This excludes that period of steam blowdown and initial DW purging, and subcooled injection where there are either high non-condensable flows, or low RPV steam rates. This is a small fraction of the 72 hr passive cooling mission of the PCCS, and the PCCS total heat rejection from containment is low in this period. A test will be conducted to simulate the post blowdown, DW purging, and initial steaming which occurs at 2.5 hours in the DBA analysis. This captures the PCCS operation as the vessel begins steaming after GDCS injection. A test at 76 hours will be included to simulate PCCS operation with the vent fan running. Tests will be conducted with boundary conditions simulating the DBA LOCA at 2.5, 6, 12, 24, 48, 72 and 76 hours.

Test Matrix

Pressure and temperature conditions for the inlet flows will be taken from the DW conditions at the PCCS inlet, in the bounding DBA LOCA analysis, (analysis results are in DCD Tier 2 Table 6.2-7h and Figures 6.2-14j1 through 6.2-14o3).

Time into DBA LOCA (hrs)	Steam Flow Rate	Non-Condensable Flowrate
2.5	DBA LOCA Steam flow rate	Air volumetric flow rate corresponding to DBA analysis
6	DBA LOCA Steam flow rate	He/Air volumetric flow rate based on bounding DBA radiolytic H ₂ /O ₂ volumetric flow
12	DBA LOCA Steam flow rate	He/Air volumetric flow rate based on bounding DBA radiolytic H ₂ /O ₂ volumetric flow
24	DBA LOCA Steam flow rate	He/Air volumetric flow rate based on bounding DBA radiolytic H ₂ /O ₂ volumetric flow
48	DBA LOCA Steam flow rate	He/Air volumetric flow rate based on bounding DBA radiolytic H ₂ /O ₂ volumetric flow
72	DBA LOCA Steam flow rate	He/Air volumetric flow rate based on bounding DBA radiolytic H ₂ /O ₂ volumetric flow
76	DBA LOCA Steam flow rate	Air volumetric flow rate corresponding to DBA analysis

The gases present in a LOCA are the nitrogen initially present in the DW, which is subject to residual venting through the PCCS, steam that is generated by decay heat in the core, and hydrogen and oxygen, which are generated by radiolysis in the core. To simplify the facility design; hydrogen is not used, in stead a gas of similar density, helium is used. Air is substituted for nitrogen and oxygen. The steam flow rate will be controlled to match the DBA LOCA value.

The 2.5 & 76 hr tests involve higher non-condensable fractions, in which Nitrogen is the dominant non-condensable. In these tests air will be provided at the volumetric flowrate in the LOCA analysis.

In the tests simulating the 6, 12, 24, 48 and 72 hr conditions, the individual mixture flowrate of the air & helium non-condensables will be set to values which provide the same volumetric flowrate and non-condensable mixture density as the LOCA non-condensable gases.

The water level on the shell side of the PCCS will be set to the corresponding LOCA water level, considering boil off from the PCCS pool, and actuation of the PCCS/expansion pool make up function.

The steady-state tests using steam/air/helium mixtures will be conducted as follows. The test loop and PCC condenser will be purged with steam to remove any residual air from the system and to heat the PCC pool to saturation. When the pool is boiling, the required steam flow rate will be established, followed by the non-condensable flow rate to the PCCS. The desired PCC inlet pressure is then established by adjusting the position of a vent flow control valve. When steady conditions had been established, data will be taken for a period of approximately 15 minutes.

The acceptance criteria for the PCCS heat exchanger type test is that the heat removal by the unit exceeds the DBA LOCA analysis value at each of the time points tested.

2.5 POSTULATED DETONATION SCENARIOS

The two detonation scenarios analyzed in Appendix B are for a detonation in one PCCS tube and in the PCCS lower drum. The evaluation considers the cumulative effect of [[]] detonation cycles. Detonations are not assumed to propagate into a component where a detonation has already occurred.

2.5.1 Detonation in Tubes

The detonation wave in a tube travels into the upper and the lower drums with it quenching in upper drum due to high steam fractions and with a possibility of reflecting back into the tube once it reaches the lower drum wall. This reflection is accounted for in the peak pressure ratio of 2.5 times 19.0 used in determining the detonation pressure for the PCCS condenser.

2.5.2 Detonation in Lower Drum

A postulated detonation in the lower drum will vent through the tubes. The potential for the reflected waves at the flanges to amplify the detonation pressure are accounted for by the 2.5 factor.

2.6 DISCUSSION OF UNCERTAINTY AND CONSERVATIVE ASSUMPTIONS

The methodology described in this report relies heavily upon theory from literature and experimental data from scientific reports. Because of the complexity and uncertainty associated with predicting detonation properties, this report has made conservative assumptions as appropriate. These assumptions are summarized below.

2.6.1 Overestimation of Radiolytic Gas Concentration

In Section 2.1, it is stated that the initial gas mixture inside the PCCS is a pure stoichiometric mixture of hydrogen and oxygen with no steam presence. This is not a realistic scenario, especially for the upper drum and upper portion of the tubes in which less condensation will have taken place. By assuming a pure stoichiometric mixture, this methodology maximizes the amount of combustible gas in the condenser.

2.6.2 Overestimation of Initial Pressure

As described in Section 2.2, the initial PCCS pressure prior to a detonation is assumed to be the drywell peak pressure following the most limiting LOCA. Because of the inherent design of the PCCS the pressure in the system will always be lower than the drywell pressure, and will not reach a value as high as 407 kPa. For the majority of the accident, the drywell pressure is actually much lower than this, and slowly increases to a peak value over the course of the first 3 days. This trend is illustrated in Table 6.2-14e11 of the ESBWR DCD. The overestimation of initial pressure is a conservative assumption to address uncertainties associated with the experimentally determined peak pressure ratio of 19.0.

2.6.3 Underestimation of Initial Temperature

As described in Section 2.2, the ratio of peak pressure to initial pressure is also dependent on the initial temperature. The references cited in the section have concluded that a lower initial temperature, which allows for a denser mixture of combustible gas, results in a higher peak pressure ratio.

The ratio of 19.0 used in this report was taken from experimental data in which a stoichiometric mixture of hydrogen and oxygen was detonated at an initial temperature of 25°C. The realistic temperature inside the PCCS remains steady in the range between 90°C - 100°C. The underestimation of initial temperature is a conservative assumption to address uncertainties associated with the experimentally determined peak pressure ratio of 19.0.

2.6.4 Bounding the Effects of Tube Bend Reflections

Section 2.2 discusses the bends associated with the PCCS tubes. The literature referenced in Section 6.0 provides experimental data to account for amplification due to the presence of bends or tees. Reference 9 states that the peak pressures resulting from reflected waves in closed vessels are "approximately 2.5 times higher than the CJ pressure". Because the tubes in the PCCS condenser are bent to angles no greater than $[[\quad]]$ with bend radii of $[[\quad]]$, they are considered less susceptible to reflections than the case in Reference 9, yet the full 2.5 factor

is applied for conservatism prior to the application of a dynamic load factor (which is determined in 2.2.2).

2.6.5 Critical Velocity for Bounding DLF Estimate

Following the guidance of Reference 3, the V_{c0} calculated for the PCCS condenser tubes was [[]], which is considerably less than the detonation velocity 2800 m/s for the assumed stoichiometric mixture of hydrogen and oxygen in the PCCS. Although the assumption of no steam is conservative for estimating peak pressure, is not necessarily conservative for the determination of DLF. Reference 17 is a thorough report dealing with the topic of combustion of radiolytic gases typical in BWRs. Chapter 5 of that report specifically examines flame accelerations and detonation properties for a range of gas mixtures. Table 5.1.8 of that report contains calculated detonation velocities based on the thermo-chemical properties of the mixture, and shows good agreement with experimental data. The data reported in this table indicates that the CJ velocities are much higher than V_{c0} , justifying the choice of a DLF of 2. It is noted that if extrapolated to 80% steam, CJ velocities could approach the value of V_{c0} , however, the corresponding CJ pressures under these conditions are much lower than the conservative value of 19, which is described in Section 2.2.1.1. At steam concentrations of 65%, the CJ velocity is 1,962 m/s (much higher than V_{c0}). The reported CJ ratio at this steam concentration is 9.3, which is already low enough to accommodate a DLF of 4 while still remaining bounded by a factor of 2 combined with a CJ ratio of 19.

2.6.6 Elastic Range of Material

The design requirements use acceptance criteria that are within the elastic range of the materials used. Although there may be local stresses that exceed the yield limit, the linearized stresses will be shown to remain essentially elastic when subjected to a detonation load (consistent with Service Level C acceptance criteria).

The reported Reference 15 response of a tube with 15 mm ID and 3 mm wall thickness subjected to hydrogen/oxygen detonations with initial pressures up to 20 bar remained within the elastic range. The tube material had comparable yield and ultimate strength to that of SA-312 TP XM-19. The PCCS condenser is analyzed at much lower initial pressure of about 4 bar.

2.6.7 Deleted

3.0 CONSIDERATION FOR OTHER PCCS COMPONENTS

Section 2.0 of this report discussed the methodology for calculating detonation loads for the various portions of the PCCS. This section classifies those components and describes what pressures they are designed to withstand.

3.1 DELETED

3.2 APPLICABLE SUBSECTIONS OF ASME CODE SECTION III

The applicable subsection of ASME Code Section III for each PCCS component is given in Table 3-1.

Table 3-1: PCCS Components Applicable ASME Code III Subsection

<u>Component</u>	<u>ASME Code Section III, Subsection</u>
Steam Supply Piping (drywell)	NE
Steam Supply Piping (pool)	NE
Upper Drum	NE
Tubes	NE
Lower Drum	NE
Vent Pipe (pool)	NC
Vent Pipe (drywell)	NC
Vent Fan Ball Valve (drywell)	NC
Vent Fan Pipe ¹ (drywell)	NC
Drain Pipe (pool)	NC/NE ²
Drain Pipe (drywell)	NC

¹Vent fans and vent fan piping are nonsafety-related components but are conservatively designed to the criteria in Subsection NC.

²The portion of the drain that interfaces with the lower drum is NE. There is a transition to NC as depicted in Figure 1c.

3.3 PCCS COMPONENT DETONATION LOADS

The following table is a breakdown of the diameters and thicknesses of components of the PCCS components, and a description of the detonation loads assumed, or a summary of the mitigation strategy.

Table 3-2: Evaluation of Other Components of the PCCS

[[

1.

]]

- 2. Deleted
- 3. Deleted
- 4. Deleted
- 5. Deleted

4.0 ICS METHODOLOGY

The Isolation Condenser System (ICS) contains four condensers that are of a tube-and-drum design similar to the PCCS condensers. During a LOCA, these condensers are also vulnerable to the buildup and detonation of combustible gases.

Several design changes have been implemented for the ICS to prevent the accumulation of detonable concentrations of hydrogen.

4.1 ICS OPERATION (HIGH PRESSURE)

During scenarios in which the ICS is credited with heat removal (plant transients, station blackout, etc), the condenser vent function will be modified to keep the unit continuously purged of noncondensable gas.

The ICS vent had previously been designed to open automatically only on high pressure (indicative of a buildup of noncondensable gas). By the time this high pressure is reached, the concentration of hydrogen is expected to have already reached combustible levels (this is shown to occur after approximately 10 hours of ICS operation). In order to prevent this buildup, a logic change is implemented in which the vent valves automatically open 6 hours after the ICS is initiated regardless of the system pressure. Once open, the vent will bleed steam and noncondensables from the condenser to the suppression pool, keeping the steam fraction at high levels throughout the event. The vent valves are designed to fail open on a loss of power to provide additional reliability for this function.

A flow restriction shall be included in the vent line such that the maximum flow area is 0.167 cm². This flow restriction is provided to minimize the amount of water inventory lost from the reactor as a result of the constant flow through the vent lines. The flow restriction had been evaluated and shown to provide sufficient flow to keep the condensers purged, and the RPV water level is shown to remain above Level 1 for 72 hours.

4.1.1 Analysis of ICS During Station Blackout (SBO) with Venting

The Station Blackout (SBO) event was analyzed using TRACG with venting of the ICS lower drum at 6 hours after the onset of the event. The ICS vent line, which is connected to the lower drum, is equipped with a flow-restricting orifice of flow area 0.167 cm². The SBO event was analyzed with a vent line flow area 0.167 cm², which is conservative with respect to build up of non-condensable gases, and a flow area of 0.667 cm², which is conservative with respect to RPV inventory. Results for both show that adequate venting is provided and remains below combustible levels of 20% for ICS components, and the RPV level is still maintained above Level 1. Figure 5 presents results for the 0.167 cm² flow area calculation. Figure 5 presents the fractional noncondensable (NC) partial pressure in multiple segments of the ICS drain line. The drain line fractional NC partial pressure envelopes the fractional NC partial pressure in the lower IC tubes and lower drum. Reactor water inventory levels are lower for the larger flow area and remain above Level 1 for 72 hours. The larger flow area results, with respect to RPV inventory, are reported in ESBWR Design Control Document, Tier 2, Section 15.5.5.3 and Table 15.5-10b.

[[

]]

Figure 5: Noncondensable Gas Fractions in ICS During SBO with Venting (Orifice Flow Area of 0.167 cm²)

Note: The values in Figure 5 are below 0.2 except for Node 3 which shows oscillations between 2 and 4 hours that exceed 0.2 by approximately 0.08. All other nodes are below values of 0.2. Nodes 1 through 20 represent the full length of the drain line in the TRACG model where node 1 is at the top of the drain line and 20 is at the bottom and where nodes 1 through 4 represent a vertical run of the line.

4.1.2 Radiolytic Gas In Solution Prior to SCRAM

Results presented for SBO in Section 4.1.1 assumed the contribution of hydrogen in solution prior to SCRAM is negligible. The amount of hydrogen in solution contributes 0.033% to the total amount produced during the six hour period before venting. Therefore the amount of hydrogen contributed from solution prior to SCRAM is negligible.

The amount of hydrogen in solution was derived using existing BWR plant data for hydrogen production. Typical BWR's produce a volumetric flow rate (combined hydrogen and oxygen) of 0.045 CFM/MW_t (with CFM rated at 130°F). This was conservatively scaled up by about 50% and the result, 0.067 CFM/MW_t, was then multiplied by ESBWR's thermal power of 4500 MW_t. The equivalent molar flow rate of hydrogen from the ESBWR volumetric flow rate along with the normal steam flow rate for ESBWR was used to arrive at a hydrogen concentration in steam.

Henry's Law was then used to arrive at the hydrogen concentration in solution. The concentration was then multiplied by the amount of water in the RPV, conservatively estimated at 823 m³. The estimate of water does not take credit for reactor internals displacing water. The amount of hydrogen produced during the six hour period is taken from ESBWR's radiolytic hydrogen and oxygen production post-SCRAM, Figure 6.

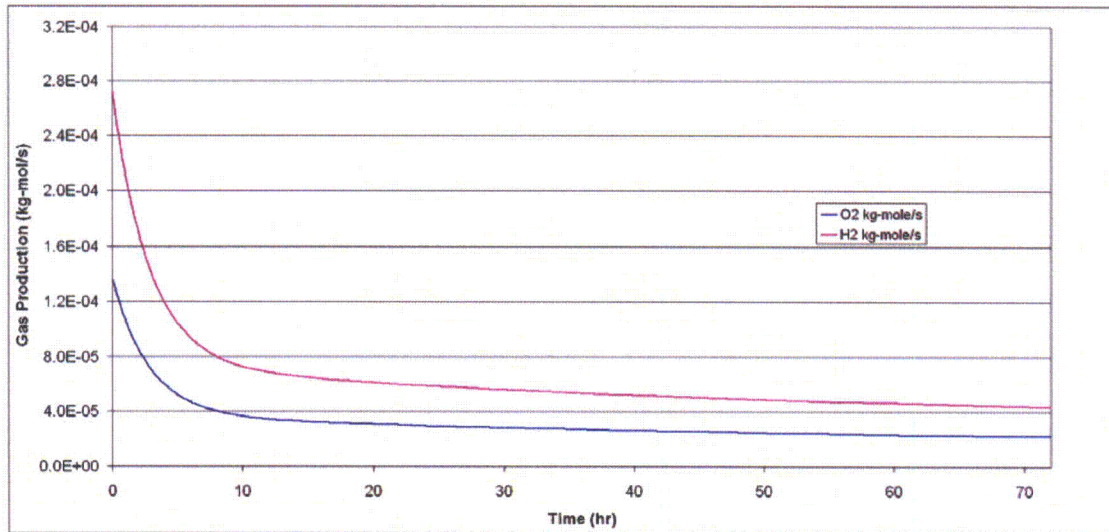


Figure 6: ESBWR Post-SCRAM Radiolytic Gas Production of Hydrogen and Oxygen

4.2 ICS DURING LOCA (LOW PRESSURE)

During a loss of coolant accident (LOCA), the ICS is needed to initiate in order to supply the condensate stored in its drain piping. This additional water is credited with keeping the core covered with margin during a design basis accident. The actual heat removal through the ICS condenser is relatively small and is not credited in this type of event. However, there is potential for condensation to occur, and given enough time it is possible for combustible gases to accumulate in the ICS condenser following a LOCA.

In order to prevent this buildup from occurring, a logic change has been implemented for the ICS containment isolation valves in which the valves now automatically close after receiving an indication that the depressurization valves on the reactor have opened. The sequence of events during a design basis accident show that there is adequate time between ICS initiation and DPV opening for the condensate in the ICS drain lines to transfer to the RPV.

A TRACG evaluation shows that once it is isolated from the vessel, the ICS condenser pressure drops below 15 psia within 2,000 seconds, and noncondensable gas partial pressure does not exceed 0.63 following isolation. A detonation under these conditions is highly unlikely, however, if one were to occur the resulting loads would be within the stated design pressure of the ICS (1264.7 psia) as shown below.

The methodology by which the PCCS CJ pressures were calculated can be applied to the ICS, however, credit will be taken for the detonation properties of the mixture, which contains no less than 37% steam (based on the TRACG evaluation described above) in the long term and greater than 37% steam immediately after isolation. The conservative CJ multiplication factor of 19.0, which was applicable to pure mixtures of hydrogen and oxygen at 25°C, can be reduced based on the thermo-chemical data contained in Reference 17. Table 5.1.8 of that report (reproduced below) contains data for a range of steam fractions.

Table 4-1: Thermodynamic Properties of Hydrogen-Oxygen-Steam Mixtures*

%H ₂ O	Initial pressure P ₀ , bar	Initial temperature T, K	Sonic velocity in reactants C _{sp} , m/s	Sonic velocity in products C _{sp} , m/s	Adiabatic combustion temperature T _a , K	Adiabatic combustion pressure P _{1cc} , bar	Expansion ratio σ	Chapman-Jouguet temperature T _{CJ} , K	Chapman-Jouguet velocity D _{CJ} , m/s	Chapman-Jouguet pressure P _{CJ} , bar	Reflection pressure P _{ref} , bar
0	1	383	607	1390	3087	7.5	6.56	3642	2815	14.5	35
20	1	383	576	1280	2867	6.9	6.12	3348	2568	13.3	32
40	1	383	548	1174	2561	6.2	5.57	2989	2329	12.0	29
60	1	383	524	1052	2048	5.3	4.65	2461	2050	10.0	24
65	1	383	518	1011	1870	4.9	4.32	2280	1962	9.3	22
68	1	383	515	984	1755	4.7	4.10	2159	1902	8.9	21
70	1	383	513	964	1677	4.5	3.94	2074	1860	8.5	20
72	1	383	511	943	1597	4.3	3.78	1984	1815	8.2	19

*Excerpt from Reference 17

Because the CJ pressure is inversely proportional to the steam fraction, the CJ pressure ratio of 13.3 (corresponding to 20% steam) will be used to bound conditions in the ICS in the long term. For CJ pressure ratios immediately after isolation, steam fractions during the transition (short-term) from high total pressure at isolation to low pressure will be used to evaluate detonation pressures.

A DLF of 2 is applied to the ICS condenser, as was done for the PCCS condenser in Section 2.2.2.1. The equation from that section is reproduced below, with parameters that are consistent with the design of the ICS condenser tubes:

$$[[\quad \quad \quad]]$$

The corresponding detonation velocity (from Table 5.1.8 of Reference 17) is nearly double the critical velocity, thus the DLF of 2 remains justified.

Long-Term ICS Detonation Pressure Load

Beginning with an ICS initial pressure of 15 psia, the final load is:

$$15.0 \cdot 13.3 \cdot 2 \cdot 2.5 = 1000 \text{ psia,}$$

which is significantly below the ICS design pressure of 1250 psia.

Short-Term ICS Detonation Pressure Load

ICS total pressure is rapidly reduced soon after ICS isolation due to further condensation of the remaining steam. Prior to isolation, steam fractions remain well above 80%, so the period before isolation was not evaluated for detonation pressure loads. The remainder of the 2000 second period was evaluated, and the peak load occurs at approximately 75 seconds after isolation (a combination of total initial pressure and CJ pressure ratio). The corresponding steam fraction and total initial pressure is 42% and 20.4 psia, respectively. The CJ pressure ratio for 42% steam is 11.83. The final load is:

$$20.4 \cdot 11.83 \cdot 2 \cdot 2.5 = 1207 \text{ psia,}$$

which is below the ICS design pressure of 1250 psia.

The maximum detonation load approaches the bounded long-term load within seven minutes of ICS isolation.

4.2.1 ICS Vent, Steam, and Drain Lines During LOCA (Low Pressure)

The design pressure rating for the ICS components (condenser, drain lines, steam lines, and vent lines) is 1250 psia and as discussed above the peak detonation pressure load soon after ICS isolation during a LOCA is 1207 psia. Therefore these components will withstand a detonation.

4.3 APPLICABLE SUBSECTIONS OF ASME CODE SECTION III

The applicable subsection of ASME Code Section III for each ICS component is given in Table 4-1.

Table 4-1: ICS Components Applicable ASME Code III Subsection

<u>Component</u>	<u>ASME Code Section III, Subsection</u>
Steam Supply Pipe (drywell)	NB
Steam Supply Pipe up to Venturi (pool)	NB
Steam Supply Pipe from Venturi to Upper Drum (pool)	NC
Upper Drum	NC
Tubes	NC
Lower Drum	NC
Vent Pipe (pool)	NC
Vent Pipe (drywell + wetwell)	NC
Drain Pipe from Lower Drum to Tee Connection (pool)	NC
Drain Pipe from Tee Connection in Pool to Reactor Pressure Vessel	NB

4.4 DEFLAGRATION TO DETONATION TRANSITION (DDT)

As discussed in Section 2.2.3, DDT can increase localized pressures to high values, and the loading due to these pressures can be accounted for by the use of a dynamic factor of 4, which is bounded by the assumption $(2 \cdot 2.5 \cdot P_{CD})$ used in Section 4.2 for ICS. As described in the summary of Reference 4, the DDT loads are impulsive and very short in duration and therefore need not be considered as an additional dynamic load on top of the dynamic factors already being applied. Section 2.2.3 provides a more detailed discussion on DDT.

The maximum possible detonation pressure load for the ICS is 1207 psia (See Section 4.2) using the above methodology. All of ICS components (condenser, drain lines, steam lines, and vent lines) that are part of the reactor coolant pressure boundary are designed for a system design pressure of 1250 psia and are bounded by the maximum detonation pressure with respect to DDT.

5.0 PCCS AND ICS INSPECTIONS AND QUALIFICATION

This section defines the nondestructive examination (NDE) and preservice and in-service inspection requirements as they pertain specifically to the welds between the tubes and drums of the ICS and PCCS condensers. Inspection of these welds is described in detail because they are of a unique design and geometry. The other pressure retaining welds are of a more standard design and are assigned standard ASME inspection requirements.

5.1 FABRICATION INSPECTIONS

5.1.1 PCCS

Non-destructive examination for the PCCS is governed by ASME Section III, Subsection NE-5000. Paragraph NE-5200 calls for radiographic examination (RT) for all types of welded joints with the exception of socket welds (which do not apply to the PCCS). However, the requirements of NE-5280 allow for the substitution of ultrasonic (UT) and liquid penetrant (PT) testing in lieu of RT if the joint detail does not permit RT. Because of the close spacing and confined geometry of the tube-to-drum welds, this substitution of UT and PT for RT is considered appropriate.

5.1.2 ICS

Non-destructive examination for the ICS is governed by ASME Section III, Subsection NC-5000. Per NC-5220, radiographic examination is called out for circumferential welded joints; however, these requirements only apply to members that are at least 4.8 mm thick. The ICS will adhere to these rules for conservatism although the tube thickness is only [[]].

Like the PCCS, there is a paragraph for special substitutions for RT in which a combination of UT and PT may be used instead (Paragraph NC-5279). This substitution will be credited for the ICS condenser, as its geometry is nearly identical to the PCCS.

5.2 PRE-SERVICE / IN-SERVICE INSPECTIONS

5.2.1 PCCS

The PCCS condenser is a Class MC component that is subject to the requirements of ASME Section XI, Subsection IWE. Because the PCCS resides in a low-pressure low temperature environment, it is not subject to accelerated wear or degradation and therefore does not qualify for augmented visual inspections per the requirements of IWE-1240.

Table IWE-2500-1 defines examination requirements. Item E1.12 calls for "General Visual" inspection of the PCCS condensers. A VT-3 exam is appropriate based on the guidance of Reference 16.

5.2.2 ICS

The ICS condenser is a Class 2 component that is subject to the requirements of ASME Section XI, Subsection IWC. The guidance of paragraph IWC-1221 indicates that the ICS condenser meets the criteria for exemption from surface and volumetric exams due to the [[]] diameter of the ICS tubes, per IWC-1221(a)(1). Also, the requirements of IWC-1221(c) indicate that the passive nature of the condenser (statically pressurized, passive with no pumps, safety injection) also meets the exemption criteria. A General Visual inspection requirement with a VT-2 test shall be assigned to the ICS condenser tube welds.

5.3 TUBE BENDS

5.3.1 PCCS

PCCS tubes bent by cold forming shall be annealed after bending. Annealing shall be required. Annealing shall be conducted between 1065°C and 1120°C, followed by a quench to 205°C within 5 minutes. Process includes tube bends + 150 mm on each side. Interior of tubes is purged with a protective atmosphere during the process.

Tube thickness shall be verified post-bending. A qualification sample with smallest bend radius shall be sectioned to confirm wall thickness requirement is met. Tests shall also be performed to qualify the tubes for tensile, yield, and elongation requirements post-bending.

The hardness of XM-19 for PCCS tubes is limited to Rockwell C 30 for the final product.

5.3.2 ICS

Induction bending of ICS tubes shall be qualified based on the bend radius and the diameter.

Tubes shall be UT examined before bending according to the requirements of NB-2551. After bending, tubes shall be PT examined according to NB-2556. Section NB requirements are applied here for conservatism.

Tube thickness shall be verified post-bending. A qualification sample with smallest bend radius shall be sectioned to confirm wall thickness requirement is met. Tests shall also be performed to qualify the tubes for tensile, yield, and elongation requirements post-bending.

5.4 WELD AND WELD FILLER MATERIAL

Appropriate weld filler metal for XM-19 shall be 308L, or ER209. Appropriate weld filler metal for Nb-modified Alloy 600 shall be Nb-modified Alloy 82.

For the PCCS, there are no dissimilar metal welds. XM-19 to 304L or to 316 is not considered a dissimilar metal weld. PCCS materials are listed in Figure B-2a of Appendix B.

6.0 REFERENCES

1. W.A. Strauss and J.N. Scott, "Experimental Investigation of the Detonation Properties of Hydrogen-Oxygen and Hydrogen-Nitric Oxide Mixtures at Initial Pressure up to 40 Atmospheres". *Combustion and Flame* 19, 141-143, 1972.
2. R. Edse and L.R. Lawrence Jr., "Detonation Induction Phenomena and Flame Propagation Rates in Low Temperature Hydrogen-Oxygen Mixtures". Elsevier Science Inc., October 1969.
3. J. E. Shepherd, "Structural Response of Piping to Internal Gas Detonation". ASME Pressure Vessels and Piping Conference, 2006. VP2006-ICPVT11-93670, presented July 23-27 2006 Vancouver BC Canada.
4. F. Pintgen, Z. Liang, and J. E. Shepherd, "Structural Response of Tubes to Deflagration-to-Detonation Transition". Extended abstract for 21st International Colloquium on the Dynamics of Explosions and Reactive Systems, Poitiers, France, 23-27 July 2007.
5. NUREG/CR-4905, "Detonability of H₂-Air-Diluent Mixtures". Sandia National Laboratories, June 1987.
6. E. Schultz, J. Shepherd, "Validation of Detailed Reaction Mechanisms for Detonation Simulation". Graduate Aeronautical Laboratories California Institute of Technology, Pasadena, CA 91125, Explosion Dynamics Laboratory Report FM99-5.
7. NUREG/CR-6213, "High-Temperature Hydrogen-Air- Steam Detonation Experiments in the BNL Small-Scale Development Apparatus". Brookhaven National Laboratory, August 1994.
8. W.E. Baker et al., "Fundamental Studies in Engineering 5: Explosion Hazards and Evaluation". Elsevier Scientific Publishing Company, New York, 1983.
9. J. E. Shepherd, A. Teodorczyk, R. Knystautas, J. H. Lee, "Shock Waves Produced by Reflected Detonations". *Progress in Astronautics and Aeronautics* 134, 244-264.
10. R.K. Kumar, "Detonation Cell Widths in Hydrogen-Oxygen-Diluent Mixtures". *Combustion and Flame* 80, 157-169. 1990.
11. Y. N. Shebeko et al., "The Influence of Inert Retardants on the Combustion of Hydrogen-Oxygen Mixtures Under Elevated Temperatures and Pressures". *Combustion, Explosion, and Shock Waves* Vol. 30, No. 2, 1994.
12. Z. Liang, T. Curran, and J.E. Shepherd, "Structural Response of Piping Components to Detonation Loading". Explosion Dynamics Laboratory Report FM2006.008, December 20, 2008.
13. NEDC-32615P, "Post-Test Analysis of PANTHERS PCC Tests". GE Nuclear Energy, June 1996.
14. "PANTHERS-PCC Data Analysis Report". SIET Document No. 00394RA95, Rev. 0. June 20, 1995. Transmitted under MFN 098-95, Docket STN 52-004.

15. M. Kuznetsov et al., "Structural Response of DN15-Tubes Under Radiolysis Gas Detonation Loads for BWR Safety Applications". 18th International Conference of Structural Mechanics in Reactor Technology (SmiRT 18), Beijing, China, August 7 – 12, 2005, SmiRT 18-J09-1.
16. "Containment Inspection Program Guide Update", Electronic Power Research Institute, Report 1015151 Technical Update December 2007.
17. "Combustion of BWR-Typical Radiolytic Gas Mixtures," Final Report for the International Radiolytic Gas Combustion Project, VGB-Contract SA"AT" 13/04, December 2007.
18. Kelm, Jahn, and Reinecke, "Operational Behavior of Catalytic Recombiners – Experimental Results and Modeling Approaches", Institute for Energy Research, Safety Research and Reactor Terminology (IEF-6), Jülich, Germany
19. "Qualification of Passive Autocatalytic Recombiners for Combustible Gas Control in ALWR Containments," Prepared by the Electric Power Research Institute (EPRI) ALWR Program, April 8, 1993.
20. G. Ciccarelli and S. Dorofeev, "Flame Acceleration and Transition to Detonation in Ducts", Progress in Energy and Combustion Science, Vol. 34, Issue 4, pp 499-550, 2007
21. Flame Acceleration and Deflagration-to-Detonation Transition in Nuclear Safety, OECD Nuclear Energy Agency/CSNI/R(2000)7, August 2000.
22. Kuchta, J. M., "Investigation of Fire and Explosion Accidents in the Chemical, Mining, and Fuel-Related Industries", United States Department of the Interior, Bureau of Mines, Bulletin 680.
23. "Passive ALWR Source Term. Advanced Reactor Severe Accident Program," Prepared by EG and G Idaho, Inc., Idaho Falls, February 1991.
24. W.M. Beltman and J.E. Shepherd, "Linear Elastic Response of tubes to Internal Detonation Loading," Department of Mechanical Engineering, University of Twente, Netherlands. Graduate Aeronautical Laboratories, California Institute of Technology, Pasadena, CA.
25. Response to RAI 19.1-8 Supplement 1, Part B, MFN 06-313, September 12, 2006.
26. Response to RAI 19.1-8 Supplement 2, MFN 06-313 Supplement 6, August 13, 2007.

APPENDIX A - SUPERSEDED PCCS STRUCTURAL ANALYSIS

A.1 Description of Model

This Appendix archives the previous configuration of the PCCS that has since been superseded by Appendix B.

A finite element analysis model (FEM) using the approved ANSYS computer code was performed on the PCCS condenser with a supplemental hand calculation. Approved versions of ANSYS are given in ESBWR DCD Tier 2, Table 3D.1-1.

- The FEM models the current geometry of the PCCS condenser and supports described in Figures A-1a, A-1b, and A-2, including all components between the steam inlet passages through the RCCV Top Slab and the condensate drain/vent passages through the RCCV Top Slab.
- The following components of the PCCS condenser were modeled with [[]]
ANSYS elements:

[[

o

]]

- The tubes of the PCCS condenser were modeled with [[]]
ANSYS elements with the following properties:

[[

*** Appendix A Superseded By Appendix B ***

○]]

- The [[]] of the dynamic steel frame were modeled with [[]] ANSYS elements with the following properties:

[[]]

○]]

A.2 Load Definitions

Consideration of the following loads has been taken into account for the PCCS condenser:

- D (+B) Dead Weight (+ Buoyancy)
- P_t Test Pressure
- P_a Design accident pressure generated by a LOCA
- T_t Thermal effects during tests
- T_a Thermal effects generated by a LOCA
- SSE Safe Shutdown Earthquake
- SRVD Safety Relief Valve Discharge
- LOCA Loss of Coolant Accident

A.3 Load Combinations

Enveloping Load Combinations are described in Table A-1.

*** Appendix A Superseded By Appendix B ***

Table A-1: PCCS Load Combinations

Service Level (elastic analysis)	Load Combination
Test Condition	$D + P_t + T_t$
Design Condition	$D + P_a + T_a$
Levels A, B	$D + P_a + T_a + SRV + LOCA$
Levels C, D	$D + P_a + T_a + SSE + SRV + LOCA$

*** Appendix A Superseded By Appendix B ***

A.4 Finite Element Model Inputs

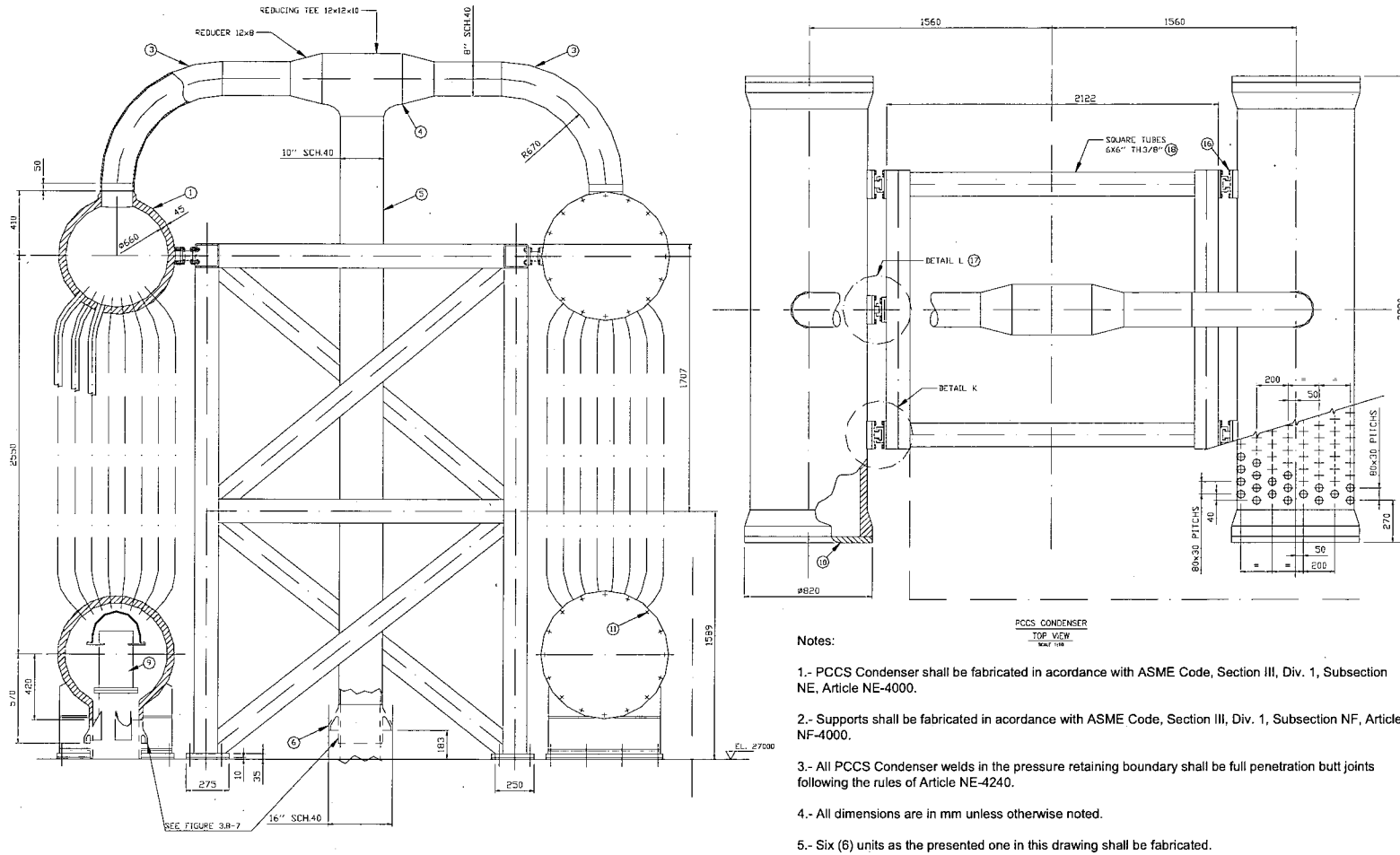


Figure A-1a: PCCS Condenser and Supports

*** Appendix A Superseded By Appendix B ***

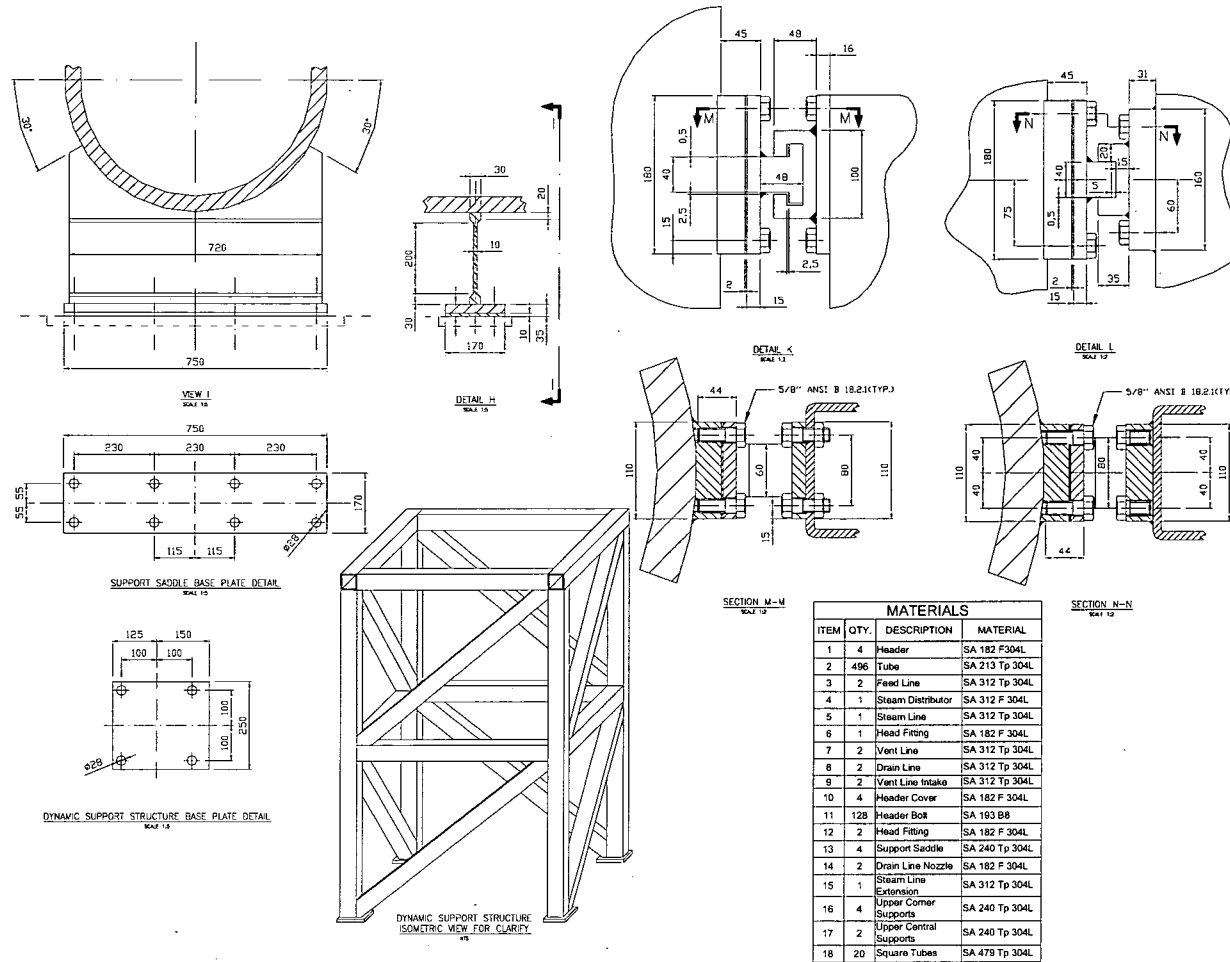


Figure A-1b: PCCS Condenser and Supports Details

*** Appendix A Superseded By Appendix B ***

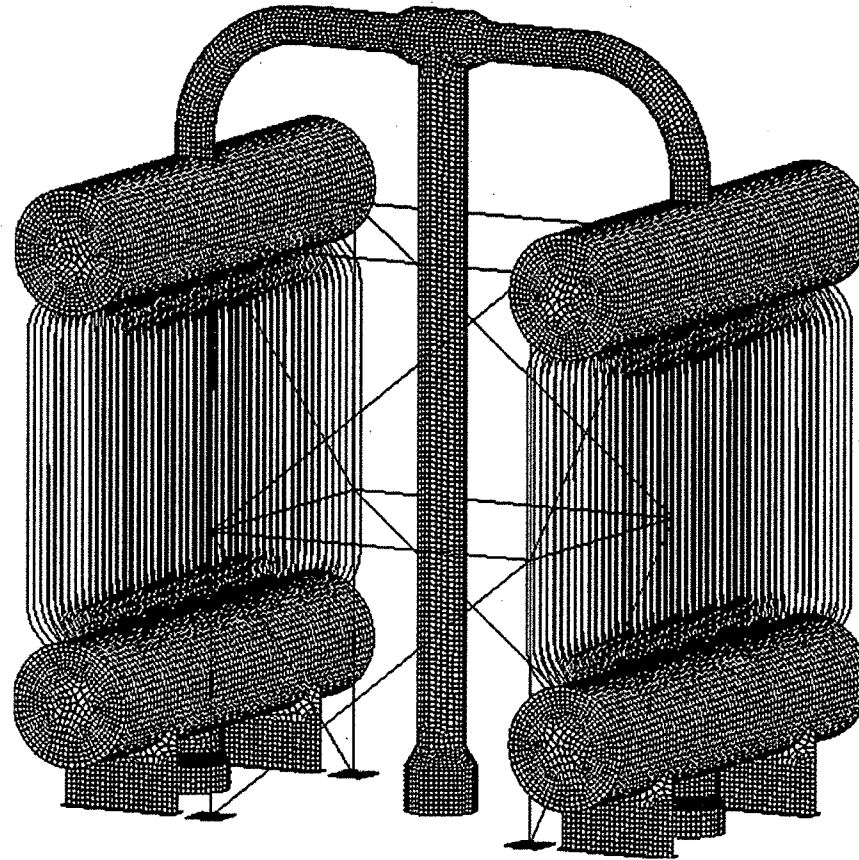


Figure A-2: FEM of PCCS Condenser and Supports

*** Appendix A Superseded By Appendix B ***

A.5 Stress Results and Margin to Allowable

Table A-2: Stress Summary of the PCCS Condenser and Supports

Component	Stress Category	Test			Design			Service Level A/B			Service Level C/D		
		Calculated Stress (MPa)	Allowable Stress (MPa)	Stress Margin (%)	Calculated Stress (MPa)	Allowable Stress (MPa)	Stress Margin (%)	Calculated Stress (MPa)	Allowable Stress ⁽¹⁾ (MPa)	Stress Margin (%)	Calculated Stress (MPa)	Allowable Stress ⁽²⁾ (MPa)	Stress Margin (%)
Upper Header	P_m	11.8	119.8	90	11.8	114.9	90	16.8	114.9	85	37.8	137.9	73
	$P_L + P_b$	11.8	183.7	94	11.8	150.6	92	16.8	150.6	89	39.8	180.7	78
Lower Header	P_m	11.8	119.8	90	11.8	114.9	90	24.8	114.9	78	47.8	137.9	65
	$P_L + P_b$	11.8	183.7	94	11.8	150.6	92	26.8	150.6	82	55.8	180.7	69
Tubes	P_m	11.4	119.8	91	11.4	114.9	90	15.4	114.9	87	19.4	137.9	86
	$P_L + P_b$	11.4	183.7	94	11.4	150.6	92	33.4	150.6	78	66.4	180.7	63
Feed Line	P_m	9.9	119.8	92	9.9	114.9	91	23.9	114.9	79	79.9	137.9	42
	$P_L + P_b$	9.9	183.7	95	9.9	150.6	93	29.9	150.6	80	110.9	180.7	39
Steam line	P_m	10.9	119.8	91	10.9	114.9	91	25.9	114.9	77	80.9	137.9	41
	$P_L + P_b$	10.9	183.7	94	10.9	150.6	93	31.9	150.6	79	112.9	180.7	38
Steam Distributor	P_m	12.6	119.8	89	12.6	114.9	89	24.6	114.9	79	67.6	137.9	51
	$P_L + P_b$	12.6	183.7	93	12.6	150.6	92	26.6	150.6	82	73.6	180.7	59
Condensate Lines	P_m	12.6	119.8	89	12.6	114.9	89	31.6	114.9	73	66.6	137.9	52
	$P_L + P_b$	12.6	183.7	93	12.6	150.6	92	37.6	150.6	75	80.6	180.7	55
Header Cover	P_m	87.0	119.8	27	87.0	114.9	24	89.0	114.9	23	92.0	114.9	20
	$P_L + P_b$	87.0	183.7	53	87.0	150.6	42	89.0	150.6	41	92.0	180.7	49
Header Bolt	Average Stress	70.3	144.7	51	70.3	110.1	36	70.3	220.2	68	70.3	220.2	68
Support Saddle	P_m	Negligible						29.0	112.6	74	87.0	168.9	48
	$P_L + P_b$							30.0	168.9	82	88.0	253.4	65
	Shear							9.0	67.6	87	26.0	101.3	74
Truss Support Structure	Tension							14.0	76.6	82	69.0	114.9	40
	Shear							3.0	51.1	94	12.0	76.6	84
	Compression							14.0	47.9	71	69.0	71.9	4
	Bending	14.0	84.3	83	70.0	126.4	45						

1) Allowable stress values correspond to Level A 2) Allowable stress values correspond to Level C

APPENDIX B - PCCS STRUCTURAL ANALYSIS WITH DETONATION LOADING

B.1 Description of Model

This Appendix summarizes the evaluation of the PCCS for detonation loads based on the revised configuration described in this report. The inputs to the modified analysis are as follows:

B.1.1 Tube Analysis Model

A 3-D finite element model (FEM) for the analysis of one tube under hydrogen detonation load is built with ANSYS 10.0. The forces at the boundary conditions have been defined to equalize the internal pressure. A description of the FEM follows:

- The FEM physically represents the current geometry of [[]] tubes and the portion of the headers that join to the tubes.
- The entire model is built with [[]] ANSYS elements. The mesh of the tube where the detonation pressure is applied is very refined to get accurate results.
- The detonation load of 19.333 MPa multiplied by the DLF of 2, i.e. 38.7 MPa is applied as internal pressure in one tube and along the tube length, including the hole in the headers.
- Displacement restrictions are applied at the different cut section of the headers as boundary conditions. Boundary conditions far of the analyzed tube, no impact in the results obtained
- Several analysis cases have been executed changing the tube where the detonation occurs, and the maximum resultant stress is not significantly affected.

B.1.2 Lower Header Analysis Model

A 3-D finite element model (FEM) for the analysis of the lower header under hydrogen detonation load is built with ANSYS 10.0. To capture tube-to-header connection interaction due to circumferential expansion of the lower header, tube-to-header connections are also included in the model. See Figure B-1b of model. Detail F of Figure B-2b shows the tube-header-connections as modeled. This configuration provides conservative results, and stress concentrations seen in the analysis can be alleviated through an optimized tube-to-header connection.

The portion having the condensate nozzle has been selected as the most critical header area. A description of the FEM follows:

- The FEM physically represents the current geometry of a cylindrical section of the lower header, corresponding to a [[]] array of the tube bank, containing the reinforced condensate nozzle and the vertical run up to the anchored flange. The FEM does not include the end covers and end cover bolts; they are evaluated separately in Section B.1.4.
- The entire model is built with [[]] ANSYS elements.
- The detonation load of 19.333 MPa multiplied by the DLF of 2, i.e. 38.7 MPa is applied as an internal pressure on the inner face of the header, including the nozzle opening, the drain line and the holes for the tubes. Equivalent edge pressures are applied at the two cut sections of the header to account for the edge effects. Displacement restrictions in the nodes at the sixteen bolt locations are applied.

B.1.3 Global PCCS Condenser Analysis Model

A 3-D finite element model (FEM) for the analysis of the PCCS Condenser and support under loads for all service levels listed in Table B-1 except Service Level C-2 is built with ANSYS 10.0. A description of the FEM follows:

- The FEM physically represents the revised geometry of the PCCS Condenser and support, including all components between the steam inlet passage through the RCCV Top Slab and the condensate drain/vent passages through the RCCV Top Slab.
- The following components of the PCCS Condenser are modeled with SHELL 63 ANSYS elements: upper headers [[]], lower headers [[]], upper header covers [[]], lower header covers [[]], steam line [[]], feed lines [[]], steam distributor [[]], steam line sleeve [[]], steam line head fitting [[]], condensate nozzle [[]], condensate line sleeve [[]], support saddle [[]], support saddle base plates [[]], and steel frame support structure base plates [[]].
- The reinforced area of the lower header at the condensate nozzle is conservatively not considered in this global model.

[[]]

○

○

]]

- The steam line, condensate lines (from the head fittings downwards), and the vent lines, which run inside condensate lines, are not included in the model, since they do not have any structural influence in the PCCS Condenser behavior.
- The internal and external water masses are introduced in the model by increasing the material density. All components of the PCCS Condenser are cylindrical form. All members of the steel frame support structure are square tubes.

- Displacement restrictions are applied as boundary conditions at the bolt point locations of the base plates and at sixteen nodes in each lower section of the line sleeves through the RCCV Top Slab.
- In the node corresponding to the upper support location, the appropriate directional coupling is applied between the upper headers and the steel frame support structure.
- The coordinate system adopted in the FEM is the right hand Cartesian coordinate system. Direction X of the FEM follows the Y-direction (E-W) of the plant, direction Y of the FEM follows the X-direction (N-S) of the plant, and direction Z of the FEM coincides with Z-direction (vertical).

B.1.4 Lower Header Covers and Lower Header Cover Bolts

The lower header covers and lower header cover bolts are not included in the lower header FEM. The stresses due to a detonation load are evaluated separately using ASME Section III formula found in NE-3325 and Appendix XI-3223 for the covers and bolts, respectively.

To provide flexibility for final routing and supporting of pipes and components, sizing that has been performed by formula can be changed during detailed design to use design by analysis, as permitted by the ASME Code. This analysis will require the use of the detonation pressure load as defined in this section along with the service level load combinations as defined in Appendix B and acceptance criteria as provided by the ASME Code.

Lower Header Cover

The following formula, derived from Article NE-3325.2, used for the flat circular plates, is used to evaluate the lower header covers:

$$\sigma = \frac{C \cdot P \cdot d^3 + 1.27 \cdot W \cdot h_G}{d \cdot t^2}$$

where:

C = 0.2, for covers bolted to the vessel

P = design pressure = 38.666 MPa

d = gasket circle diameter = 0.572 m

t = shell thickness = 0.150 m

G = diameter at location of gasket load reaction = 0.572 m

w = width used to determine the basic gasket seating = 0.012 m

b = effective gasket width = w/8 = 0.0015 mm (estimated)

m = gasket factor = 6 (estimated)

h_G = radial distance from gasket load reaction to the bolt circle = 0.079 m

$W = W_{m1}$ = total flange design bolt load = $0.785 \cdot G^2 \cdot P + 2 \cdot b \cdot \pi \cdot G \cdot m \cdot P = 11181638 \text{ N}$

Then:

σ = maximum stress = 199.6 MPa

Lower Header Bolts

The following expression is derived from Appendix XI-3223 and is used to determine the maximum stress on the lower header cover bolts:

$$W_{m1} = 0.785 \cdot G^2 \cdot P + 2 \cdot b \cdot \pi \cdot G \cdot m \cdot P$$

$$\sigma = \frac{W_{m1}}{n \cdot A_B}$$

$$A_B = \frac{\pi \cdot d_B^2}{4}$$

where:

P = design pressure = 38.666 MPa

G = diameter at location of gasket load reaction = 0.572 m

n = number of bolts = 28

d_B = minimum bolt section diameter = 0.03467 m (1 1/2"-8 UN)

m = gasket factor = 0 (self-energized hollow o-ring seal, per Appendix XI, Table XI-3221.1-1)

Then:

A_B = minimum bolt cross section area = $9.441 \times 10^{-4} \text{ m}^2$

W_{m1} = total flange design bolt load = 9930954 N

σ = maximum bolt stress = 375.7 MPa

Of note, a gasket factor of zero is credited because the design will use a self-energized hollow o-ring seal.

B.2 Load Definitions

Consideration of the following loads has been taken into account for the PCCS condenser:

- D (+B) Deadweight (+ Buoyancy)
- P_t Test pressure
- P_a Design accident pressure generated by a LOCA
- T_t Thermal effects during tests
- T_a Thermal effects generated by a LOCA
- SSE Safe Shutdown Earthquake
- SRVD Safety Relief Valve Discharge
- LOCA Loss of Coolant Accident
- DET Detonation pressure load

B.3 Load Combinations

Enveloping Load Combinations are described in Table B-1. These load combinations are consistent with and bound ESBWR Design Control Document, Tier 2, Table 3.8.4, SRP 3.8.2 and Reg. Guide 1.57.

Detonation loads determined in the Tube Submodel and Lower Drum Submodel are combined with other loads (calculated from the Global PCCS Condenser Model) as a direct summation of maximum stresses.

As per DCD Tier 2, Table 3.8-4 "The peak responses of dynamic loads do not occur at the same instant. SRSS method to combine peak dynamic responses is acceptable for steel structures." Therefore, dynamic stresses are combined using the SRSS method and then directly added together as a direct sum with non-dynamic stresses.

Table B-1: Modified PCCS Load Combinations

Service Level (elastic analysis)	Load Combination*
Test Condition	$D + P_t + T_t$
Design Condition	$D + P_a + T_a$ **
Levels A, B	$D + P_a + T_a + SRV + LOCA$ **
Level C-1	$D + P_a + T_a + SSE + SRV + LOCA$ **
Level C-2	$D + DET + T_a + SSE$

* Live loads (L) are not significant loads for the equipment considered in this analysis.

** Pipe reactions (R_a) will be minimized during detailed design, by considering mitigating factors such as pipe flexibility and reduced pipe size in the pipe routing. Also, there are large margins to the allowable for cases where pipe reactions contribute to the calculated stress. This footnote clarifies that load combinations evaluated in the report do not include pipe reaction loads due to events inside the drywell. These reaction loads are expected to be negligible due to the difference in size of piping connected to the drain line penetration and low pressure (not high-energy pipes). The drain line outer diameter, from Section 2.2.4.4, is approximately 16 inches while the largest pipe connected is 4 inches. Also the design of the piping (as explained above) will minimize operational loads such as thermal expansion by allowing the pipe routing to have flexible expansion of piping segments without loading the anchor points.

B.4 Finite Element Model Inputs

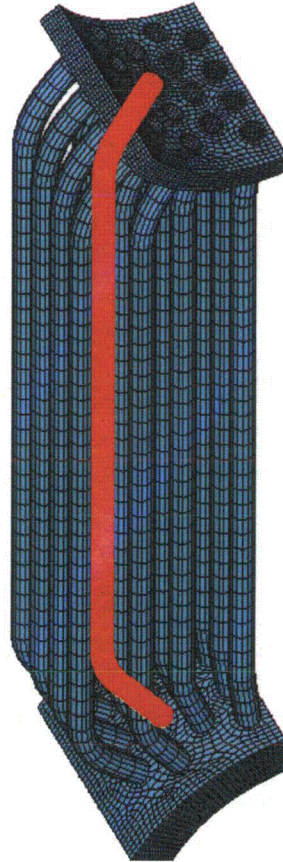


Figure B-1a: Tube FEM of and Pressure Load

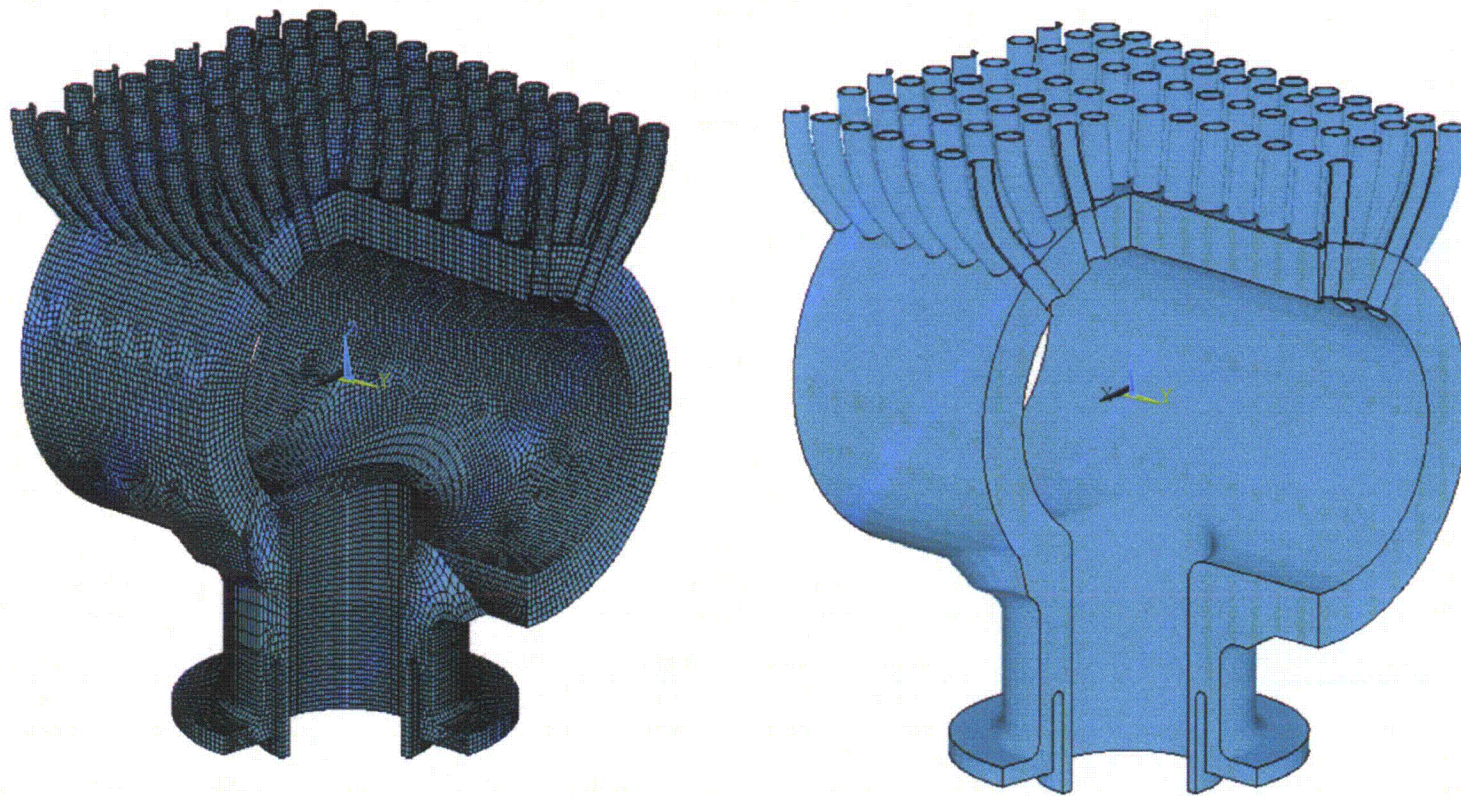


Figure B-1b: Lower Header FEM

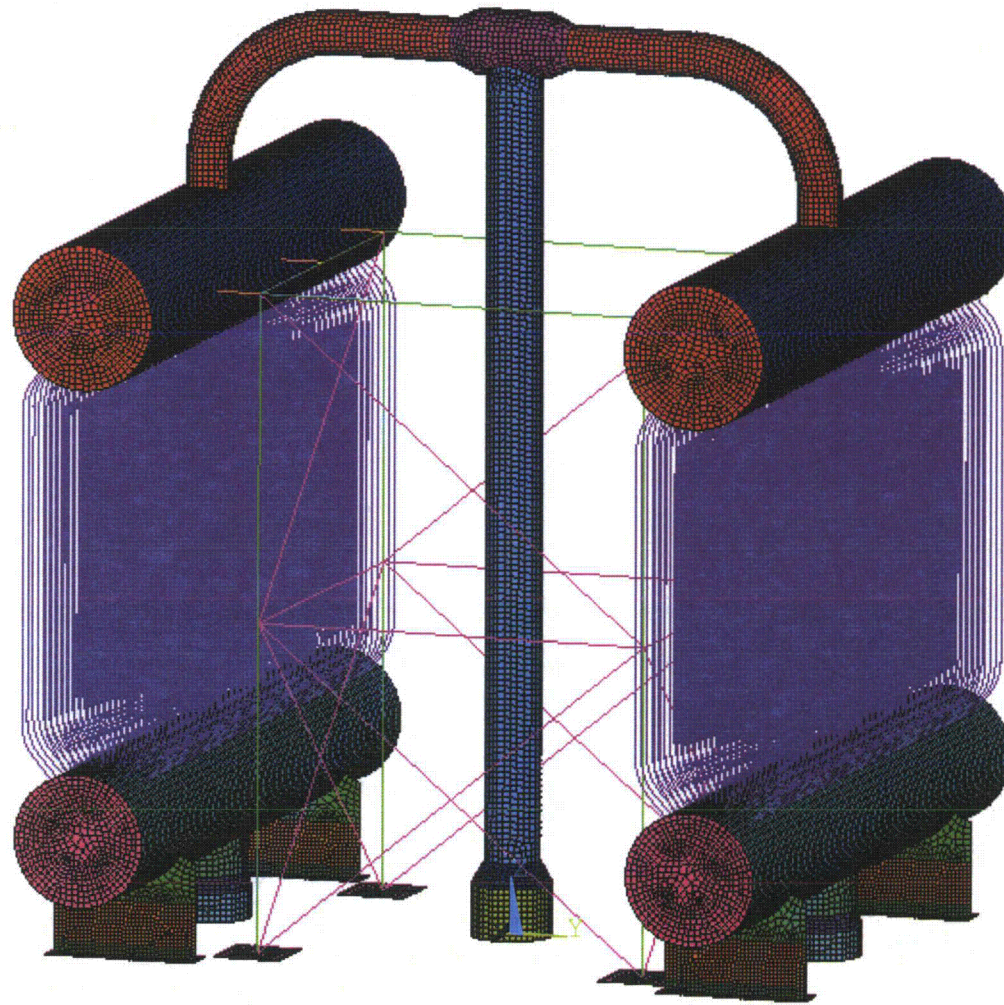


Figure B-1c: PCCS Condenser FEM

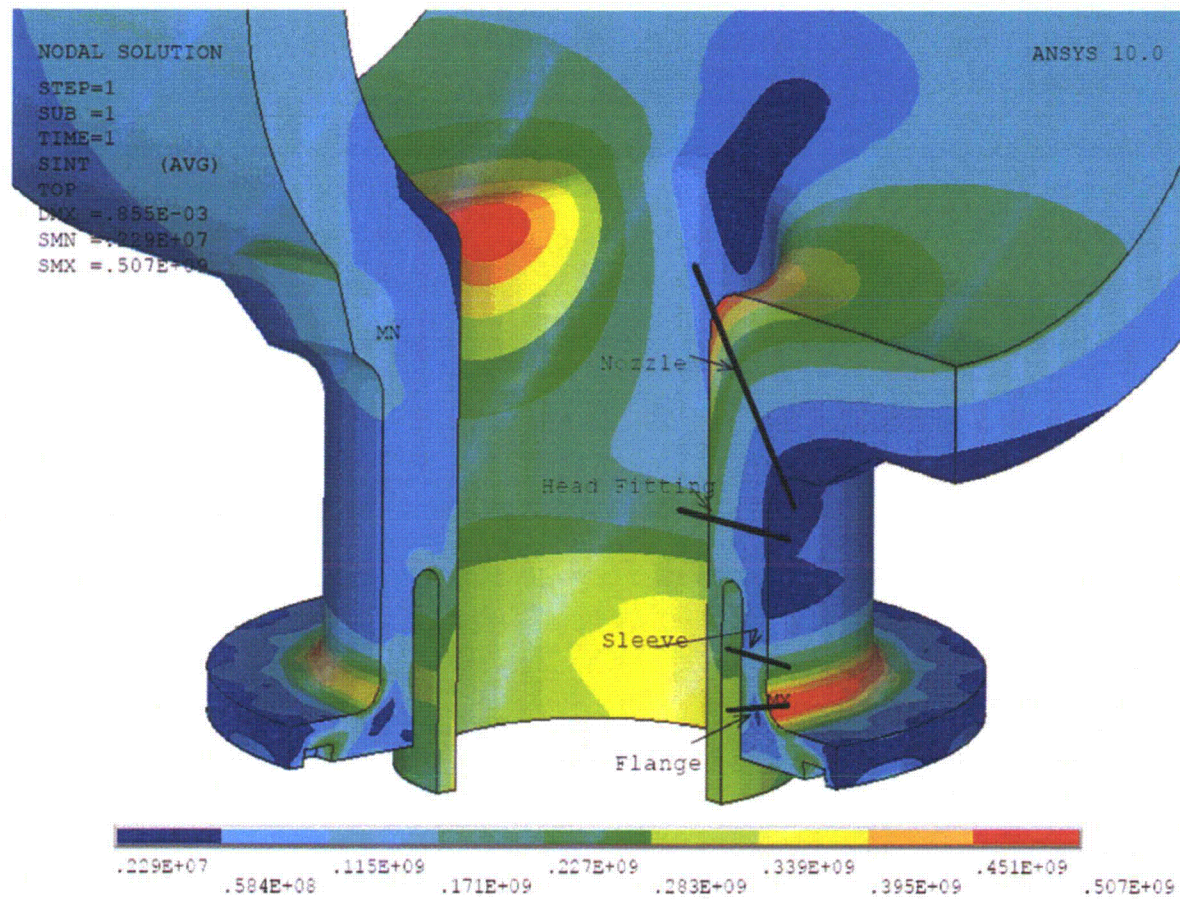


Figure B-1d: Lower header FEM. Nozzle, Head Fitting, Sleeve and Flange Sections for Linearized Stress Intensities (MPa)

NEDO-33572, Revision 3

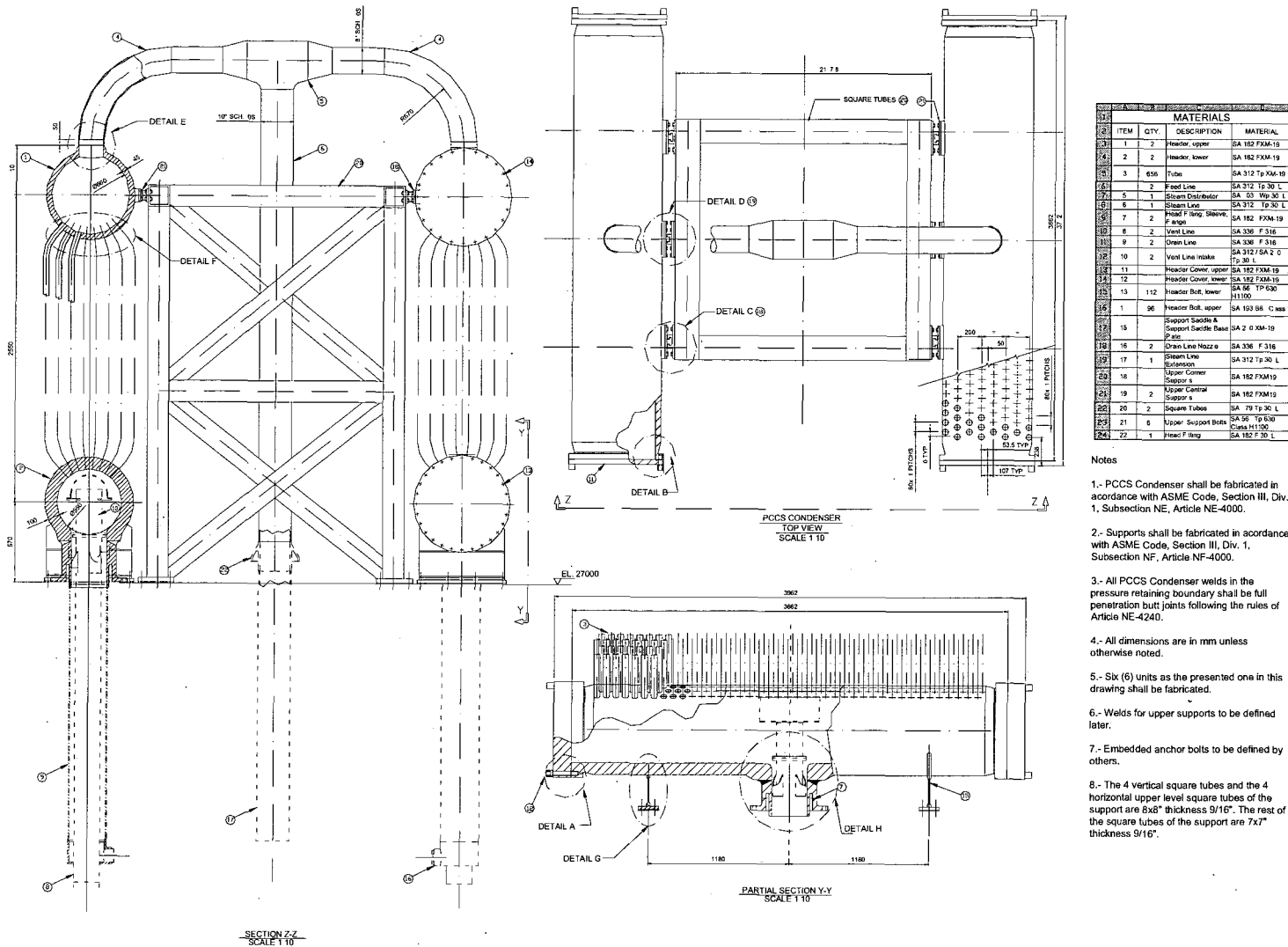


Figure B-2a: PCCS Condenser and Supports Details

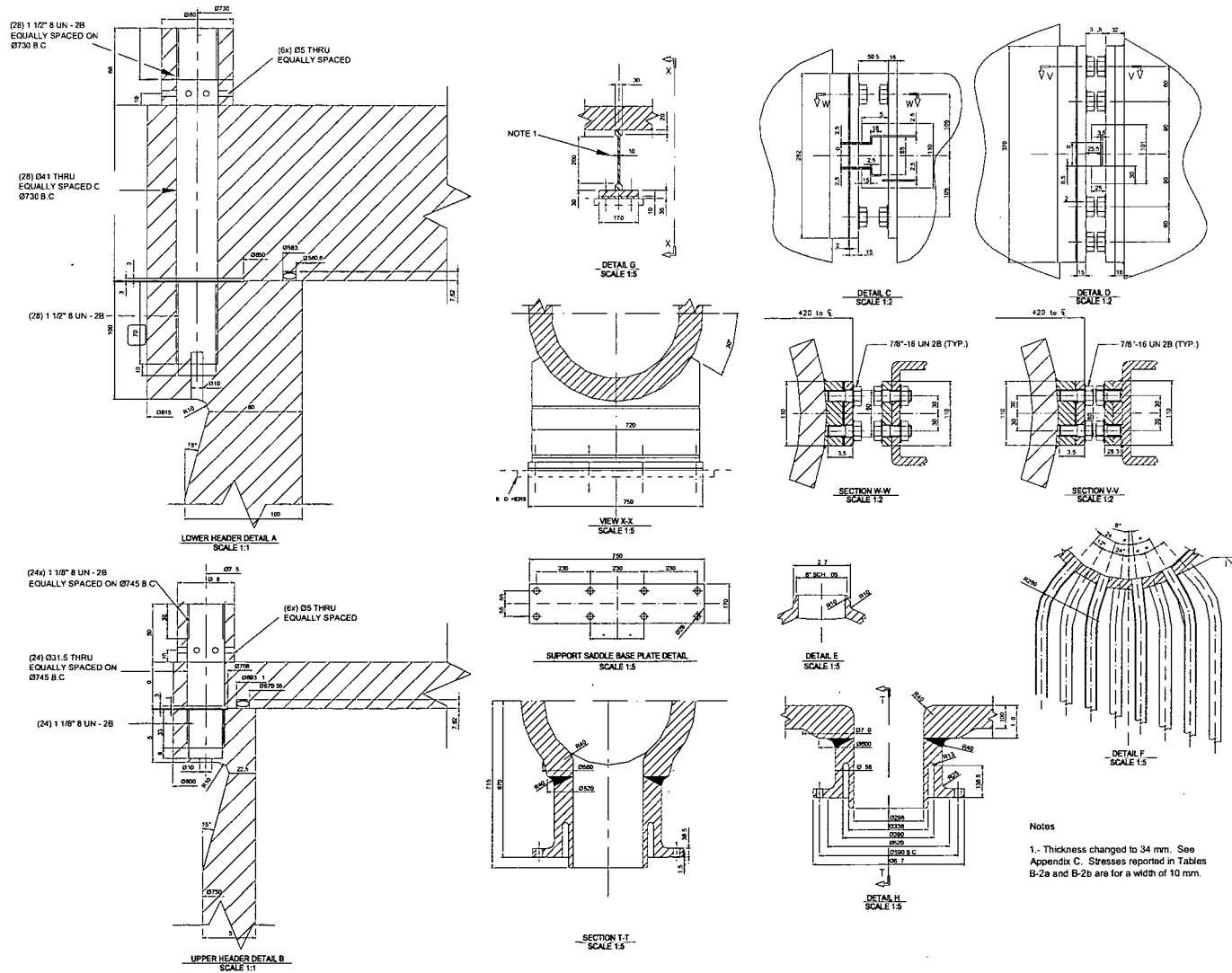


Figure B-2b: PCCS Condenser and Supports Details

NEDO-33572, Revision 3

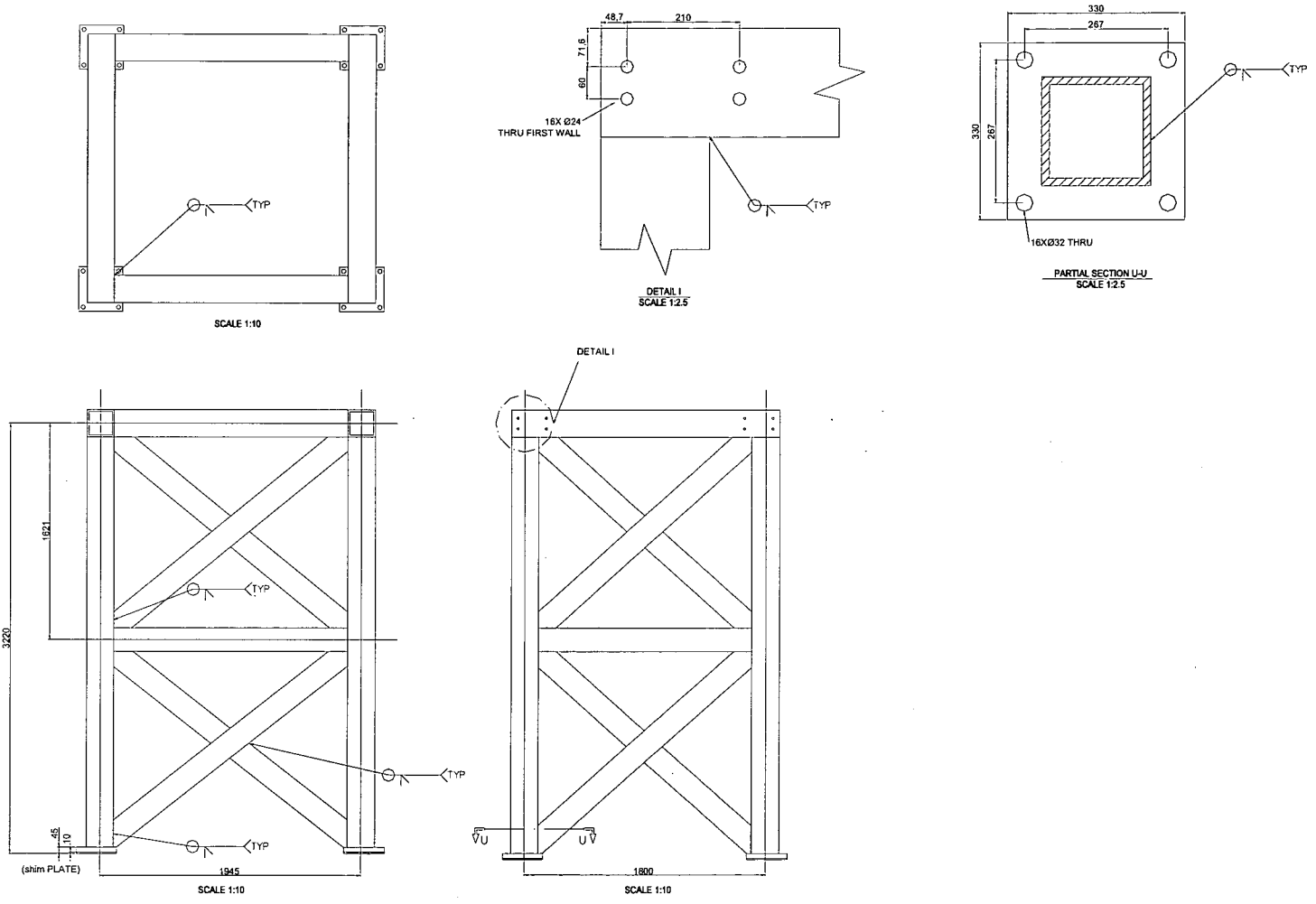


Figure B-2c: PCCS Condenser and Supports Details

B.5 Stress Results and Margin to Allowable

Table B-2a: Stress Summary of the PCCS Condenser and Supports

Component	Stress Category	Test			Design			Service Level A/B		
		Calculated Stress (MPa)	Allowable Stress (MPa)	Stress Margin (%)	Calculated Stress (MPa)	Allowable Stress (MPa)	Stress Margin (%)	Calculated Stress (MPa)	Allowable Stress (MPa)	Stress Margin (%)
Upper Header	P _m	11.1	262.9	95.8	11.1	201.3	94.5	13.7	201.3	93.2
	P _L + P _b	11.1	403.1	97.2	11.1	263.7	95.8	14.6	263.7	94.5
Lower Header (ligaments)	P _m	4.4	262.9	98.3	4.4	201.3	97.8	5.5	201.3	97.3
	P _L + P _b	4.4	403.1	98.9	4.4	263.7	98.3	5.7	263.7	97.8
Lower Header (drain nozzle)	P _m	4.4	262.9	98.3	4.4	201.3	97.8	5.5	201.3	97.3
	P _L + P _b	4.4	403.1	98.9	4.4	263.7	98.3	5.7	263.7	97.8
Tubes	P _m	4.6	262.9	98.3	4.6	201.3	97.7	4.9	201.3	97.6
	P _L + P _b	4.6	403.1	98.9	4.6	263.7	98.3	7.2	263.7	97.3
Feed Line	P _m	9.9	119.8	91.7	9.9	114.9	91.4	15.7	114.9	86.3
	P _L + P _b	9.9	183.7	94.6	9.9	150.6	93.4	18.2	150.6	87.9
Steam line	P _m	10.9	119.8	90.9	10.9	114.9	90.5	13.2	114.9	88.5
	P _L + P _b	10.9	183.7	94.1	10.9	150.6	92.8	14.9	150.6	90.1
Steam Distributor	P _m	12.6	119.8	89.5	12.6	114.9	89.0	15.1	114.9	86.9
	P _L + P _b	12.6	183.7	93.1	12.6	150.6	91.6	16.1	150.6	89.3
Condensate Lines	P _m	12.6	218.6	94.2	12.6	201.3	93.7	16.9	201.3	91.6
	P _L + P _b	12.6	335.1	96.2	12.6	302.0	95.8	16.9	302.0	94.4
Upper Header Cover	P _m	55.3	262.9	79.0	55.3	114.9	51.9	55.5	201.3	72.4
	P _L + P _b	55.3	403.1	86.3	55.3	150.6	63.3	55.5	263.7	79.0
Lower Header Cover	P _m	3.9	262.9	98.5	3.9	201.3	98.1	4.0	201.3	98.0
	P _L + P _b	3.9	403.1	99.0	3.9	263.7	98.5	4.0	263.7	98.5
Upper Header Bolt	Average Stress	25.7	144.7	82.2	25.7	110.1	76.7	25.7	220.2	88.3
Lower Header Bolt	Average Stress	8.3	570.7	98.5	8.3	212.3	96.1	8.3	424.6	98.0
Support Saddle	P _m	Negligible						5.4	183.0	97.0
	P _L + P _b							5.4	274.5	98.0
	Shear							1.1	109.8	99.0
Steel Frame Support Structure	Tension							2.7	76.6	96.5
	Shear							0.6	51.1	98.8
	Compression							2.7	47.9	94.4
	Bending	2.8	84.3	96.7						

Table B-2b: Stress Summary of the PCCS Condenser and Supports

Component	Stress Category	Service Level C-1			Service Level C-2 ¹		
		Calculated Stress (MPa)	Allowable Stress (MPa)	Stress Margin (%)	Calculated Stress (MPa)	Allowable Stress (MPa)	Stress Margin (%)
Upper Header	P _m	52.8	137.9	61.7	41.6	291.4	85.7
	P _L + P _b	64.8	180.7	64.1	53.5	381.7	86.0
Lower Header (ligaments)	P _m	16.4	291.4	94.4	271.9	291.4	6.7
	P _L + P _b	18.5	437.1	95.8	326.0	437.1	25.4
Lower Header (drain nozzle)	P _m	16.4	291.4	94.4	202.9	291.4	30.4
	P _L + P _b	18.5	421.3	95.6	383.0	421.3	9.1
Tubes ²	P _m	7.4	291.4	97.5	274.8	291.4	5.7
	P _L + P _b	42.1	381.7	89.0	344.3	381.7	9.8
Feed Line	P _m	100.9	137.9	26.8	90.8	137.9	34.2
	P _L + P _b	139.9	180.7	22.6	130.0	180.7	28.1
Steam line	P _m	43.1	137.9	68.7	32.1	137.9	76.7
	P _L + P _b	45.7	180.7	74.7	34.7	180.7	80.8
Steam Distributor	P _m	47.1	137.9	65.8	34.5	137.9	75.0
	P _L + P _b	66.5	180.7	63.2	53.8	180.7	70.2
Condensate Line Head Fitting ^{2,3}	P _m	65.5	241.6	72.9	125.0	241.6	48.3
	P _L + P _b	65.9	362.0	81.8	184.0	362.0	49.2
Condensate Line Sleeve ^{2,3}	P _m	65.5	241.6	72.9	124.0	241.6	48.7
	P _L + P _b	65.9	330.7	80.1	171.0	330.7	48.3
Condensate Line Flange ^{2,3}	P _m	65.5	241.6	72.9	136.7	241.6	43.4
	P _L + P _b	65.9	316.4	79.2	53.2	316.4	83.2
Upper Header Cover	P _m	58.1	201.3	71.1	2.8	201.3	98.6
	P _L + P _b	58.4	381.7	84.7	3.1	381.7	98.8
Lower Header Cover	P _m	4.4	201.3	97.8	200.1	201.3	0.6
	P _L + P _b	4.5	381.7	98.8	200.2	381.7	47.6
Upper Header Bolt	Avg Stress	25.7	220.2	88.3	0.1	220.2	100.0
Lower Header Bolt	Avg Stress	8.3	424.6	98.0	375.7	424.6	11.5
Support Saddle ^{2, 3, 5}	P _m	53.3	274.5	80.6	53.1	274.5	80.7
	P _L + P _b	53.4	411.7	87.0	53.2	411.7	87.1
	Shear	11.1	164.7	93.3	11.0	164.7	93.3
Steel Frame Support Structure ⁴	Tension	41.5	131.0	68.3	82.8	131.0	36.8
	Shear	9.5	87.3	89.1	18.8	87.3	78.5
	Compression	41.5	83.6	50.4	82.8	83.6	1.0
	Bending	44.5	144.1	69.1	88.8	144.1	38.4

NEDO-33572, Revision 3

Notes:

1. All components are evaluated with a static detonation pressure load of 38.7 MPa.
2. See Table C-6 of Appendix C for Service Level C-2 stresses due to a detonation wave (dynamic load) in the lower header.
3. Condensate line material changed to SA182 FXM-19 from that reported in Revision 1 of this report. Allowable stresses for these components are changed to reflect SA FXM-19. Calculated stresses reported in this table are the same as those reported in Revision 1. Discussion on material change is provided in Appendix C.
4. For Service Level C-2, seismic load is doubled to account for detonation loading.
5. Support saddle material changed to SA240 XM-19 from that reported in Revision 1 of this report. Allowable stresses for these components are changed to reflect SA240 XM-19. Calculated stresses reported in this table are the same as those reported in Revision 1. Discussion on material change is provided in Appendix C.

Table B-3a: PCCS Condenser Top Slab Penetration Anchor Bolt Dynamic Reactions

Service Level	Steam Line Reaction (per bolt)		Condensate Line Reaction (per bolt)	
	Tension (kN)	Shear (kN)	Tension (kN)	Shear (kN)
A/B	0.7	0.1	3.2	1.0
C-1	11	0.9	40	16
C-2	22	1.8	See Table C-7, Appendix C	See Table C-7, Appendix C

Table B-3b: PCCS Condenser Top Slab Penetration Anchor Bolt Thermal Reactions

Service Level	Steam Line Reaction (per bolt)		Condensate Line Reaction (per bolt)	
	Tension (kN)	Shear (kN)	Tension (kN)	Shear (kN)
Design A/B/C/D	1.6	31	73	114

Table B-4a: PCCS Condenser Support Base Plate Anchor Bolt Dynamic Reactions

Service Level	Steel Frame Support Structure Reaction (per bolt)		Support Saddle Reaction (per bolt)	
	Tension (kN)	Shear (kN)	Tension (kN)	Shear (kN)
A/B	13	6	3.0	0.5
C-1	194	81	26	5
C-2	386	192	See Table C-7, Appendix C	See Table C-7, Appendix C

Table B-4b: PCCS Condenser Support Base Plate Anchor Bolt Thermal Reactions

Service Level	Steel Frame Support Structure Reaction (per bolt)		Support Saddle Reaction (per bolt)	
	Tension (kN)	Shear (kN)	Tension (kN)	Shear (kN)
Design A/B/C/D	-	-	55	-

Table B-5: Lower Header Condensate Line under DET, Linearized Stress¹

Section	Stress Category	Calculated Stress (MPa)	Level C-2 Allowable Stress (MPa)
Tube End	P_m	254	291.4
	P_L+P_b	307	381.7
Lower Header (Drain Nozzle)	P_m	191	291.4
	P_L+P_b	369	421.3
Condensate Line Head Fitting	P_m	108	241.6
	P_L+P_b	163	362.0
Condensate Line Sleeve	P_m	107	241.6
	P_L+P_b	149	330.7

1. Stresses from Lower Header Model as described in Section B.1.2, static detonation pressure load of 38.7 MPa.

B.6 Conclusions on Service Level C Allowable

The results tabulated in Tables B-2a and B-2b indicate that the PCCS condenser seismic and hydrodynamic loads fall within the allowables, and the detonation load meets the allowables for a Service Level C.

B.7 Fatigue

From experimental observation, up to 100 reversing stress cycles may accompany a detonation inside of a closed-end cylinder. However, as shown from the experimental data, there are a few significant cycles, but the remainder of the cycles will experience a significant decay in stress amplitude due to the limited ability of the structural mass to react to the quick speed of the detonation load and associated dampening. Since it is difficult to quantify the peak load for individual cycles, it is conservatively assumed that within the first 50 cycles, the peak cyclic stress amplitude has decayed to at least one-half of the maximum amplitude. The conservative assumption is then made that the first 50 cycles are equal in magnitude to the maximum peak stress. Due to the lower stress intensity range that occurs for the remaining 50 cycles, these cycles are assumed to be inconsequential contributors to fatigue due to the log function associated with the cyclic fatigue curve. These assumptions are carried forward for all the PCCS condenser components that experience DET loads.

For all components other than the lower drum cover bolts, the stress range is defined as two times the DET stress, recognizing from experimental data that there is a stress reversal cycle that is compressive where negative strains occur. Since the seismic and thermal cycles induce relatively low stresses that have a very small associated fatigue usage, only the DET stress intensity range is used to calculate the stress intensity range, and the total is then halved to determine the alternating stress as defined by the ASME code methodology.

In the case of the lower drum cover bolts, the bolts do not directly experience DET loads, but receive a reaction load from those DET loads that are applied to the cover plate. As such, the cover plate will experience alternating stresses in response to the DET event, but the bolts will only experience tensile stress loads in reaction to the DET load on the cover plate when internal pressure conditions exist. During the negative part of stress reversal cycle of the cover plate, the flange of the lower steam drum absorbs the compressive load at the flange interface instead of the bolts. Therefore, the compressive or negative strain does not occur in the bolts, and the stress range is equal to the initial pressure amplitude of the DET event. The stresses due to seismic and thermal are again negligible. Consistent with NE-3232.3(c), the DET stress is then multiplied by a factor of four to account for the stress concentrations associated with the threads. This total stress is then halved to determine the alternating stress.

The stress values, allowed cycles, expected cycles and usage factors for all components that have the potential for significant cyclic loading are reported in Table B-5. All usage factors fall below 1.0 and therefore detailed fatigue analysis is not required.

Table B-5: PCCS Condenser Fatigue Assessment

Component	DET Stress (MPa)	Stress Range (Mpa)	Alternate Stress (MPa)	Allowed Cycles	Expected Cycles at Fatigue Levels ⁽¹⁾	Usage Factor
Tubes	272.0	544.0	272	$9 \cdot 10^4$	600	0.00667
Lower Header	513.0	1026.0	513	$5 \cdot 10^3$	600	0.12
Lower Header Cover	199.6	399.2	199.6	$7 \cdot 10^5$	600	0.00086
Condensate Drain	507	1014	507	$5 \cdot 10^3$	600	0.12
Lower Header Cover Bolt	$346.8^{(2)}$	$346.8 \times 4^{(3)} = 1387$	693.5	983	600	0.61

⁽¹⁾ Expected cycles equal 50 cycles times [[]] detonations

⁽²⁾ Detonation stress adjusted by elastic modulus ratio of 0.923 in accordance with NE-3232.3(d)

⁽³⁾ Strength Reduction Factor of 4 for Fatigue Evaluation of Threaded members

APPENDIX C - ANCHOR BOLT REACTIONS DUE TO DETONATION AND STRESSES FOR SELECTED PCCS COMPONENTS

C.1 Introduction

The dynamic loads due to a hydrogen detonation in the PCCS lower header are of short duration and large amplitude. To calculate the effects of these loads a finite element (FE) model of the PCCS system was employed. A postulated traveling pressure wave was applied to the inner faces of the lower header and the transient response of the PCCS was calculated. From these, results peak loads were extracted at the PCCS lower header mounting points and bottom tube ends and then multiplied by a factor of 2.5.

C.1.1 Detonation Wave Profile

The detonation wave profile used was developed to be consistent with Reference 1 in which wave profiles traveling down pipes were experimentally measured. The initial detonation wave profile is characterized by a sharp pressure discontinuity followed by an exponential rarefaction curve, which ends in a steady state pressure greater than the initial pressure.

The profile used is defined in Equation 1 where $t_{cj} = x/v_{cj}$ which is the time required for the detonation wave to travel from the origin to the location of interest. P_1 , P_2 , and P_3 are the gas pressure before, during and after the wave has traveled through the gas, and $T \approx t_{cj}/3$ is the time constant for rarefaction wave following the initial pressure pulse. The pressure P_2 (peak pressure in the wave) is also denoted as P_{cj} which is the pressure at which the Rayleigh and Hugoniot curves become tangent, Reference 2. P_{cj} is a thermodynamic property of the detonating media alone. In addition to yielding the peak pressure this tangency point also yields the steady state velocity of the wave front with respect to the material in front of the wave. This velocity is defined as the Chapman- Jouguet velocity (v_{cj}). The v_{cj} value used in this analysis is 2910.75 m/s. Table C-1 presents the parameters used to define the detonation wave profile.

$$P(x,t) = \begin{cases} P_1 & 0 < t < t_{cj} \\ (P_2 - P_3)e^{-\frac{(t-t_{cj})}{T}} + P_3 & t_{cj} < t < \infty \end{cases} \quad 1$$

C.1.2 Load Definition and Modeling Assumptions

The load applied to the PCCS system will tend to be self equilibrating in that as the detonation wave dies out and a steady state pressure ensues leading to a zero net load on the PCCS bolting or support structure. For this reason when considering hydrogen detonation only the transient response of the system is of interest. In this case the postulated worst case detonation points are assumed to be those points which yield the longest transient non-equilibrating loads. The following assumptions have been used in the analysis.

1. Detonation occurs at one face of the lower header and pressurizes that face.
2. The wave front shown in Figure C-2 runs the length of the lower header and pressurizes the other face of the lower header eventually equilibrating the load on the other face of the lower header. Additional wave interactions have been neglected.
3. The wave profile is a function of propagation distance. The propagation distance being used to calculate the time constant used in this analysis is one half the length of the PCCS drum in the direction of propagation. The time constant being used is $T=t_{cj}/6$ where t_{cj} is the time for the wave to propagate through the drum. The wave profile used at the midpoint of the lower header is shown in Figure C-2. Wave profiles at other locations along the length of the lower header are the same with P_2 occurring at time $t_{cj} = x/v_{cj}$.
4. No hydrodynamic effects are considered in the calculation. The water surrounding the PCCS system would act to radiate energy away from the PCCS system, which would tend to reduce the loading seen at the mount points.
5. One half of the PCCS system is considered; the half of the system not included in the model will not contribute to the response in the time frame of interest.
- 6. Damping is not included in the model.**
7. The final load reported here are directly recovered from the analysis, any additional scale factors have not been applied.

C.1.3 Finite Element Model

The FE model shown in Figure C-3 - Figure C-5 was created using ANSYS solid 92 and shell 181 elements. The model consists of ~412000 Elements and ~140000 nodes (See Table C-2: Simulation Parameters). As mentioned previously, the pressure transient is applied to the lower drum using an ANSYS Table. The table was populated with pressure values as a function of time and position. The detonation was assumed to begin at one face of the PCCS header. As the analysis stepped through time the pressures applied to the inner faces of the lower header was updated to account for the propagation of the detonation front. As the detonation front reaches the opposite side of the header it is assumed to continue on rather than reflecting, this approach decreases the pressure load acting to oppose the momentum of the bottom header. Once the wave has completely propagated through the lower header, the pressure in the lower header is assumed to remain at the steady state pressure behind the wave front (P_3).

The transient simulation approach here is a direct integration implicit approach. The simulation has been split into two distinct times. The first being the time in which the wave is propagating through the PCCS Lower Header. This time was defined as 1.25 times the length of the lower header divided by V_{cj} (1.57 ms). This first time segment was divided into 100 steps leading to a time step size of 16 μ s. After the wave propagation was finished the

simulation was continued in order to capture at least one cycle of the structural mode being excited. The time step used in this time phase was 100 μ s. The time period for this portion of the simulation is between 1.6 to 18.3 ms. As mentioned previously, no damping was included in the model.

Each individual mount point on the PCCS bottom header was coupled to a node fixed in all directions. The loads seen by the fixed nodes were used to extract the transient mount point loads.

Figure C-6 shows a schematic cross-section of the condensate line as it was modeled. Figure C-1 is a figure of the entire PCCS condenser.

C.1.4 Finite Element Model Results

The displacement results shown in Figure C-7 - Figure C-12 show various time points in the simulation. The plotted displacements are actual scale. The first 4 plots show time in which the wave is still propagating in the PCCS header. Figure C-12 shows the time at which lateral loads are maximum on the drain line.

The overall loads (horizontal & vertical) seen by the mounting points are shown in Figure C-13. With reference to this figure, the horizontal load response has two major frequency components. This response is characterized by one relatively low frequency mode with a high frequency mode superimposed on top.

C.1.4.1 Horizontal (Direction of Wave Propagation), Vertical, and Moment Loads

When the horizontal load from each support is shown individually in Figure C-14 (2 saddle supports and the drain line), it can be seen that the drain line sees a much greater proportion of the total load. The peak lateral load on the drain line from this simulation was found to be 909 kN while the peak load on the saddle bolting was found to be 152 kN, Table C-3a.

Peak vertical loads are 895 kN and 683 kN for the drain line and each saddle support, Table C-3a.

Peak moment loads are shown in Figure C-15

C.1.4.2 Condenser Tube Loads

The condenser tubes are modeled using solid elements with a coarse distribution. Because of this, the stresses predicted will not be accurate. For this reason the following post processing procedure was conducted to retrieve the loads found in Table C-3b.

1. The time at which the largest stress intensity occurs at the base of the tube is found by plotting stress intensities through out time.
2. At the time selected from above, a cross section cut is created at the base of the tube.
3. At the cross section of interest, the loads are extracted using the FSUM command where the loads are centered at the middle of the cross section.

C.1.4.3 Deleted

C.1.4.4 Frequency Content

To gain some understanding of the frequencies that are present in the forced response, the free vibrations time portion of horizontal load on the drain line was processed using an Fast Fourier Transform (FFT). This result can be seen in Figure C-16. The two major peaks that stand out when comparing the FFT results to the time history results are the peak between 100 and 200 Hz, which corresponds to the low frequency response. The high frequency response superimposed on the low frequency result best matches the 1800-1900 Hz peak. Frequencies with the largest time step below 2000 Hz will contain 5 time steps per wave length.

C.1.5 Wave Reflections and Multiplication Factors

In this analysis the free field wave form discussed above was assumed to load the structure. This assumption neglects the impacts due to the complex wave reflections and interactions that would be found in an actual event. The wave reflection of greatest importance is that due to the reflection of the pressure wave on the face opposite to the assumed detonation face. The justification for neglecting the wave reflections is as follows.

Upon reflection, the peak pressure seen by the end plate can be as high as 2.5 times the peak free field pressure. After reflection, having already propagated through the media, the detonation wave would have spent its reactants and can then be treated as a nonreactive shock front. This front would be followed by a rarefaction wave steeper than that seen in Figure C-2. For this reason, the wave would die down relatively quickly. This statement is supported by Reference 3, in which peak pressure of the incident and reflecting waves are compared at specific locations along the length of detonation tubes. From this work, the experimentally measured peak reflected pressure had been found to reduce to 1.3 times the incident peak pressure after having only traveled back through 10% of the total length of the detonation tube. Using this information, the effects of the wave reflections along the length of the lower header can be assumed to be negligible after one reflection.

The wave transit time for one length on the bottom header is ~1.26 ms. By also considering the results presented in Figure C-14 and C-16 it can be seen that the major structural modes leading to drain line loading have a frequency of ~150Hz which equates to a period of 6.67 ms. The ratio of the response period over the transient time yields a value of 5.3. As this ratio is greater than four, it can be understood that the pressure due to the wave reflection on the opposing face will act against the momentum of the structure. In other words, the structure will still be moving in the direction in which it was initially forced when the reflection wave pressure is seen on the opposing face. In Figure C-14 this can be seen as the sharp drop in load at ~1.3ms. As this is the case, neglecting the spike in reflected pressure is actually conservative when considering the loads experienced by the mounting bolts. Considering the higher reflection pressure will lead to a lower peak momentum, which also leads to lower overall loads on the mounting bolts.

C.1.6 Peak Loads and Calculated Stress Intensities

Although wave reflection is not expected to add to the anchor bolt loads (Section C.1.5), the loads given in Tables C-3a and C-3b are multiplied by a factor of 2.5 and are shown in Table C-4. These loads are used to calculate stress intensities for the condensate line head fitting, condensate line sleeve, support saddle, and bottom of tube end.

C.1.6.1 Support Saddle and Condensate Line Stresses

Stresses for the support saddle, condensate line head fitting, condensate line sleeve, and tube end were calculated using the loads shown in Table C-4 and are given in Table C-5. The shear (τ) and tensile/compressive (σ) stresses were calculated by dividing the horizontal forces and the vertical forces by the cross-sectional area of interest. The bending stresses were calculated using Equation 2.

$$\sigma_b = \frac{Mc}{I} \quad 2$$

where:

σ_b = bending stress, MPa

M = moment, N-m

I = moment of inertia for cross-section of interest, m⁴

c = distance to extreme fiber from neutral axis, m

C.1.6.2 Stress Intensities

Principal stresses can be calculated using the following equation for a given cross-section.

$$S_1, S_2 = \frac{\sigma_x + \sigma_y}{2} \pm \sqrt{\left(\frac{\sigma_x - \sigma_y}{2}\right)^2 + \tau_{xy}^2} \quad 3$$

where:

S₁, S₂ = principal stresses 1 and 2, MPa

σ_x = normal stress in x direction, MPa

σ_y = normal stress in y direction, MPa

τ = shear stress, MPa

For the PCCS case analyzed in this appendix, the normal stresses only occur in one direction due to the nature of the detonation wave traversing the lower header down its long axis, eliminating x-direction from Equation 3.

$$S_1, S_2 = \frac{\sigma_y}{2} \pm \sqrt{\left(\frac{\sigma_y}{2}\right)^2 + \tau_{xy}^2} \quad 4$$

The stress intensity, P, can then be calculated by subtracting the minimum principal stress from the maximum principal stress.

$$P = \text{Max}(S_1, S_2) - \text{Min}(S_1, S_2) \quad 5$$

The membrane stress intensities for components in Table C-5 can be calculated using Equations 4 and 5 by substituting in the tensile stress and the shear stress:

$$S_{Lb1}, S_{Lb2} = \frac{(\sigma_t + \sigma_b)}{2} \pm \sqrt{\left(\frac{(\sigma_t + \sigma_b)}{2}\right)^2 + \tau^2} \quad 6$$

and

$$P_m = \text{Max}(S_{Lb1}, S_{Lb2}) - \text{Min}(S_{Lb1}, S_{Lb2}) \quad 7$$

P_m is the membrane stress intensity. With values from Table C-5 and Equations 6 and 7, P_m calculated values are shown in Table C-6.

C.1.6.3 Service Level C-2 Load Combination Stresses

Seismic stress was combined with the detonation stress in Table C-6 using SRSS and then dead weight plus thermal stresses were added directly, $D + Ta + \text{SQRT}(SSE^2 + DET^2)$, and are shown as Service Level C-2 calculated stresses in Table C-6. The seismic, dead weight, thermal stresses used are the same used to calculate values shown in Table B-2b of Appendix B. The shear value in Table C-6 is the same given in Table B-2b.

Stresses for the condensate line sleeve exceed the calculated stresses for Service Level C-2 shown in Table B-2b but are within the allowable for SA 182 Grade FXM-19 as shown in Table C-6. The condensate line material (head fitting, sleeve, flange) was changed from a 304L stainless steel to a XM-19 stainless steel from that shown in Revision 1 of this report. See section C.1.6.5 for material difference discussion.

Calculated Service Level C-2 stresses for the support saddle are shown Table C-6 and exceed the calculated stresses for Service Level C-2 in Table B-2b but are within the allowable limits for SA 240 XM-19. The width of the thinnest section at the saddle and the base and the attachment to the lower header has been increased to be slightly more than the width of the base and the attachment shown in Figure B-2a. The width for the entire saddle support assembly is now 34 mm. In addition, to the increased width, the material was changed from 304L to SA 240 XM-19. See section C.1.6.6 for material difference and thickness discussion.

C.1.6.4 PCCS Condenser Lower Header Mount Dynamic Reactions

Mount reaction loads for the PCCS lower header condensate line and the support saddle are given in Table C-7.

C.1.6.5 PCCS Condensate Line and Support Saddle Material

Forging material SA-182 Grade FXM-19 is an approved material for Class MC components. The change from 304L (in Revision 1 of report) to XM-19 for the drain line does not impact ANSYS analysis in Appendix B or Appendix C. Both materials behave very similar in that re-running the analyses would produce approximately the same results.

C.1.6.6 PCCS Support Saddle Material and Dimensions

The support saddle is a Subsection NF component that supports a Class MC component. The mechanical behavior of 304L is similar to that of XM-19 with respect to dynamic behavior.

The change to a thicker cross-section for the whole support saddle plate will increase the stiffness of it but will not significantly change the overall response of the lower header with respect to the condensate line. The condensate line dominates the response of the system; this can be seen in Figure C-15. The moments for the condensate line are about 13 times larger than those of the support saddles. The moments of inertia for condensate line sleeve and condensate line head fitting are three orders of magnitude larger than that of the thickened support saddle. In addition, a margin of 20.4% exists to the allowable stress of the support saddle, Table C-6. This margin will accommodate any increase to the additional load from the increase in stiffness.

C.1.7 References

1. W.M. Beltman and J.E. Shepherd, "Linear Elastic Response of tubes to Internal Detonation Loading," Department of Mechanical Engineering, University of Twente, Netherlands. Graduate Aeronautical Laboratories, California Institute of Technology, Pasadena, CA.
2. Davis, W. Fickett W.C., "Detonation Theory and Experiment. Mineola," Dover Publications, 2000. 0-486-41456-6.
3. J.E. Shepherd, et. al., "Shock Wave Produced by Reflected Detonations," Progress in Astronautics and Aeronautics, Troy, NY, 1989, Vol. 134.
4. J. E. Shepherd, "Structural Response of Piping to Internal Gas Detonation". ASME Pressure Vessels and Piping Conference, 2006. VP2006-ICPVT11-93670, presented July 23-27 2006 Vancouver BC Canada.

Table C-1: Input Data for Detonation Wave Profile and Load

Parameter	Value	Notes
P ₁ , pressure, (Pa)	407 x 10 ³	Peak containment pressure for limiting ESBWR LOCA
P ₂ pressure, (Pa)	8.0 x 10 ⁶	Initial pressure of 407 kPa times a factor of 19 for hydrogen oxygen detonations.
P ₃ pressure, (Pa)	3.2 x 10 ⁶	Pressure behind the expansion wave is approximately 0.4 times P ₂ , Reference 4.
v _{ej} velocity, (m/s)	2910.75	Chapman-Jouguet velocity for hydrogen and oxygen mixture at initial pressure and temperature of 4 atm and 25 °C, respectively
Length of lower header, (m)	3.662	See Appendix B, Figure B-2a.
Inner diameter at end cover, (m)	0.550	See Appendix B, Figure B-2a.

Table C-2: Simulation Parameters

Parameter	Value
Nodes	~140000
Elements	~412000
Analysis Type	Full Transient, Direct Integration
Time Step 1	16 μ s
Time Step 2	100 μ s
Total Time	18.3 ms
Number of Steps	267
Damping	No Damping Applied

Table C-3a: Mounting Loads¹

Parameter	Description	Load
Condensate Line (kN)	Horizontal	909
Condensate Line (kN)	Vertical	+895
		-1368
Condensate Line Moment (kN-m)	Moment About X	198
Saddle Support (kN)	Horizontal	152
Saddle Support (kN)	Vertical	+683
		-210
Saddle Support Moment (kN-m)	Moment About X	14

1. (+) designates tension and (-) designates compression

Table C-3b: Tube End Loads

Parameter	Description	Load
Condenser Tube Moments (maximum moment at the base of tubes)	Shear Load (kN)	6.3
	Axial Load (kN)	12.2
	Moment About X (kN-m)	0.3514

Table C-4: Loads with 2.5 Multiplier¹

Parameter	Description	Load
Condensate Line (kN)	Horizontal	2272.5
Condensate Line (kN)	Vertical	+2237.5
		-3420.0
Condensate Line Moment (kN-m)	Moment About X	495.0
Saddle Support (kN)	Horizontal	380.0
Saddle Support (kN)	Vertical	+1707.5
		-525.0
Saddle Support Moment (kN-m)	Moment About X	35.0
Tube End (kN)	Shear Load	15.75
Tube End (kN)	Axial Load	30.5
Tube End Moment (kN-m)	Moment About X	0.8785

1. (+) designates tension and (-) designates compression

Table C-5: Stresses Due to Detonation Wave in Lower Header⁴

Parameter	Load Description	Stress (See Section C.1.6.1 for Definitions)	Calculated Stresses from Loads in Table C-4				
			Condensate Line Sleeve, Cross-Section ¹ , MPa	Condensate Line Head Fitting, Cross-Section ¹ , MPa	Support Saddle Cross-Section ² , MPa	Tube End Cross-Section ³ , MPa	
Condensate Line	Horizontal	τ	50.18	23.92			
Condensate Line	Vertical	σ_t	+49.40	+23.55			
Condensate Line	Vertical	σ_c	-75.51	-36.00			
Condensate Line	Moment About X	σ_b	110.7	63.94			
Support Saddle	Horizontal	τ					15.52
Support Saddle	Vertical	σ_t					+69.75
Support Saddle	Vertical	σ_c			-21.45		
Support Saddle	Moment About X	σ_b			252.3		
Tube End	Horizontal	τ					27.03
Tube End	Vertical	σ_t					52.34
Tube End	Moment About X	σ_b	138.64				

1. The analyzed sleeve section of condensate line is 34 mm thick with outer radius of 229 mm and inner radius of 195 mm; head fitting section of condensate line is 80 mm thick with outer radius 229 mm and inner radius of 149 mm, (See Figure B-2b for dimensions).
2. The analyzed thinnest section for the support saddle is 720 mm x 10 mm in the ANSYS model. 24 mm is added to this section of the support saddle shown in Figure B-2b for a consistent cross-section top-to-bottom of 720 mm x 34 mm. Calculated stresses shown are respect to new cross-section.
3. The analyzed tube section is [[]] mm thick with an out radius of [[]] and inner radius of [[]] mm, (See Figure B-2b for dimensions).
4. (+) designates tension and (-) designates compression.

Table C-6: Stress Summary for Selected PCCS Components: Detonation Wave in Lower Header

Section	Stress Category	Calculated Stress, Under Detonation Load ^{1,4} (MPa)	Calculated Stress for Service Level C-2 Load Combination ² , MPa	Allowable Stress for Service Level C-2, MPa	Margin, %
Condensate Line Head Fitting ³	P _m	99.7	125.5	291.4	56.9
	Deleted				
Condensate Line Sleeve ³	P _m	188.9	209.1 ⁶	291.4	28.2
	Deleted				
Support Saddle ^{5,7}	P _m	76.3	93.0 ⁶	274.5	66.1
	P _L + P _b	323.6	327.9 ⁶	411.7	20.4
	Shear	15.5	19.1 ⁶	164.7	88.4
Tube End ⁷	P _m	75.2	96.1	291.4	67.0
	P _L + P _b	198.5	237.0	381.7	37.9

1. Stresses calculated using Table C-5 values and Equations 7 and 9 in Section C.1.6.2. Shear stress for the support saddle was carried forward from Table C-5.
2. Seismic stress was combined with the detonation stress using SRSS and then dead weight plus thermal stresses were added directly, $D + T_a + \text{SQRT}(\text{SSE}^2 + \text{DET}^2)$. Seismic, dead weight, thermal stresses used are the same shown in Table B-2b of Appendix B.
3. Condensate line material changed to SA182 Grade FXM-19 from that reported in Revision 1 report.
4. These stress values can be directly compared to those provided in Table B-5b of Appendix B for the tube end and condensate line head fitting and condensate line sleeve.
5. Support Saddle material changed to SA240 XM-19 from that reported in Revision 1 of report.
6. The stresses shown are higher than the stresses reported in Table B-2b for Service Level C-2. All other locations shown in this column have stresses that are less than those shown in Table B-2b.
7. P_L + P_b is calculated using Equations 6 and 7 in Section C.1.6.2. P_m is also calculated using Equations 7 and 8 but with the term ob set equal to zero.

Table C-7: PCCS Condenser Lower Condenser Mount Dynamic Reactions: Detonation Wave in Lower Header

Service Level ¹	Support Saddle Mount Reaction			Condensate Line Mount Reaction		
	Tension (kN)	Shear (kN)	Moment About X (kN-m)	Tension (kN)	Shear (kN)	Moment About X (kN-m)
C-2	+683-210	14	14	+895 -1368	909	198
C-2 with 2.5 Multiplier	+1707.5 -525.0	380.0	35.0	+2237.5 -3420.0	2272.5	495.0

1. See Section B.3 of Appendix B for service level load combinations.

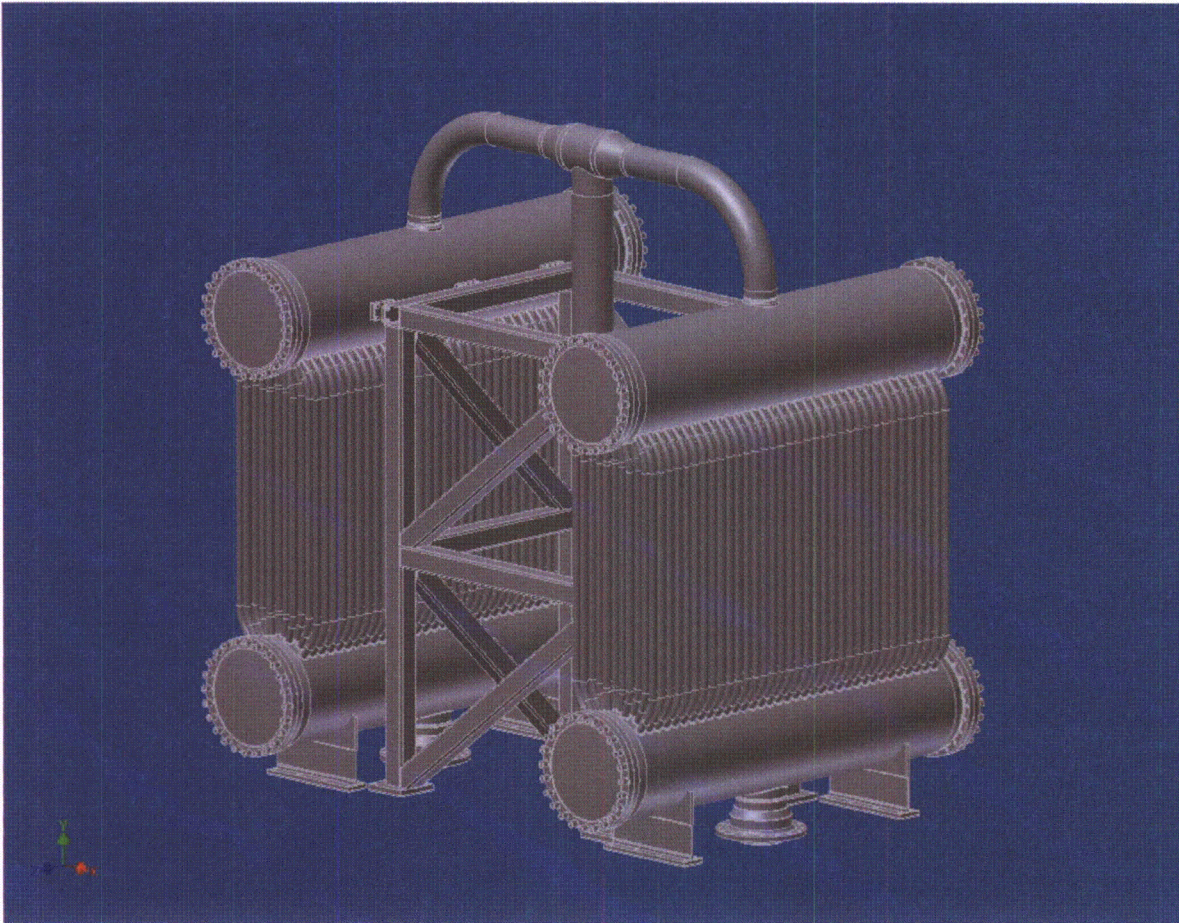


Figure C-1: PCCS Condenser

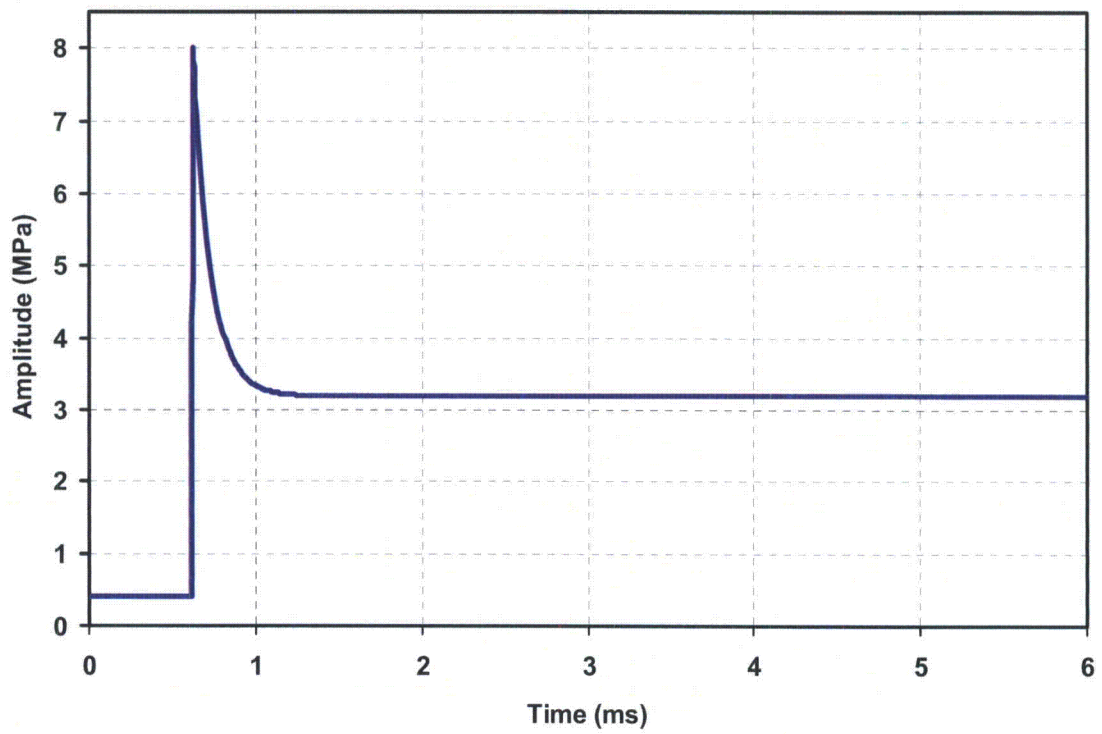


Figure C-2: Pressure Profile of Detonation Wave at Midpoint of PCCS Lower header

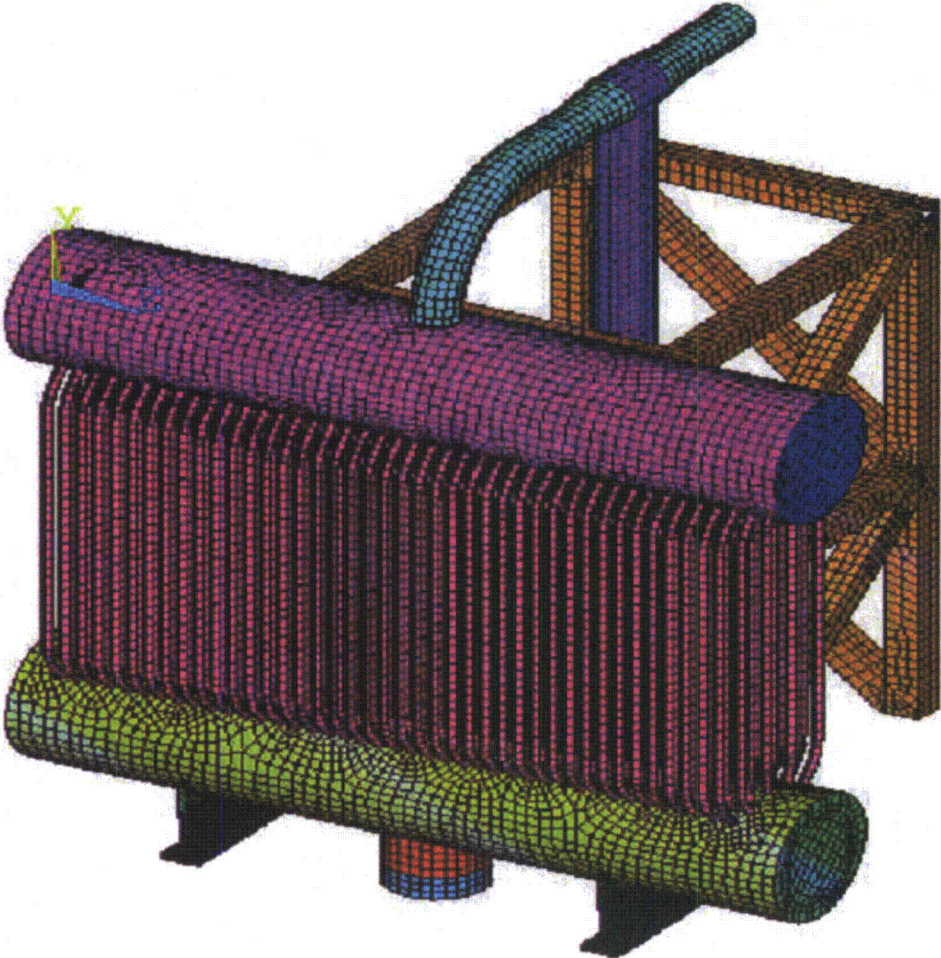


Figure C-3: Finite Element Model of PCCS System

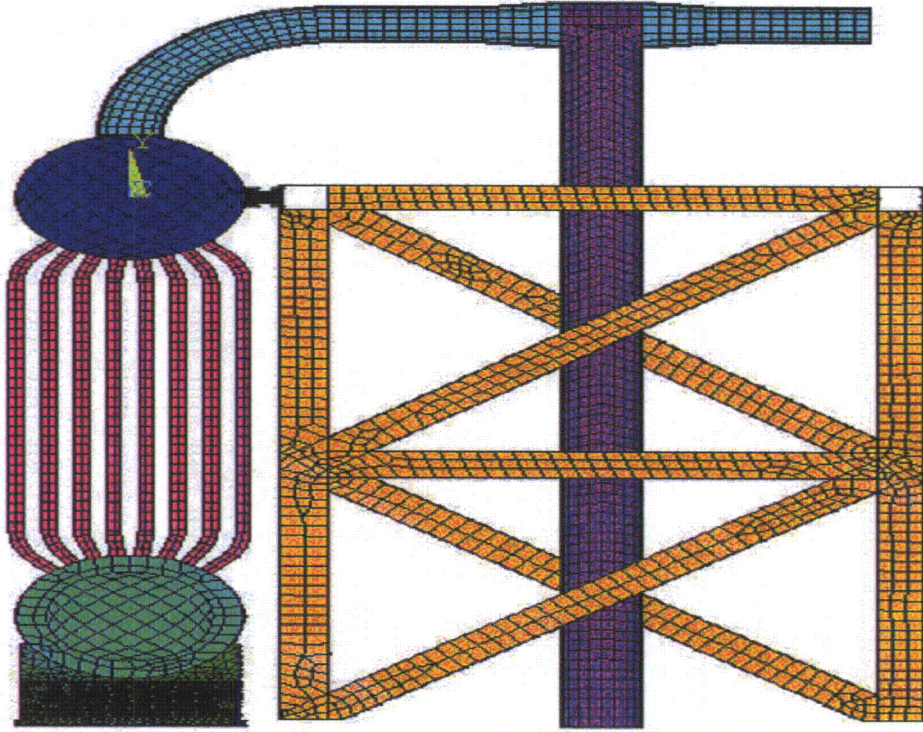


Figure C-4: Finite Element Model of PCCS System

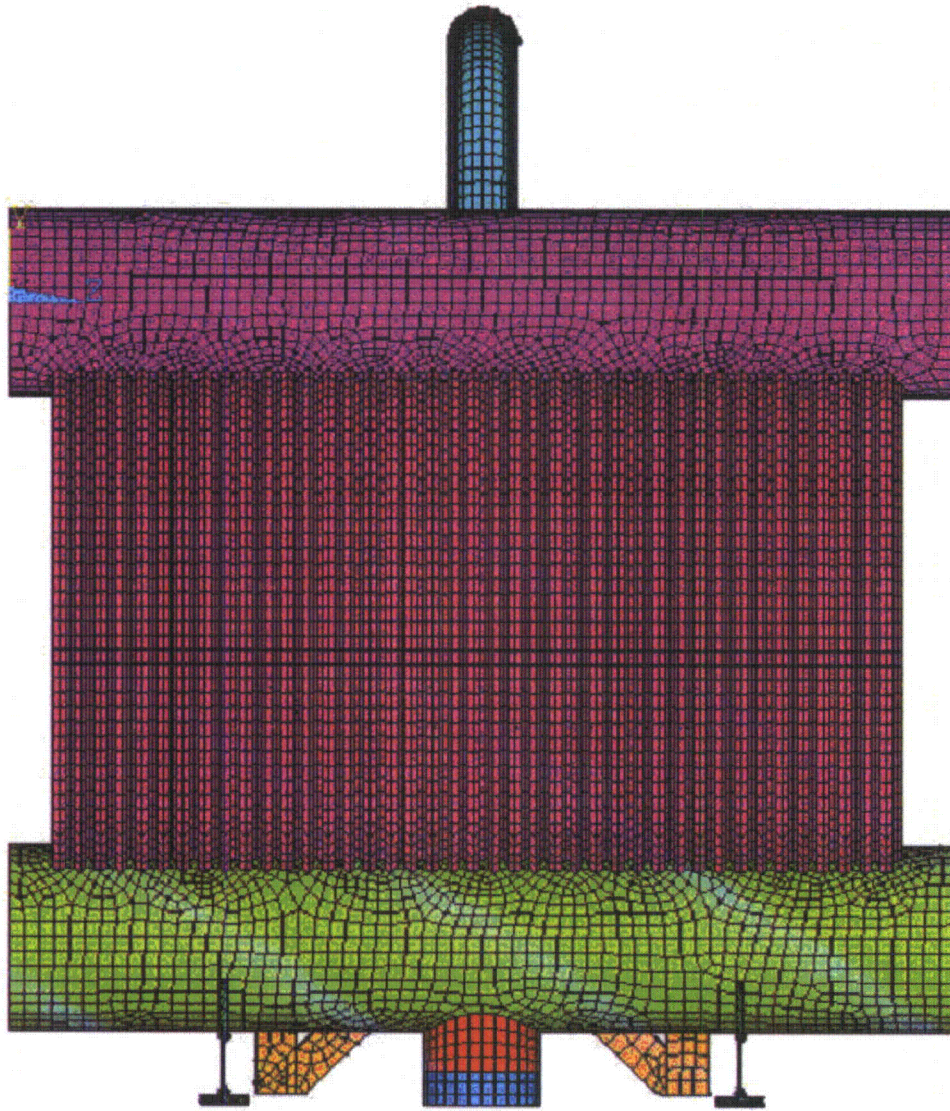


Figure C-5: Finite Element Model of PCCS System

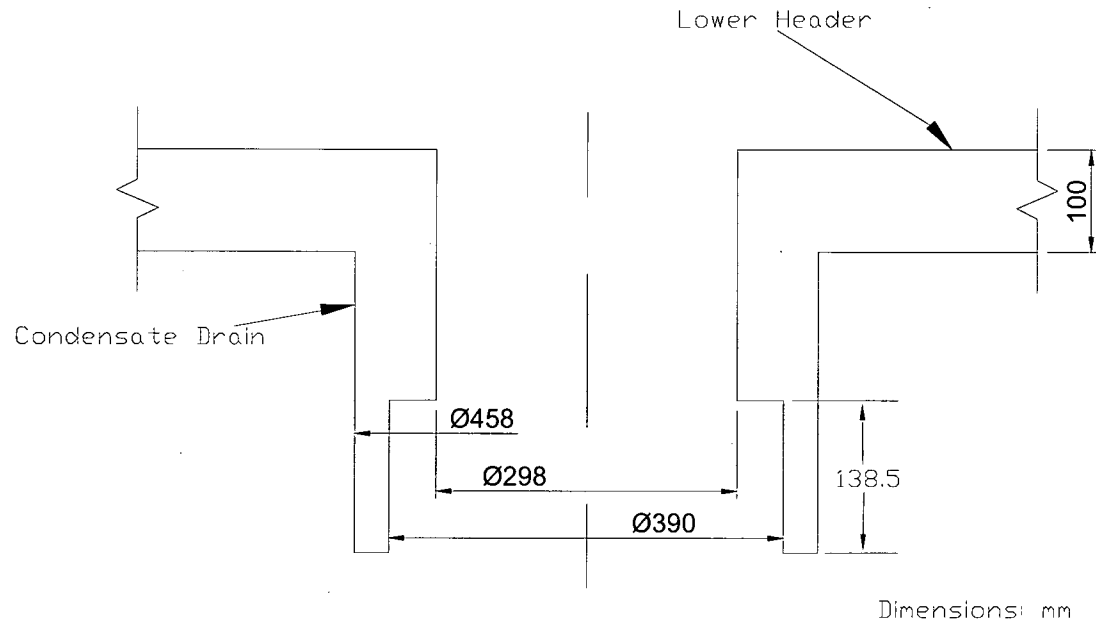


Figure C-6: PCCS Condensate Line Dimension as Modeled

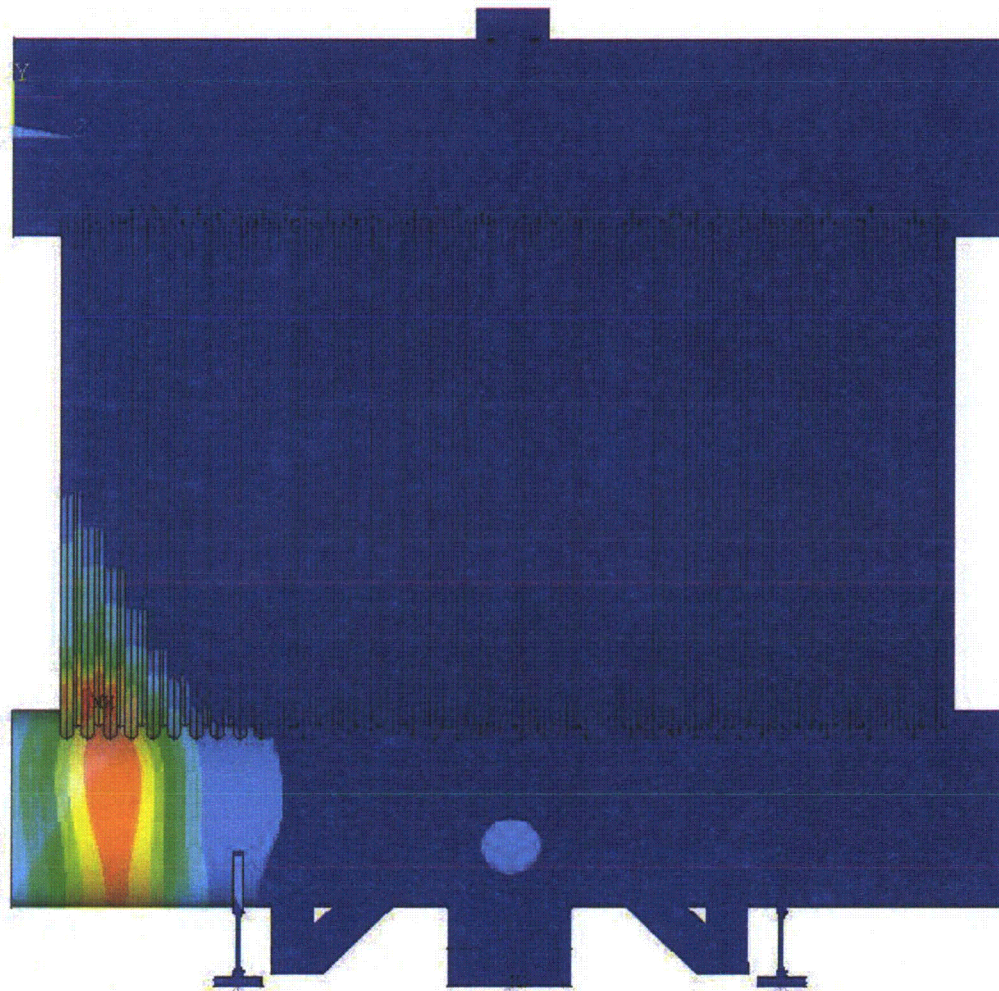


Figure C-7: Lower Header Displacement Contour (pressure wave front $\frac{1}{4}$ through Lower Header, displacement plots actual scale)

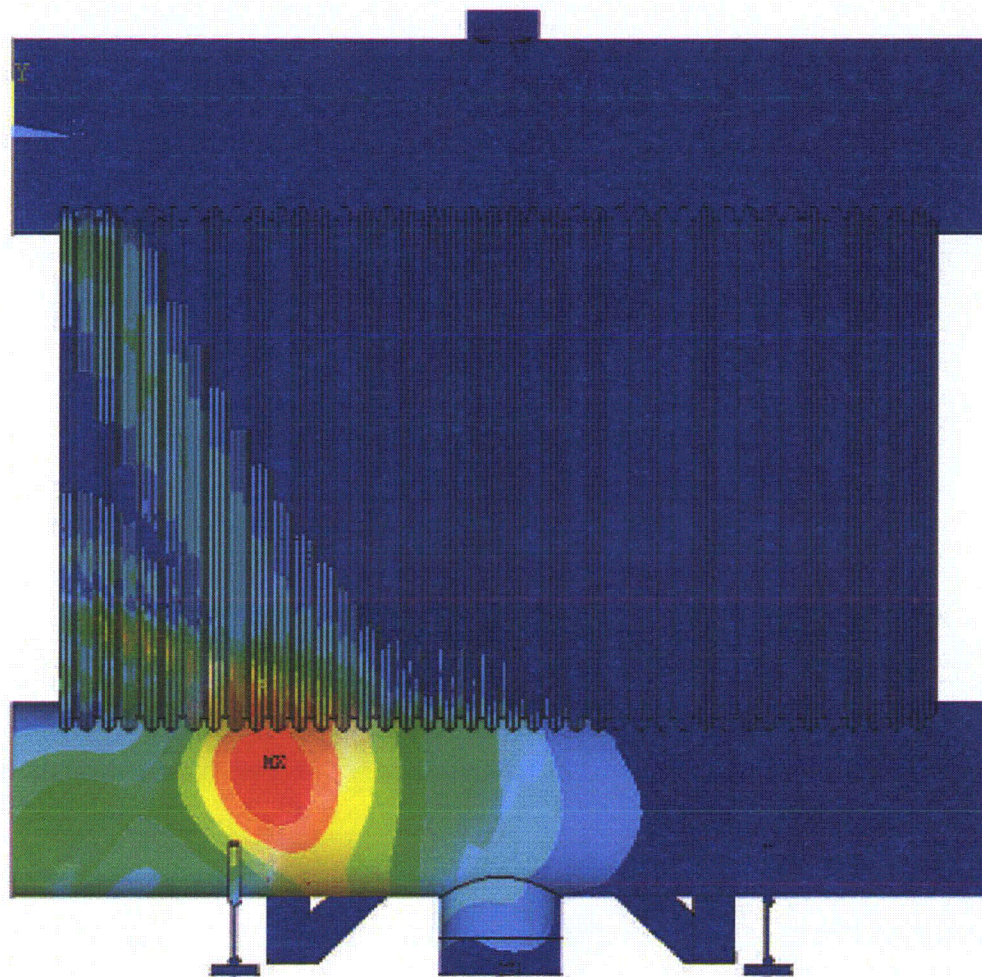


Figure C-8: Lower Header Displacement Contour (pressure wave front ½ through Lower Header, displacement plots actual scale)

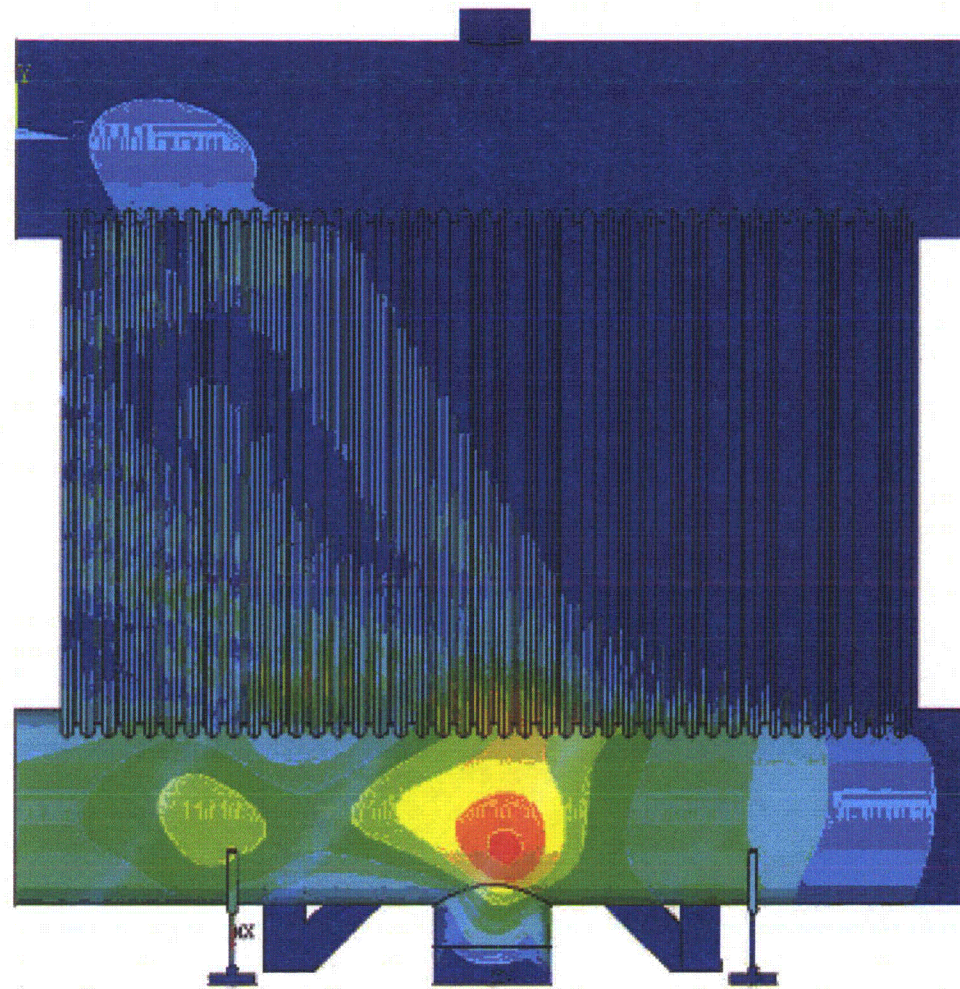


Figure C-9: Lower Header Displacement Contour (pressure wave front $\frac{3}{4}$ through Lower Header, displacement plots actual scale)

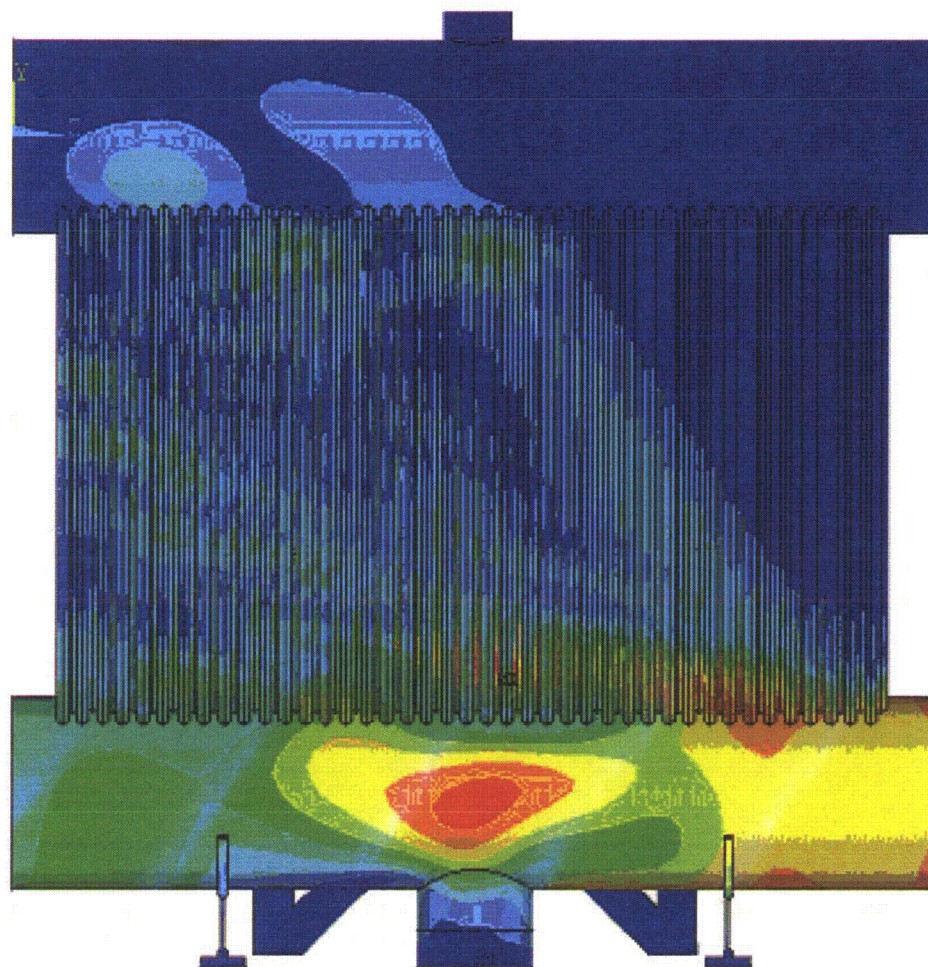


Figure C-10: Contours of displacement, start of steady state pressure in Lower Header, displacement plots actual scale

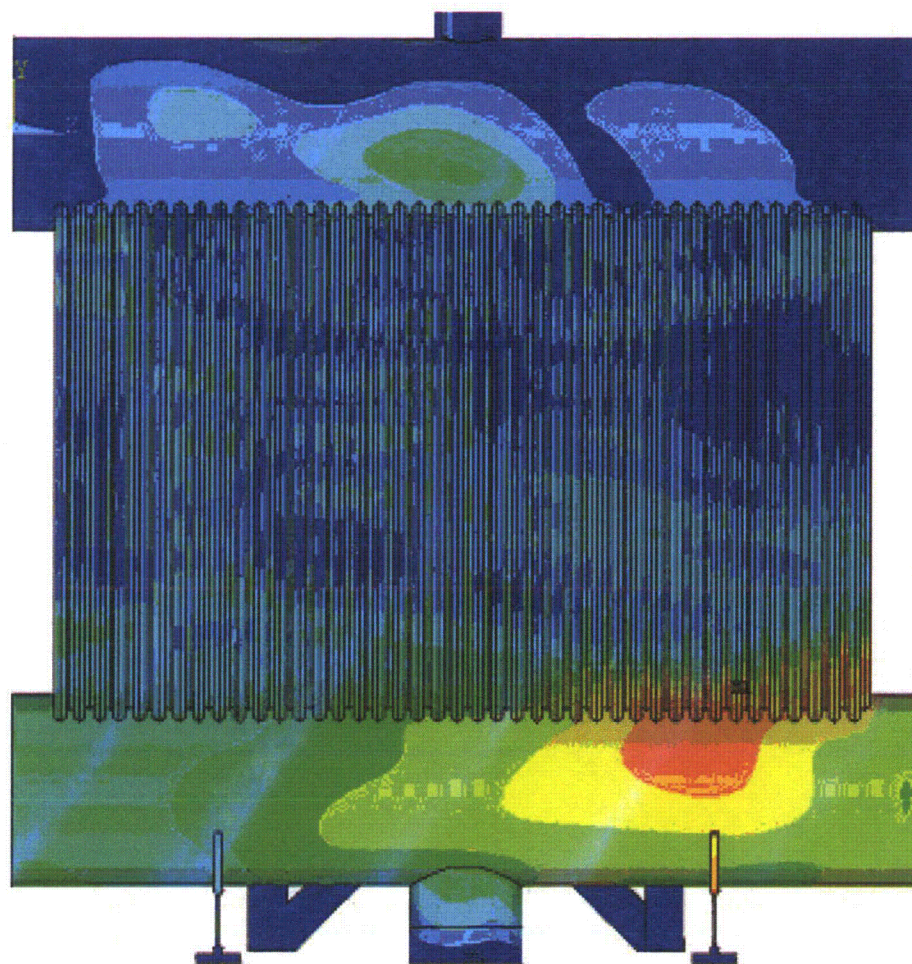


Figure C-11: Lower header Displacement Contour at Start of Steady State Pressure (displacement plots actual scale)

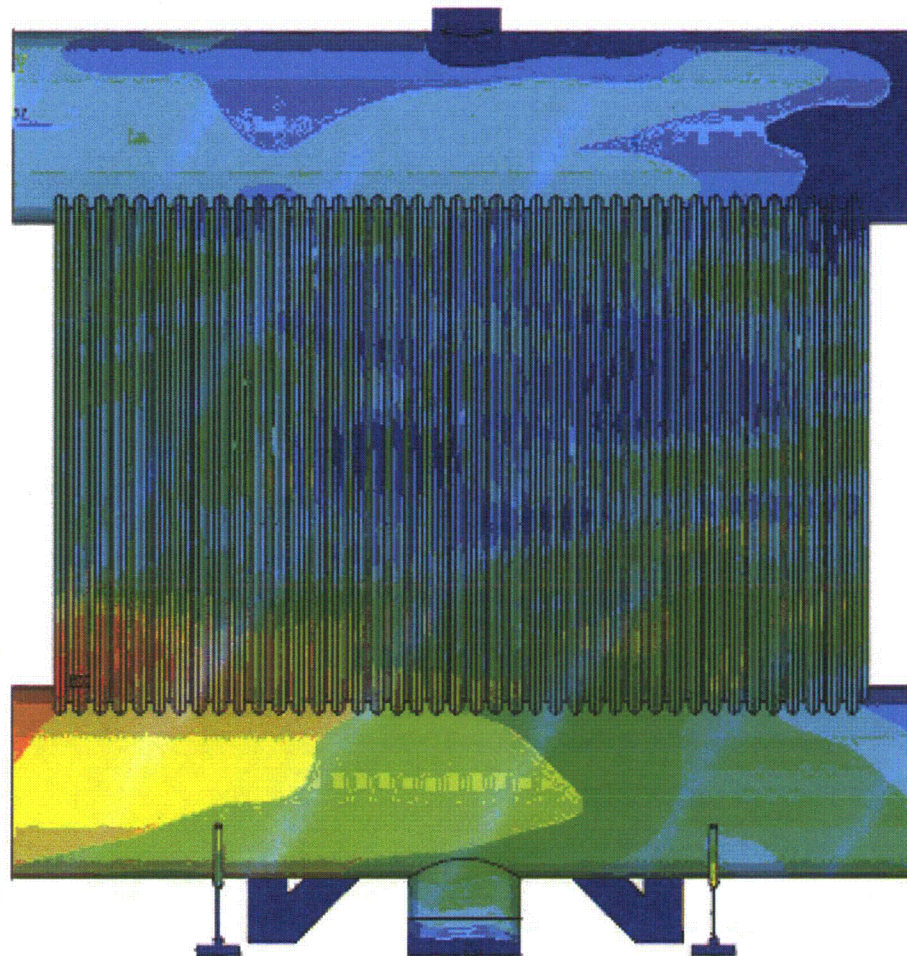


Figure C-12: Lower Header Displacement Contour at Peak Lateral Load on Drain Line (displacement plots actual scale)

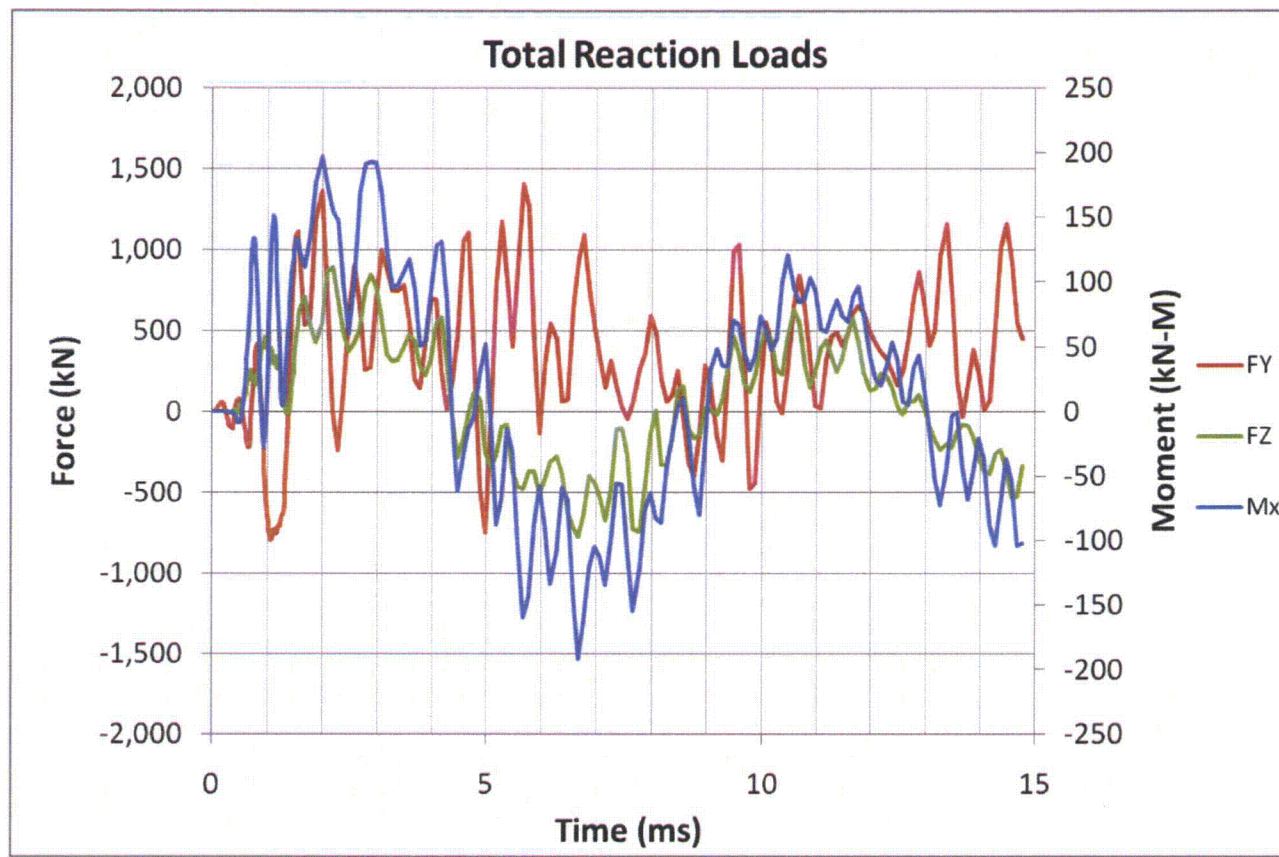


Figure C-13: Net Reaction Loads at PCCS Lower Header Mount Points

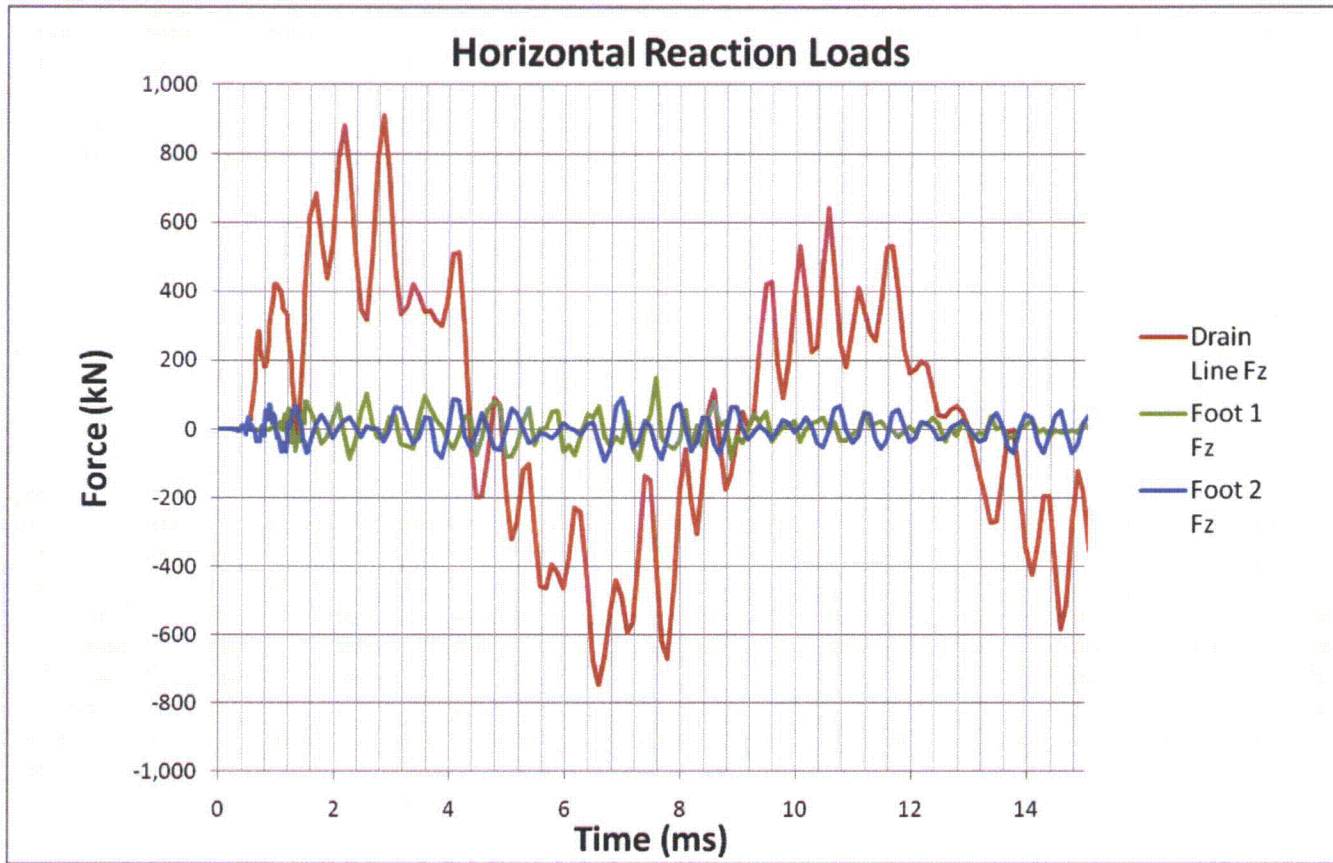


Figure C-14: Individual Horizontal Reaction Loads (2 Saddles and Condensate Line)

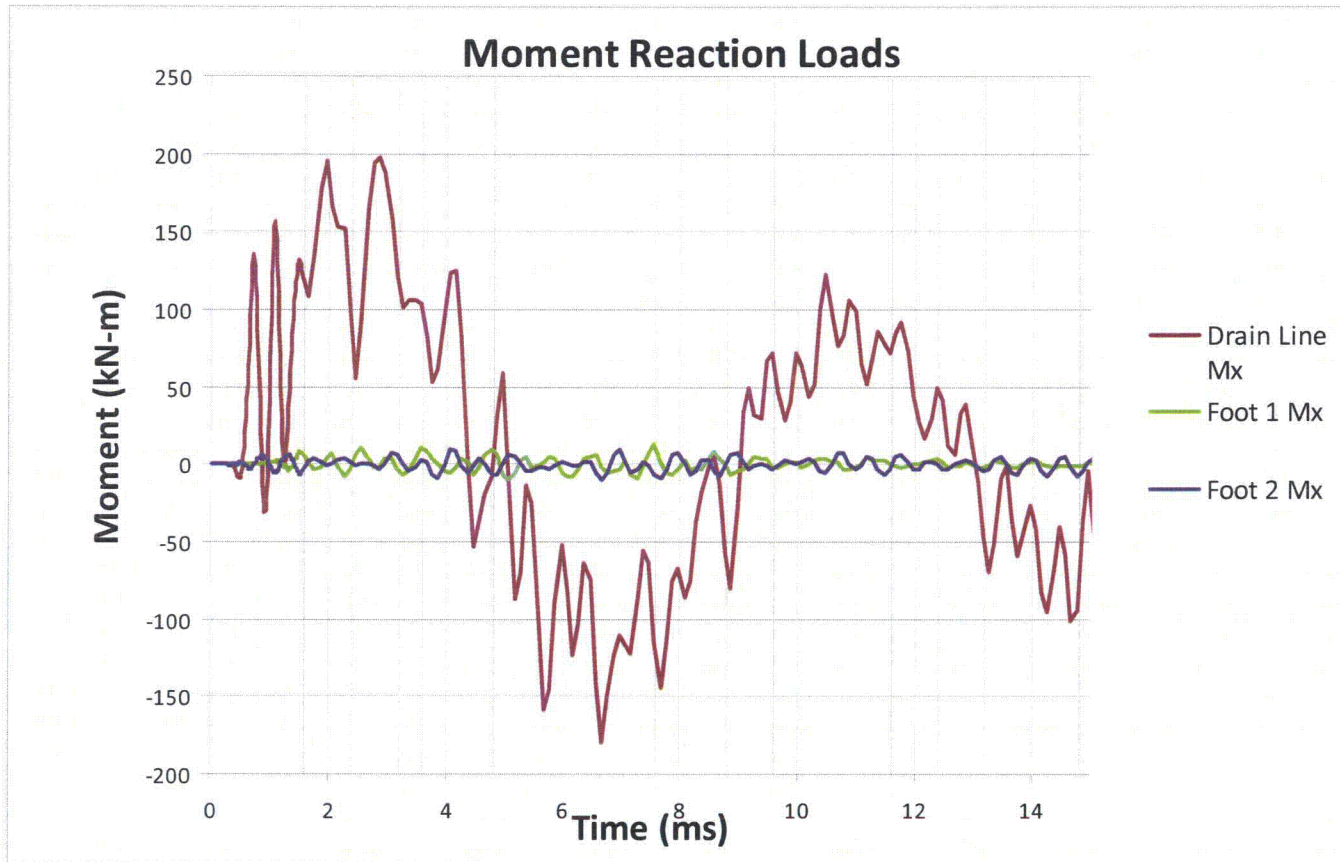


Figure C-15: Individual Moment Loads (2 Saddles and Condensate Line)

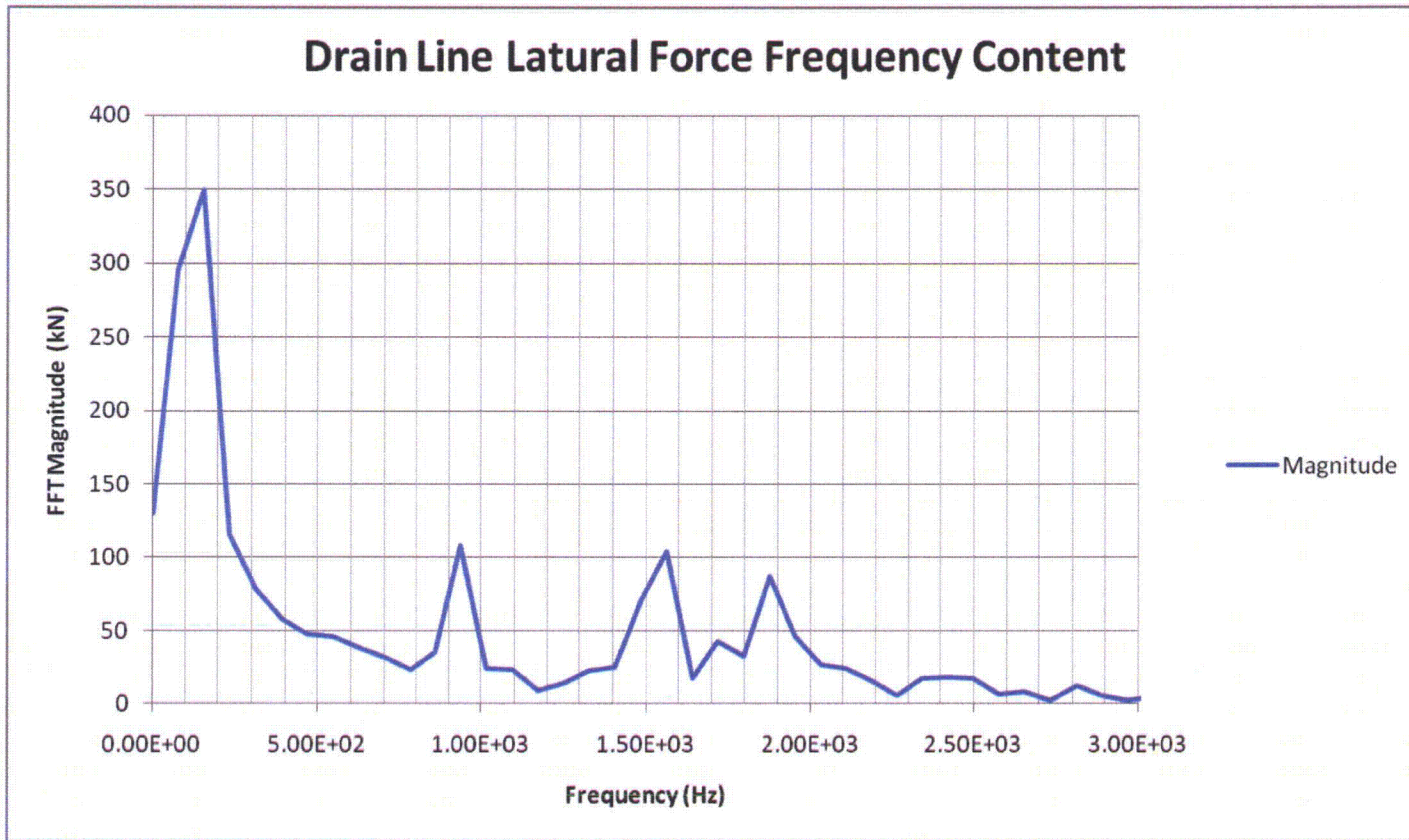


Figure C-16: Frequency Content in Condensate Line, Horizontal Force. Signals less than 2000 Hz will be captured with at least 5 time steps

Enclosure 6

MFN 10-044 Supplement 3

**Revised Response (Revision 3) to NRC Request for
Additional Information Letter No. 411
Related to ESBWR Design Certification Application**

Engineered Safety Features

RAI Number 6.2-202 S01

**Markups to NEDO-33251 Revision 2, "ESBWR I&C Diversity
and Defense-In-Depth Report," May 2009**

ACRONYMS AND ABBREVIATIONS

GDCS	Gravity-Driven Cooling System
GDS	Gated Diode Switch
HCU	Hydraulic Control Unit
HFE	Human Factors Engineering
HMI	Human-Machine Interface
HP CRD	High Pressure Control Rod Drive (or Control Rod Drive high pressure makeup water injection)
HSI	Human-System Interface
HVAC	Heating, Ventilation and Air Conditioning
I&C	Instrumentation & Control
IAS	Instrument Air System
IC	Isolation Condenser
ICP	Independent Control Platform
ICS	Isolation Condenser System
<u>IDIF</u>	<u>ICS DPV Isolation Function</u>
IEEE	Institute of Electrical and Electronics Engineers
INOP	Inoperable
kV	Kilovolt (1000 volts)
LD&IS	Leak Detection and Isolation System
LFCV	Low Flow Control Valve
LOCA	Loss-of-Coolant-Accident
LPRM	Local Power Range Monitor
LTR	Licensing Topical Report
Deleted	Deleted
MCR	Main Control Room
MRBM	Multi-Channel Rod Block Monitor
MSIV	Main Steam Isolation Valve

- Safety-related Reactor Trip and Isolation Function (RTIF) cabinets. These cabinets include the fail-safe logic for the following systems and functions (in four redundant divisions):
 - Reactor Protection System (RPS),
 - (Nuclear Boiler System (NBS)) Main steam isolation valve (MSIV) and drain valve logic and MSIV and drain valve isolation functions of the Leak Detection and Isolation System (LD&IS)
 - Suppression Pool Temperature Monitoring (SPTM) function of the Containment Monitoring System (CMS) – a process sensing function supporting RPS.
- Safety-related Neutron Monitoring System (NMS), including APRM, LPRM and Startup Range Neutron Monitor (SRNM) functions (four redundant divisions)
- Safety-related Independent Control Platform (ICP) - this functional group of fail-as-is logic consists of chassis that are physically located in the RTIF cabinets (four redundant divisions):
 - Anticipated Transient Without Scram/Standby Liquid Control System (ATWS/SLC) functions (includes ATWS mitigation logic processors and SLC system control logic processors),
 - Vacuum Breaker Isolation Function (VBIF) of the Containment System, ~~and~~
 - HP CRD Isolation Bypass function, and
 - ICS DPV isolation function

Space consideration may dictate locating the ICP hardware in separate cabinets.

- Safety System Logic and Control (SSLC)/ESF which provides safety-related fail-as-is ESF logic. Emergency Core Cooling System (ECCS) functions (four redundant divisions) which includes:
 - Isolation Condenser System (ICS) functions,
 - Automatic Depressurization System (ADS) functions of the NBS,
 - Gravity-Driven Cooling System (GDCCS) functions, and
 - Standby Liquid Control (SLC) System functions, and
 - LD&IS functions (non-MSIV),
 - Control Room Habitability System (CRHS) functions,
 - Containment Monitoring System (CMS) functions, and
 - Safety-related information systems.
 - The Process Radiation Monitoring System provides process-sensing inputs to the LD&IS and CRHS to support the isolation functions.
- Nonsafety-related nuclear systems of the N-DCIS that are divided into the following network segments
 - GENE systems (including DPS)

Figure 1 ESBWR DCIS Architecture

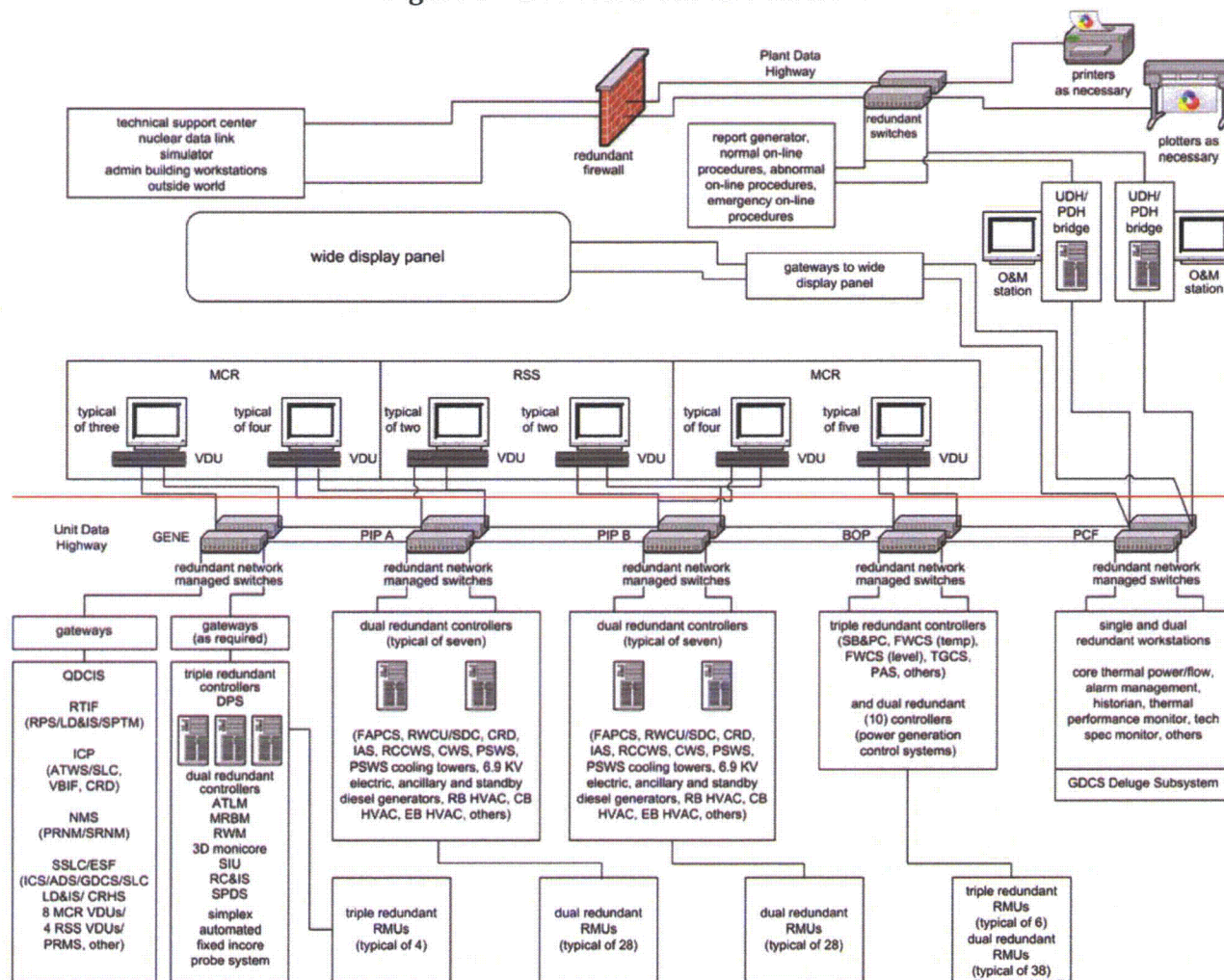
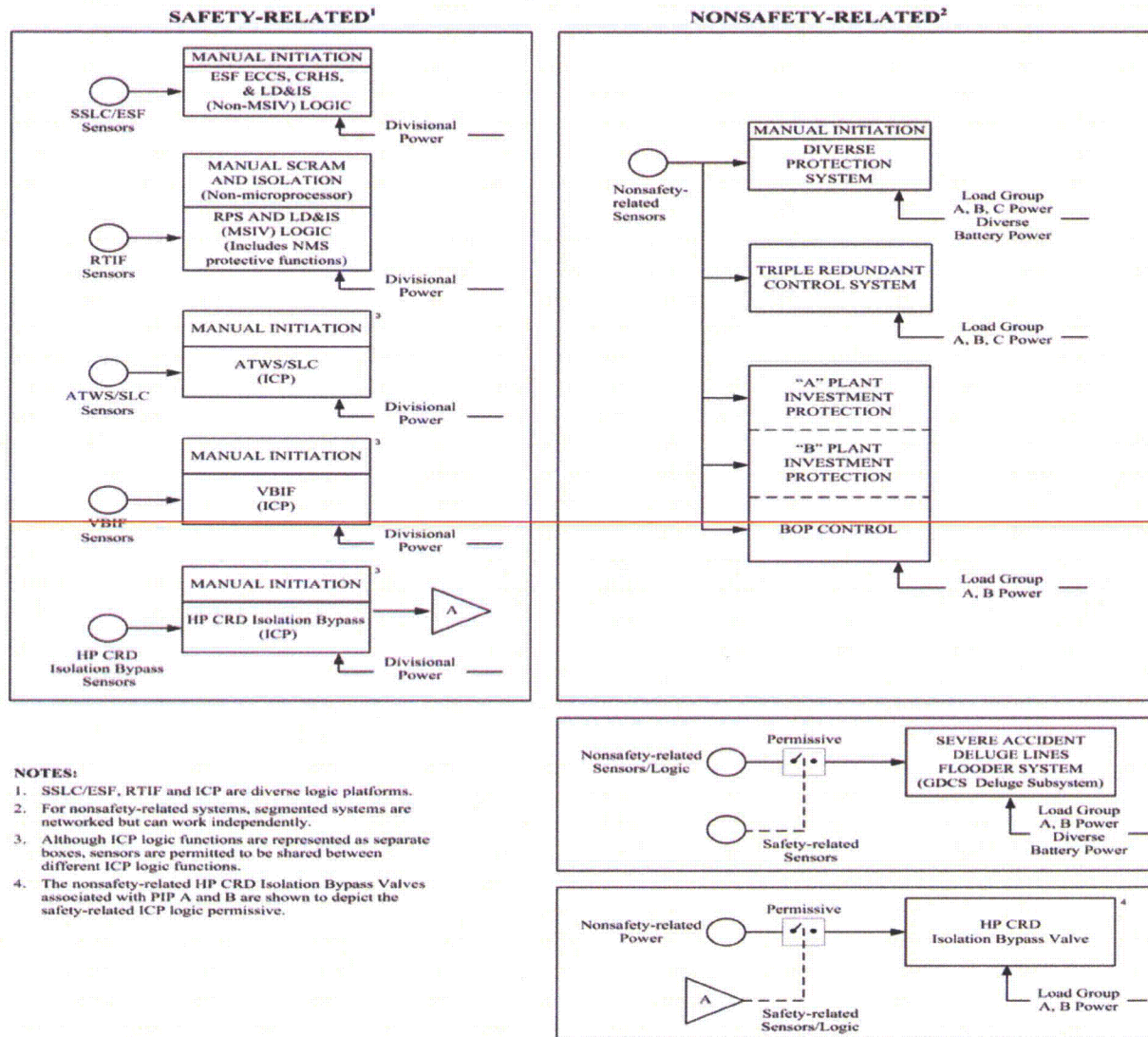


Figure 3 ESBWR Logic Platform and Power Diversity



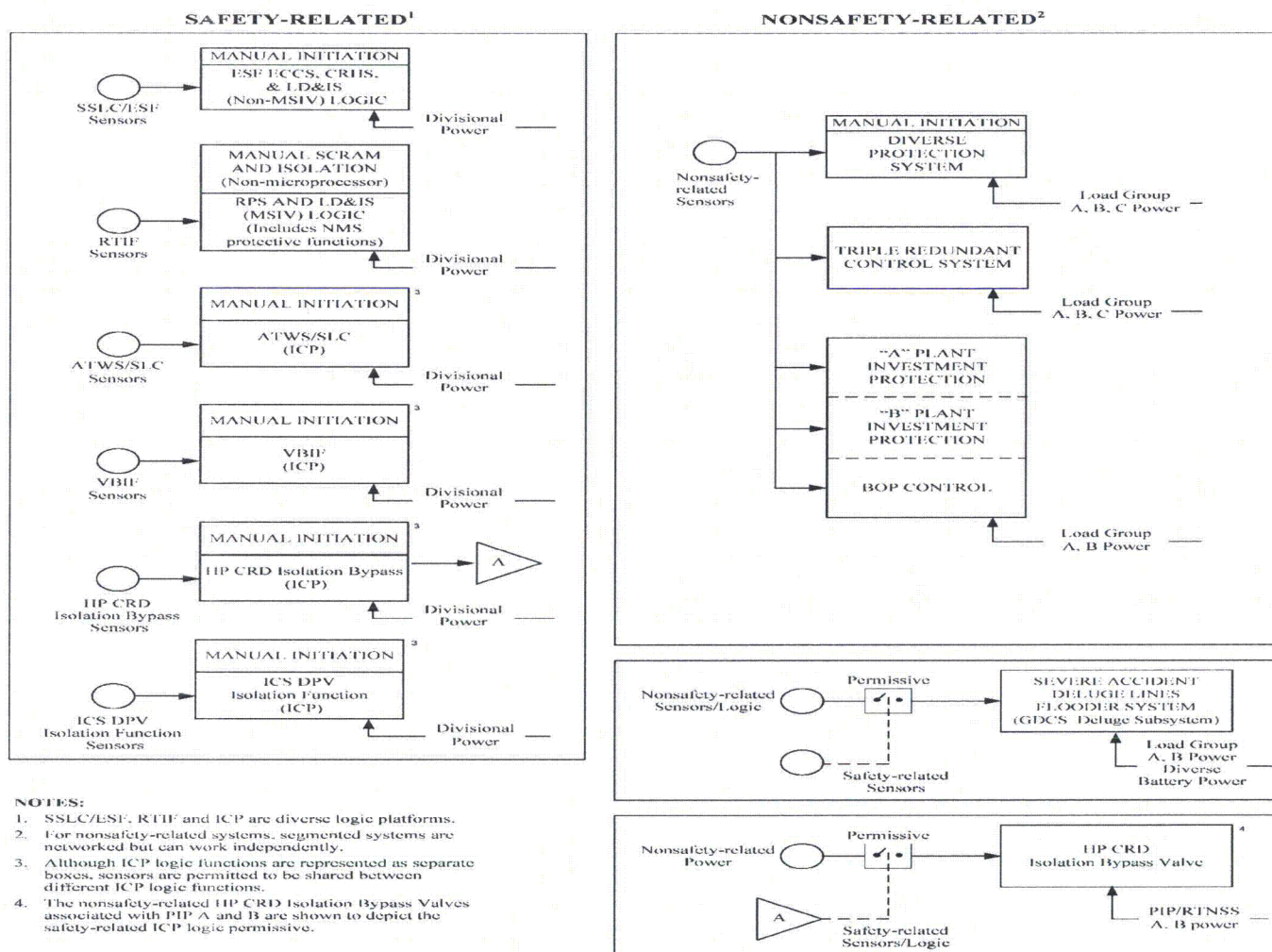


Figure 4 Main Control Room Layout - Typical

2.2 SAFETY-RELATED DISTRIBUTED CONTROL AND INFORMATION SYSTEM OVERVIEW

The Q-DCIS consists of the RTIF-NMS logic platform, the ICP and the SSLC/ESF logic platform. These systems and their associated sensors are organized into four divisions; the VDUs associated with each division provide for the control of the safety-related ESF equipment and additionally provide the necessary monitoring of the plant safety-related functions during and following an accident as required by Regulatory Guide (RG) 1.97 (Reference 6-13). The two-out-of-four logic associated with the RTIF-NMS logic platform, ICP and SSLC/ESF logic platform and the unique nature of the ESBWR solenoid and squib actuators allow the plant to be designed as "N-2"; specifically, any two divisions can accomplish the safety-related trip and ESF functions. N-2 is a significant element of the defense-in-depth design of the ESBWR DCIS.

The general relationship of the Q-DCIS is shown in Figure 6. (There are also nonsafety-related functions of NMS that are part of the N-DCIS.) The RTIF logic processors are located in the RTIF cabinet (one per division in separate Q-DCIS rooms) that combines the RPS, LD&IS (for MSIVs and drains only), SPTM, VBIF, HP CRD Isolation Bypass Function ~~and~~, ATWS/SLC functions, and ICS DPV isolation function. Although all equipment located in the RTIF cabinet is appropriate to the division and everything in the cabinet is powered by the appropriate divisional uninterruptible and battery power, the VBIF, HP CRD Isolation Bypass ~~and~~, ATWS/SLC functions, and ICS DPV isolation function (which are part of the ICP) are segregated to separate chassis from the remaining RTIF logic processors and from one another. The ICP (i.e., VBIF, HP CRD Isolation Bypass ~~and~~, ATWS/SLC, and ICS DPV isolation) is diverse from the RTIF-NMS and SSLC/ESF logic platforms. All of the safety-related functions are implemented in hardware/software platforms diverse from the DPS.

The ESBWR RPS design has several important differences from other Boiling Water Reactor (BWR) scram logic and hardware (although many of these features were included in the ABWR design); these include:

- Per parameter trip (specifically there must be (for example) two un-bypassed level trips to scram, a pressure trip and a level trip will not cause a scram).
- No operator manipulation of the division of sensors and/or division of logic bypass, nor any operation of the RPS back panel inoperable switches can reduce scram logic redundancy to less than "any two un-bypassed same parameters in trip will cause a scram". Only one division at a time can be physically bypassed. The RPS (and MSIV LD&IS) is N-2 to scram/isolate.
- Communication with the nonsafety-related DCIS is one-way (Q-DCIS to N-DCIS) through fiber; the loss of this communication does not affect RPS functionality.
- Communication with other RPS divisions is one-way, fiber isolated, and does not mix divisional data.
- All signals are actively transported such that "fail safe" is not a "1" or a "0" but rather "trip on loss of communication". As a result, loss of communication from another division is interpreted as a trip signal (unless that division is bypassed) and loss of communication with a bypass joystick switch is interpreted as "no bypass".

- RPS (and Q-DCIS) logic is powered by divisional redundant (uninterruptible 120V AC) power supplies that are backed by redundant batteries; additionally, the systems are backed up by offsite power and either of the two diesel generators.
- The CRD Hydraulic Control Unit (HCU) scram solenoid power is local to the Reactor Building (RB) and switched by fiber driven two-out-of-four logic from the RPS logic processors (located in the RTIF cabinet in the Control Building (CB)). This avoids the long distance voltage drops to the solenoids in the older BWR designs and eliminates (along with using monitored, safety-related inverters for solenoid power) the need for Electric Protection Assemblies. Loss of communication from the CB RTIF cabinets is interpreted as a trip.
- The hardware, software and solenoid switching for the RPS are diverse from the DPS.

The ICP provides a safety-related platform that is diverse from the RTIF-NMS and SSLC/ESF platforms. The ICP implements the following ESF, diverse reactor shutdown, ATWS mitigation, and beyond design basis event mitigation functions (Reference 6-3 provides additional details on the ICP).

- ATWS/SLC – Certain ATWS mitigation functions are implemented as safety-related logic. The ATWS mitigation logic processors provide SLC initiation and feedwater runback signals, as well as ADS Inhibit logic that inhibits the sustained RPV Level 1, sustained drywell pressure high, and drywell pressure high-high initiation logic within the SSLC/ESF platform. SLC logic processors provide SLC system actuation and accumulator isolation functions in support of ATWS mitigation, diverse reactor shutdown, and ECCS operation. Isolation of the respective SLC accumulators on low accumulator level prevents nitrogen intrusion into containment to preclude a containment integrity or safety-related cooling system challenge.
- VBIF – To isolate a leak from (or failure of) any of the three Wetwell to Drywell vacuum breakers, the vacuum breaker isolation valve logic provides the backup means of isolating the Wetwell from the Drywell. The Vacuum Breaker Isolation valves provide a diverse means of system isolation to the mechanical vacuum breakers and are not required to mitigate a CCF of the RTIF-NMS or SSLC/ESF platforms.
- Control Rod Drive high pressure makeup water injection (HP CRD) Isolation Bypass function – HP CRD flow to the RPV is isolated by SSLC/ESF logic during accidents that could challenge peak containment pressure. As part of beyond design basis scenarios where injection of the GDCS pool inventory is not successful, HP CRD isolation is bypassed automatically by ICP logic to provide additional coolant inventory.
- ICS DPV isolation function – To automatically close the ICS steam admission valves upon opening of any two DPVs. Closing the ICS steam admission valves when the RPV is depressurized mitigates the accumulation of radiolytic hydrogen and oxygen.

The SSLC/ESF DCIS is implemented on a hardware/software platform that is a sub system of the Q-DCIS. The SSLC/ESF hardware/software platform is diverse from RTIF-NMS, ICP and the DPS. SSLC/ESF has a separate set of sensors from RTIF-NMS and ICP, and a diverse set of sensors from DPS. Since it is highly desirable to avoid the consequences of inadvertent actuation of ECCS (specifically automatic depressurization) and also important to reliably actuate ECCS

- PCCS Ventilation Fans
- Drywell Cooling, and
- RB, Fuel Building (FB), Control Building (CB), Switchgear Building Heating Ventilation and Air Conditioning (HVAC).

The PIP systems are organized mechanically into two trains (i.e., pump “A” and pump “B”) with each train powered by a different diesel generator and 6.9 KV bus. The two trains are controlled by a deliberately segmented N-DCIS, so that the RMUs, control processors and displays that operate PIP A systems are separate from those operating PIP B systems. The segmentation is implemented using managed network switches; approximately one third of the nonsafety-related control room displays are assigned to the PIP A and the PIP B switches. Normally any control room nonsafety-related display can control/monitor any PIP or BOP system but the loss of either PIP system DCIS or the BOP DCIS will not affect the operation of the remaining PIP system or its displays.

The BOP control systems are those used principally for power generation and are not normally used for shutting down the plant, nor monitoring the more important plant parameters. They specifically include the triple redundant systems used to control the turbine, reactor pressure, RPV water level and plant automation and dual redundant systems, such as, the RC&IS, hotwell level control and condensate polishing systems.

The above systems provide margins to plant safety-related limits and improve the plant's transient performance. The systems also maintain the plant conditions within operating limits. The BOP functions can also be used to shut down the plant and are also part of the ESBWR defense-in-depth automatic and manual functions.

The PCF of N-DCIS redundantly provides for the plant AMS, some of the rod blocks for the Rod Control and Information System (RC&IS), the monitoring of thermal limits including core thermal power and flow calculation and calculation of calibration information for NMS and the isolated safety-related parameter display functions. The PCF of N-DCIS provides information to and receives demands from the nonsafety-related VDUs. The N-DCIS also provides for the acquisition and display of sensor outputs for nonsafety-related plant monitoring functions.

The N-DCIS supports the Severe Accident Deluge Lines Flooder System using diverse hardware and software and separate sensors from both the safety-related and nonsafety-related DCIS systems. The Deluge Lines Flooder System uses squib valves to drain GDCS pool water underneath the RPV should all other core cooling and shutdown systems fail. The valves are actuated by sensed containment floor high temperatures attributable to the postulated core and vessel melt.

2.4 DIVERSE PROTECTION SYSTEM OVERVIEW

The DPS is a triple redundant, nonsafety-related system that provides an alternate means of initiating a reactor trip, actuating selected Engineered Safety Features and providing plant information to the operator. The relationship is shown in Figure 6. For functions credited with mitigating a digital protection system CCF, the DPS receives signals directly from a diverse set of sensors that are electrically independent from the sensors used by the Q-DCIS platforms.

Specifically, the DPS uses hardware, software and power that are diverse from those used by the safety-related systems. The DPS is described further in Tier 2 Chapter 7 of Reference 6-3.

The DPS system performs several major/minor functions:

- It scrams the plant using a subset of the safety-related RPS parameters.
- It scrams the plant on a SCRRI/SRI command with power remaining elevated, or on receipt of an RPS scram demand from two of four RPS divisions.
- It closes the MSIVs on receipt of a high steam flow signal, low RPV water level, or low reactor pressure (i.e., low turbine inlet pressure).
- It initiates Selected Control Rod Run-in (SCRRI) and Select Rod Insert (SRI) to rapidly reduce power.
- It initiates selected ECCS.
- It transmits ATWS/SLC logic signals to cause the Feedwater Control System (FWCS) to run back feedwater flow.
- It initiates a delayed feedwater runback if elevated power levels persist following either a SCRRI/SRI command or an RPS scram command from two of four RPS divisions.
- It trips the feedwater pumps on RPV water level 9 (after they have been run back to zero flow on RPV water level 8 by the FWCS).
- It opens the ICS lower header vent valves after six hours of ICS initiation.

The DPS initiates a plant scram on a per parameter two-out-of-four coincidence of:

- Detected high or low RPV water level,
- Detected high RPV pressure,
- Detected high drywell pressure,
- Detection of high suppression pool temperature, and
- Inboard or outboard MSIV closure on two or more main steam lines.

The DPS causes a scram by interrupting the current in the 120 VAC return power from the HCU scram solenoids using the same switches used to perform individual control rod scram timing. The two-out-of-three scram decision of the triple redundant processors is sent to the scram timing test panel where they are two-out-of-three voted to open all the solenoid return power switches. The operator also has the ability to initiate a manual DPS scram from either hard switches or the N-DCIS VDUs.

The DPS processes a SCRRI/SRI signal to hydraulically scram selected control rods and to command the RC&IS to perform the SCRRI function based on any of the following initiators:

- Generator load rejection signal from the Turbine Generator Control System (TGCS),
- Turbine trip signal from the TGCS,
- Loss of feedwater heating, and

Enclosure 7

MFN 10-044 Supplement 3

**Revised Response (Revision 3) to NRC Request for
Additional Information Letter No. 411
Related to ESBWR Design Certification Application**

Engineered Safety Features

RAI Number 6.2-202 S01

Affidavit